UNIVERSIDADE DE SÃO PAULO
INSTITUTO DE GEOCIÊNCIAS

FROM LARGE RIVERS TO THE ROCK RECORD: CHANNEL PATTERNS, BEDFORMS AND A FACIES MODEL FOR THE AMAZON RIVER

Cristiano Padalino Galeazzi

Orientador: Prof. Dr. Renato Paes de Almeida

TESE DE DOUTORADO

Programa de Pós-Graduação em Geoquímica e Geotectônica

SÃO PAULO

2020

Serviço de Biblioteca e Documentação do IGc/USP
Ficha catalográfica gerada automaticamente com dados fornecidos pelo(a) autor(a)
via programa desenvolvido pela Seção Técnica de Informática do ICMC/USP

Bibliotecários responsáveis pela estrutura de catalogação da publicação:
Sonia Regina Yole Guerra - CRB-8/4208 | Anderson de Santana - CRB-8/6658

GALEAZZI, CRISTIANO PADALINO
FROM LARGE RIVERS TO THE ROCK RECORD: CHANNEL PATTERNS, BEDFORMS AND A FOCIES MODEL FOR THE AMAZON RIVER / CRISTIANO PADALINO GALEAZZI; orientador RENATO PAES DE ALMEIDA. -- São Paulo, 2020.
173 p.

Tese (Doutorado - Programa de Pós-Graduação em Geoquímica e Geotectônica) -- Instituto de Geociências, Universidade de São Paulo, 2020.

1. LARGE RIVERS. 2. CHANNEL PATTERN CLASSIFICATION. 3. LARGE RIVER BEDFORMS. 4. LARGE RIVER FACIES MODELS. 5. PALEOCURRENT VARIANCE. I. ALMEIDA, RENATO PAES DE, orient. II. Título.

AGRADECIMENTOS

Agradeço ao orientador Renato Paes de Almeida por toda orientação e desorientação proporcionadas no decorrer dos anos, pela capacidade de gerar interesse e por todo conhecimento compartilhado durante esse longo tempo de convivência, que culminou com a ocupação das funções de piloto e copiloto de uma lancha em meio a uma tormenta no Rio Japurá.

Aos ilustres companheiros de pesquisa de todas as gerações do grupo Mocó – André Marconato, André Stern, Ariel Prado, Bernardo Freitas, Bruno Turra, Carlos Mazoca, Daniela Goulios, Felipe Figueiredo, Geovana Geraldo, Heitor Figueiredo, Julio César Ardito, Larissa Tamura, Liliane Janikian, Lucas Corrêa, Mariane Vivan, Maria Paula Clavijo, Natalia Hilbert e Simone Carrara – que desde a origem até o presente trabalho responderam a muitas dúvidas, contribuíram prontamente com o desenvolvimento da pesquisa e deixaram o clima amazônico mais ameno.

Os agradecimentos se estendem também aos companheiros que participaram das expedições que possibilitaram a realização de parte desse trabalho, André Sawakuchi, Carlos Grohmann, Dailson Bertassoli, Fabiano Pupim, Caio Breda e Ian Garcia e aos que viabilizaram o acesso a lugares remotos da Amazônia: Jones, Emerson, João Paulo, Vanuza, Wanderson, Daniel, Elenir, Seu Nonato, Jayane e Francisco, a bordo das valentes embarcações Priscila Mendes, Maria das Graças e Geisiela Manuela. Agradeço também aos colaboradores de pesquisa Andrea Kern, Cibele Voltani, Jim Best, Julia Cisneros e Marco Ianniruberto, os quais contribuíram significativamente com o estudo desenvolvido nesses anos e proporcionaram formidáveis momentos de pescaria miocênica.

A realização das atividades relacionadas ao presente trabalho contou com apoio financeiro do Programa de Recursos Humanos da Petrobrás, pela bolsa de doutorado inicial, e da Fundação de Amparo à Pesquisa do Estado de São Paulo (FAPESP), pela bolsa de doutorado 2017/06874-3 e por meio dos projetos de pesquisa dos processos 2012/50260-6 e 2014/16739-8.

ABSTRACT

Assumed gaps in fluvial sedimentology include large rivers, channel pattern classification and their interpretation in the rock record. Despite large rivers significance being acknowledged for decades, with a growing interest in more recent times, these fluvial systems have been relatively put aside in sedimentological research. Rivers in general have been subject of research for more than a century but the link between proposed classifications and the rock record has been problematic, with a persistent lack of effective criteria to distinguish among channel patterns in fossil fluvial systems. Channel patterns have been related to water and sediment discharge, slope, grain size, width-to-depth ratio and types of climate. Therefore, recognition of both large rivers and channel patterns in the rock record is of great significance for regional paleogeographic and paleoclimatic reconstructions, reservoir modelling, estimation of sediment input in a sedimentary basin and river management. The present work aims to cover the above-mentioned gaps concerning fluvial sedimentology by presenting three manuscripts. Manuscript (1) intends to contribute to channel pattern classification and channel pattern recognition in fluvial deposits by presenting a broad survey of alluvial rivers at a global scale to quantify channel pattern natural variability and by identifying relevant parameters for recognition in the rock record. A channel pattern classification based on quantification of sinuosity and number of channels is presented, along with a method to recognize channel patterns in the rock record based on the quantification of the variability of directions observed in the preserved bedforms in floodplains at the channel belt scale. Manuscript (2) intends to contribute to the recognition of large rivers in the rock record by discussing the relationship of channel scale and water depth with bedform morphology. The work presents high-resolution bathymetric maps of the Solimões-Amazonas River, the quantification of dune data from their riverbeds and riverbed samples. Dune morphology, height and leeside angles, as well as grain size, are related to water depth and these relationships are used to make inferences about how to identify large river in the rock record and are compared with interpreted large river fluvial deposits. Manuscript (3) intends to contribute to the recognition of large rivers in the rock record by presenting the facies models for the Solimões-Amazonas River based on the integration of morphodynamics, geophysical data and samples from the riverbed and bar tops.

RESUMO

A interpretação no registro rochoso de rios de grande escala e do estilo de canal são lacunas reconhecidas da sedimentologia fluvial. Apesar da importância dos rios grandes ser reconhecida há décadas, com um crescente interesse em tempos mais recentes, estes sistemas fluviais tem sido relativamente negligenciados em pesquisas sedimentológicas. Rios no geral tem sido objeto de pesquisa há mais de um século, mas o elo entre as classificações propostas e o registro rochoso tem sido problemático, com uma persistente falta de critérios efetivos para interpretar o estilo de canal em sistemas fluviais fósseis. Estilos de canal estão relacionados à vazão de água e sedimentos, declividade, granulação, razão entre largura e profundidade e tipos de clima. Dessa forma, o reconhecimento tanto de rios grandes quanto do estilo de canal no registro rochoso é importante para reconstruções paleogeográficas e paleoclimáticas, modelos de reservatório, estimação de entrada de sedimentos em bacias sedimentares e gestão de rios. O presente trabalho tem como objetivo cobrir as lacunas mencionadas da sedimentologia fluvial com a apresentação de três manuscritos. O Manuscrito (1) pretende contribuir com a classificação de estilos de canal e seu reconhecimento no registro rochoso. Para isso, é apresentada uma classificação baseada na quantificação de sinuosidade e número de canais e um método de reconhecimento de estilo de canal no registro rochoso baseado na quantificação da variabilidade de direções observada nas formas de leitos preservadas nas planícies de inundação na escala do cinturão de canais. O Manuscrito (2) pretende contribuir com o reconhecimento de rios grandes no registro com a discussão da relação entre formas de leito com escala e profundidade do canal. São apresentadas imagens do canal submerso do Rio Solimões-Amazonas junto com a quantificação de dados das formas de leito e amostras do leito dos rios. As relações entre morfologia das dunas, altura, ângulo lee e granulação são usadas para inferir como identificar grandes rios no registro rochoso e os resultados são comparados a depósitos interpretados de grandes rios. O Manuscrito (3) pretende contribuir com o reconhecimento de grandes rios no registro rochoso apresentando um modelo de facies para o Rio Solimões-Amazonas baseado na integração da morfodinâmica, de dados geofísicos e de amostras do leito do canal.

CONTENTS

LIST OF FIGURES

I. INITIAL CONSIDERATIONS

II. LITERATURE REVIEW AND INTRODUCTION TO THE FOLLOWING CHAPTERS

IV. THE SIGNIFICANCE OF SUPERIMPOSED DUNES IN THE AMAZON RIVER: IMPLICATIONS FOR HOW LARGE RIVERS ARE IDENTIFIED IN THE ROCK RECORD

LIST OF TABLES

I. INITIAL CONSIDERATIONS

I.1 INTRODUCTION

Assumed gaps in fluvial sedimentology include large rivers, channel pattern classification and their interpretation in the rock record. Large rivers significance has been acknowledged for decades, with a growing interest in more recent times (e.g. Holeman, 1968; Potter, 1978; Miall, 2006; Potter & Hamblin, 2006; Gupta; 2007; Reesink et al., 2014) and are defined by large drainage area, channel length and water and sediment discharges (Hovius, 1998; Potter & Hamblin, 2006; Gupta, 2007). Few large rivers are the end member of continental-scale basin drainage areas (e.g. Fielding et al., 2012) and accumulate continental-scale water and sediment discharge to oceans (e.g. Milliman & Meade, 1983; Milliman & Farnsworth, 2011). Channel patterns have been related to water and sediment discharge, slope, grain size, width-to-depth ratio and types of climate. Therefore, recognition of both large rivers and channel patterns in the rock record is of great significance for regional paleogeographic and paleoclimatic reconstructions, reservoir modelling, estimation of sediment input in a sedimentary basin and river management.

Research on large rivers has been relatively put aside in sedimentological research of fluvial systems. This fact is explained by the challenging conditions imposed by the geographic locations and scale of the rivers in the very hot and wet regions (Latrubesse et al., 2005) or in the arctic regions (Slaymaker, 2020) of the world, in addition to the necessity of the use of state-of-the-art geophysical techniques to survey their deep turbid flows. Consequently, facies models have been largely based on observations made in small fluvial systems, hampering recognition of the river scale in the rock record. Attempts to interpret river scale in fluvial deposits have relied on the relation of cross-strata set thickness, dunes and water depth (e.g. LeClair & Bridge, 2001; Miall, 2006; Fielding et al., 2007) but recent studies challenge such assumption (e.g. Best et al., 2007; LeClair, 2011; Reesink et al., 2014), leaving this subject an open question.

Several channel pattern classifications have been proposed over time, with no general agreement on criteria, nomenclature, or term boundaries. Generally, classifications consider the common meandering and braided rivers end members of a continuum of channel patterns, mainly attributing the transition from one to another to variations in water discharge, slope, sediment load and erodibility (e.g. Leopold & Wolman, 1957; Schumm, 1981; Bridge, 1993; Alabyan & Chalov 1998; Eaton et al., 2010). The profusion of different terms used to classify channel patterns, such as anabranching, wandering, incomplete meandering, or meanderthal, among others (Ethridge, 2011; Carling et al., 2014; Miall, 2014), and the necessity to thoroughly explicit the meaning attributed to a given term in every publication evidences the difficulty of communication between research groups. So far, recognition of channel patterns in the rock record has been mostly based on facies models of meandering and braided channels, whereas other channel types have been overlooked. However, special attention must be given to these other channel patterns; besides being frequent, they are often found in large rivers (Latrubesse, 2008). Although the established criteria for recognition of channel patterns have not been considered overall effective (e.g. Davidson et al., 2011; Ethridge, 2011; Colombera & Mountney, 2019), employment of paleocurrent variance at the channel belt scale appears to be a valid alternative (e.g. Selley, 1965; Le Roux, 1992; Bataille et al., 2018), due to its relation with sinuosity (Ferguson, 1977; Le Roux, 1992) which in turn is strongly related to channel patterns (e.g. Schumm, 1981; Bridge, 1985) .

This work aims to cover the above-mentioned gaps concerning fluvial sedimentology by presenting the following results: (1) a global-scale survey of alluvial rivers to define a channel pattern classification based on quantitative parameters with geological significance; (2) criteria to interpret channel patterns in fluvial deposits; (3) quantitative bedform data of a large fluvial system to investigate the relation of bedform morphology and water depth; (4) facies model of a large fluvial system based on the integration of satellite imagery, state-of-the-art geophysical methods and field work observations.

I.2 OBJECTIVES

The present work aims to improve and provide criteria for interpretation of large rivers and channel patterns in fluvial deposits. In order to do so, the intended specific objectives are:

- Conduct a global scale survey of modern alluvial rivers to encompass natural variability of rivers and propose a channel pattern classification focused on interpretation of fluvial deposits and

- Identify parameters in modern river that can contribute to propose criteria for channel pattern interpretation in the rock record;

- Survey reaches of the Solimões-Amazonas River, the largest fluvial system of the world, with state-of-the-art geophysical techniques to study the relation of bedform morphology and water depth;

- Propose a facies model for the Solimões-Amazonas River by integrating the analysis of satellite imagery, high-resolution bathymetric maps, shallow seismic and radar sections, quantitative dune data, riverbed samples and field observations.

- Develop criteria to improve recognition of large-scale fluvial systems in the rock record.

I.3 LOCATION

Part of the present work was done by conducting field work in the Solimões-Amazonas River and part by remotely surveying alluvial rivers at a global scale. The Solimões-Amazonas River is located in northern Brazil, where the Amazon River is named Solimões River from the Peruvian border to the confluence with the Rio Negro, near Manaus, and Amazonas River thereafter (Fig. 1.1). Field work consisted in performing geophysical surveys in four distinct reaches during the wet seasons of in July of 2015 and 2016. Two reaches are located in the Lower Solimões (LS), c. 5-10 km before the confluence with the Rio Negro: LS1 in the northern main channel, downstream of the Marchantaria Island (also known as Mouras Island) and LS2 in the secondary channel, at the southern side of the same island. The other two reaches are located in the Upper Amazonas (UA), c. 33 km and 95 km downstream of the confluence: UA1 in the northern side of the Careiro Island, and UA2 in the northern side of Autaz Island, c. 20 km upstream of the confluence with the Madeira River.

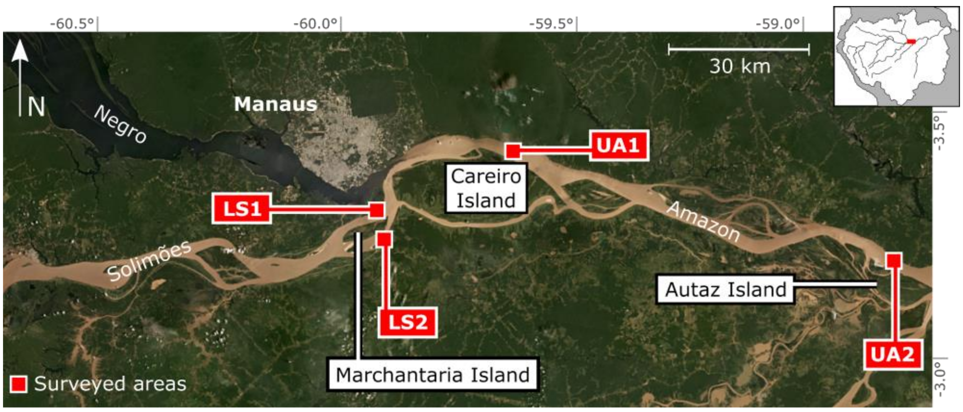

Fig. 1.1 – Location of the surveyed reaches in northern Brazil.

The remote survey of rivers at a global scale was done by the use of Google Earth software and Planet Team (2020) website. The studied modern rivers are alluvial and perennial, with developed floodplains on at least one side of the river and constant flow throughout the year. Rivers were considered adequate if they fulfilled the following requirements: occurrence of floodplain with preserved depositional elements, known discharge (minimum average monthly discharge >10 m^3s^{-1}), and preferably unoccupied by humans. Rivers from heavily populated areas were mostly ruled out due to intense human activity at their margins, leading to possible river engineering and obliteration of the preserved depositional elements. Occasionally, the same river had different reaches with known discharge and preserved depositional elements in the floodplain, therefore being measured more than once. The 361 rivers included in this work are located in Russia (88), Brazil (87), United States (31), India (22), Congo (16), Canada (13), Argentina (11), Afghanistan (10), Peru (9), Chad (7), China (6), Central African Republic (5), Bolivia (4), Kazakhstan (4), Australia (3), Colombia (3), Myanmar (3), Nigeria (3), Zambia (3), Bangladesh (2), Indonesia (2), Pakistan (2), Tanzania (2), Ukraine (2), Venezuela (2), Botswana (1), Cambodia (1), Cameroon (1), Guatemala (1), Iceland (1), Kenya (1), Kyrgyzstan (1), Mali (1), Mozambique (1), Nepal (1), Niger (1), Papua New Guinea (1), Paraguay (1), Philippines (1), Rwanda (1), Senegal (1), Tajikistan (1), Thailand (1), Turkmenistan (1), Uganda (1) (Fig. 1.2).

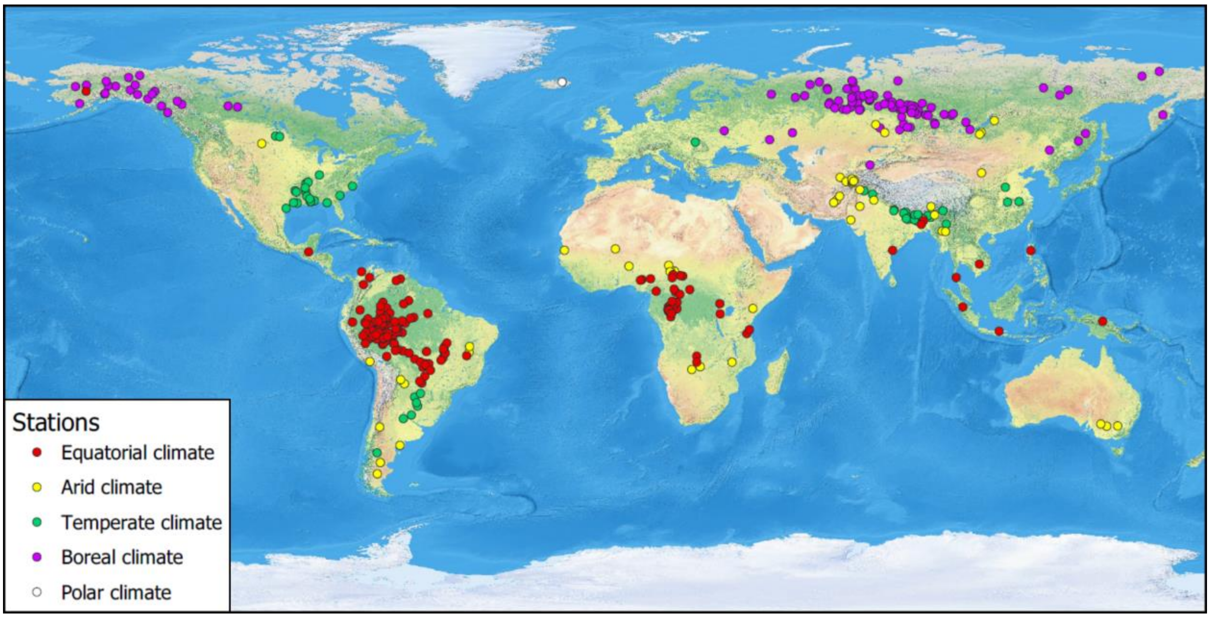

Fig. 1.2 – World map with the surveyed reaches and their respective climate zone.

I.4 METHODS

The present work was conducted partly by acquiring data during field work and partly by collecting data remotely. Data acquisition during fieldwork consisted in the employment of geophysical methods during the wet season and riverbed material sampling. Remote data acquisition included the survey of alluvial at global scale with collection of drainage basin area, water discharge, climate, channel slope, sinuosity, width, stream power, specific stream power and channel count index, as well as proportion of preserved bedform in the floodplains and the respective variance of paleocurrent within them.

I.4.1 Multibeam Echo Sounder acquisition and data processing

Multibeam Echo Sounder (MBES) is a geophysical equipment that produces high resolution 3D bathymetric images of underwater surfaces by precisely measuring the water depth (Fig. 1.3). Channel depth estimation is done by a sonar fixed on the side of the boat produces acoustic pulses towards the bottom, which are reflected back, captured and recorded (Parsons et al., 2005). The MBES used in the present work is the Teledyne-Reson Seabat 101 System, operating at a frequency of 240kHz, with 511 beam achieving 12,5 mm resolution, which functioned connected to a Vector VS330 DGPS and had live tracking. Trepidations from the engine of the boat and variations in the three dimensions caused by waves in the river were corrected by the use of a Novatel motion sensor. Survey was undertaken in lines parallel and perpendicular to river flow, with average boat velocity of 7 km/h upstream and 12 km/h downstream. Data was saved as asc files, containing longitudinal, latitudinal and depth information of every point in the grid. Bedform quantitative data was computed using Global Mapper by defining a grid and tracing profiles parallel to flow, from which dune height, wavelength and leeside angles were measured manually (Fig. 1.3).

I.4.2 Bed material sampling and processing

All surveyed riverbeds were sampled using a 10 kg Van-Veen grab sampler. Sampling was made in October 2015, three months after the MBES survey. Sampling was coupled with GPS data recorded when the sampler reached the bottom with the rope as straight downward as possible. Grain size analyses were performed with a Malvern Mastersizer 2000 for fractions smaller than 1 mm. Samples with larger fractions went through sieves and had their grain size estimated based on normalized weight proportion in relation to the whole sample. Note that Malvern gives results based on volume, while sieves results are based on weight. Bed material samples are basically composed by quartz (2,65 g/cm³) and feldspar (2,55-2,76 g/cm²), so it was assumed an average quartz density for all samples and weight was transformed to volume.

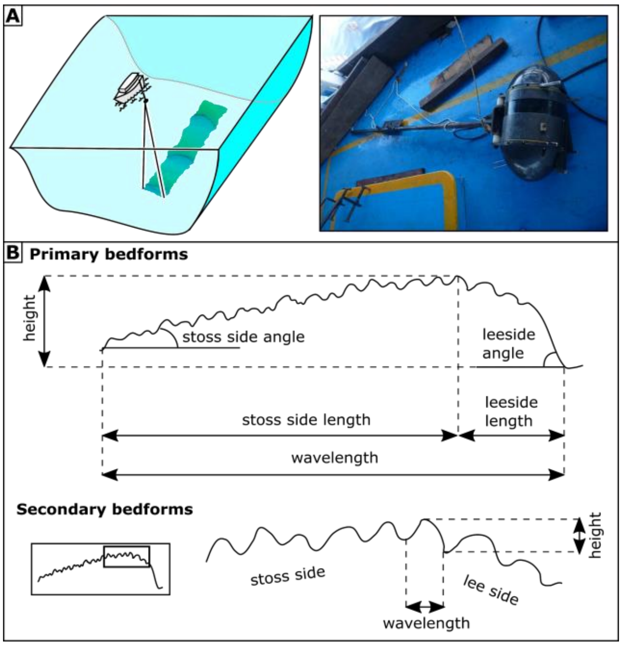

Fig. 1.3 – (a) Illustration of a MBES survey and MBES sonar head. (b) Illustration of extraction of information for (a) primary and (b) secondary bedforms from profiles parallel to the flow.

I.4.3 Collection of river data: drainage basin area, discharge, climate, channel slope, sinuosity, channel count index, width, stream power and specific stream power

Drainage basin area, water discharge and climate: Drainage basin areas and water discharge data were mostly obtained from the Global Runoff Data Centre (GRDC) website, as well as from international and governmental websites, which include the water agencies of: the Arctic region (R-ArcticNET), Africa (SIEREM; Boyer et al., 2006), Afghanistan (CAWater-info), Argentina (SNHI), Brazil (ANA), Canada (HYDAT), Russia and former Soviet Union (NCAR-UCAR) and United States (USGS). In some cases, published works were used to access discharge data. Climate was accessed by plotting the studied reaches in a simplified Koppen-Geiger climate map (Fig. 1.2) (Peel et al., 2007).

Channel slope, sinuosity, channel count index and width: River morphometric parameters were collected at bankfull or near-bankfull stage with measurement tools from Google Earth software (Fig. 1.4) with the aid of Planet Team website when a desired image did not display high-resolution in Google Earth. Channel slope was measured by tracing paths of tens of kms following the course of rivers in Google Earth and accessing their elevation profile. Sinuosity was measured as the length along the river divided by the straight-line distance along the river valley. Channel count index was computed according to Egozi and Ashmore (2008) recommendation of tracing 10 cross sections in a given reach of the river and calculate the average number of channels of all cross sections. Channel width was measured by calculating the average value of the sum of widths of the same cross sections used to measure channel count index.

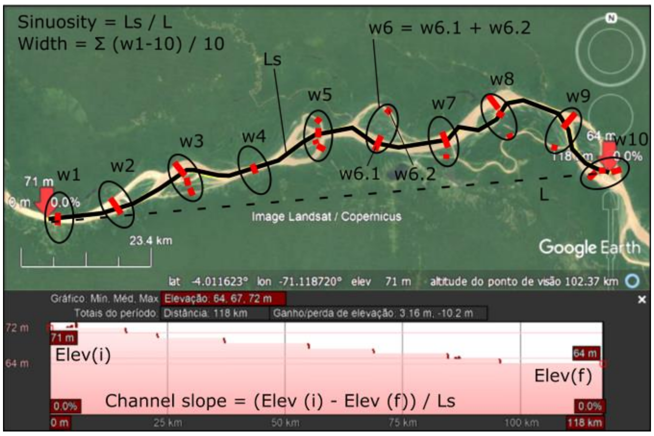

Fig. 1.4 – Google Earth software was used to compute sinuosity (black lines), width and channel count index (red lines) and channel slope (longitudinal profile).

Stream power and specific stream power: Stream power (Ω; W/m) and specific stream power (ω; W/m²) were calculated considering the interannual average of the maximum monthly discharge (Qmax, m³/s) and slope (S; cm/km x 10^{-5}) according to equations 1 and 2:

$$\text{Stream power } (\Omega) = \rho \ . \ g \ . \ Qmax \ . \ S \qquad (1)$$

$$\text{Specific stream power } (\omega) = \Omega \ / \ b \qquad (2)$$

Where *ρ* is the density of water (1000 kg/m³); *g* the acceleration of gravity (9.8 m/s²) and *b* is the width (m).

Error propagation: In order to assess the sensibility of our models to uncertainties in slope and average maximum annual discharge, two sigma errors in both measures were estimated and propagated to stream power estimates. The uncertainty in average maximum annual discharge was considered to be to the time series standard deviation of maximum annual discharge. The uncertainty in slope was estimated based on the standard error in the mean of at least 25 adjacent water surface elevation measures at each end of the considered profile. Such measurements were performed in 23 high latitude rivers, in which the elevation error in the surface elevation model is maximized, leading to a propagated error in the difference of elevation of the two profiles ends of 0.3545+-0.0454 m, with a value of 0.49 m for a confidence interval of 99.7% being the one applied to all stations. For each station, the error in altitude was propagated to the slope error considering the specific values of elevation and distance. The slope error was then combined with the maximum annual discharge uncertainty to assess the error in the stream power estimate, which is lower than 26 and 49% for 95 and 99% of the measurements, respectively.

I.4.4 Collection of floodplain data: proportion of depositional elements and paleocurrent variance

The most common depositional elements preserved in floodplains are point bars, braid bars, counterpoint bars and channelfills or abandoned channels. Proportion of depositional elements in floodplains was measured in reaches where high-resolution imagery with well-exposed bedforms was available. Measurements were done using Google Earth software (Fig. 1.5).

Paleocurrent variances (circular variances *sensu* Fisher, 1993) for more than 350 rivers worldwide were computed by tracing on satellite imagery the inferred paleoflow directions in barforms preserved in the floodplain at the channel belt scale. That resulted in paleoflow maps (Fig. 1.5) and datasets which were and processed with a Python code written for that purpose that: i) interpolates the distance between two collected points; ii) computes flow direction according to the sequence of the traced points, and iii) calculates the variance of flow direction, i.e. paleocurrent variance. This approach is similar to that adopted by Le Roux (1992) for a very small dateset (only four rivers) to determine channel sinuosity from preserved bar-forms and abandoned channel reaches preserved on the alluvial plains.

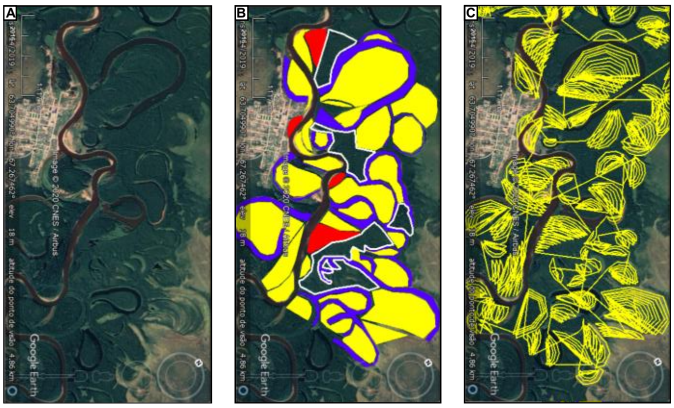

Fig. 1.5 – (a) Alluvial river with high-resolution satellite imagery and well-exposed bedforms. (b) Quantification of bedforms computed in Google Earth software. (c) Paleoflow map traced on Google Earth software.

REFERENCES

Alabyan, A.M., and Chalov, R.S., 1998. Types of river channel patterns and their natural controls: Earth Surface Processes and Landforms, v. 23, p. 467-474, doi:10.1002/(SICI)1096-9837(199805)23:5<467::AID-ESP861>3.0.CO;2-T

ANA (Agência Nacional De Águas). HidroWeb: sistemas de informações hidrológicas. Available at: http://hidroweb.ana.gov.br/HidroWeb

Bataille, C.P., Ridgway, K.D., Colliver, L., and Xiao-Ming Liu, 2018. Early Paleogene fluvial regime shift in response to global warming: A subtropical record from the Tornillo Basin, west Texas, USA: Geological Society of America Bulletin, v. 131, p. 299–317, doi:10.1130/B31872.1

Best, J.L., Ashworth, P.J., Sarker, M.H., and Roden, J.E., 2007. The Brahmaputra-Jamuna River, Bangladesh. In: Large Rivers: Geomorphology and Management (Ed. A. Gupta), p. 395–433. Wiley InterScience, Sussex, doi:10.1002/9780470723722.ch19

Boyer, J.F., Dieulin, C., Rouche. N., Cres, A., Servat, E., Paturel, J.E., and Mahé, G., 2006. SIEREM an environmental information system for water resources. 5th World FRIEND Conference, La Havana - Cuba, November 2006 in Climate Variability and Change – Hydrological Impacts, IAHS Publication, v. 308, p. 19-25.

Bridge, J.S., 1985. Paleochannel patterns inferred from alluvial deposits: a critical evaluation: Journal of Sedimentary Petrology, v. 55, p. 579-589, doi: 10.1306/212F8738-2B24-11D7-8648000102C1865D

Bridge, J.S., 2003. Rivers and Floodplains. Blackwell, Oxford, 491 pp.

Carling, P.A., Jansen, J., and Meshkova, L., 2014. Multichannel rivers: their definition and classification: Earth Surface Processes and Landforms, v. 39, p. 26-37, doi:10.1002/esp.3419

CAWater-info (Central Asia Water information). Available at: http://www.cawater-info.net/index_e.htm

Colombera, L., and Mountney, N.P., 2019. The lithofacies organization of fluvial channel deposits: A meta-analysis of modern rivers: Sedimentary Geology, v. 383, p. 16-40, doi:10.1016/j.sedgeo.2019.01.011

Davidson, S.K., Leleu, S., North, C.P., 2011. From river to rock record: The preservation of fluvial sediments and their subsequent interpretation. In S.K. Davidson, S. Leleu, C.P. North (Eds.), From river to rock record: The Preservation of Fluvial Sediments and Their subsequent Interpretation. SEPM Special Publication, v. 97, p. 3-5, doi: 10.2110/sepmsp.097

Eaton, B.C., Millar, R.G., and Davidson, S., 2010, Channel patterns: braided, anabranching, and single thread. Geomorphology, v. 120, p. 353-364, doi:10.1016/j.geomorph.2010.04.010

Egozi, R., and Ashmore, P., 2008. Defining and measuring braiding intensity: Earth Surface Processes and Landforms, v. 33, p. 2121-2138, doi:10.1002/esp.1658.

Ethridge, F.G. 2011. Interpretation of ancient fluvial channel deposits: review and recommendations. In: Davidson, S.K., Leleu, S., North, C.P. (eds) From River to Rock Record: The Preservation of Fluvial Sediments and their Subsequent Interpretation. SEPM Special Publication, v. 97, p. 9-35, doi:10.2110/sepmsp.097.009

Ferguson, R.I., 1977. Meander sinuosity and direction variance. GSA Bulletin, v. 88, p. 212-214, doi: 10.1130/0016-7606(1977)88<212:MSADV>2.0.CO;2

Fielding, C.R., 2007. Sedimentology and stratigraphy of Large River Deposits: recognition in the ancient record, and distinction from ‘Incised Valley Fills’. In: Large Rivers: Geomorphology and Management (Ed. A. Gupta), p. 97-113. Wiley InterScience, Sussex, doi:10.1002/9780470723722.ch7

Fielding, C.R., Ashworth, P.J., Best, J.L., Prokocki, E.W., and Sambrook Smith, G.H., 2012. Tributary, distributary and other fluvial patterns: What really represents the norm in the continental rock record? Sedimentary Geology, v. 261-262, p. 15-32, doi:10.1016/j.sedgeo.2012.03.004

Fisher, N. (1993). Statistical Analysis of Circular Data. Cambridge: Cambridge University Press. doi:10.1017/CBO9780511564345

GRDC (Global Runoff Data Center), 56068 Koblenz, Germany. Available at: https://www.bafg.de/GRDC/EN/Home/homepage_node.html

Gupta, A., 2007. Large Rivers; Geomorphology and Management. John Wiley and Sons, Chichester, UK, 689 pp, doi:10.1002/9780470723722

Holeman, J.N., 1968. The sediment yield of major rivers of the world. *Water Resources Research*, v. 4, p. 737-747, doi:10.1029/WR004i004p00737

Hovius, N., 1998. Controls of sediments supply by large rivers. In: Relative Role of Eustasy Climate and Tectonism in Continental Rocks (Eds K. Shanley and P. McCabe). SEPM Special Publication, v. 59, p. 3-16, doi:10.2110/pec.98.59.0002

HYDAT (National Water Data Archive). Available at: https://www.canada.ca/en/environment-climate-change/services/water-overview/quantity/monitoring/survey/data-products-services/national-archive-hydat.html

Latrubesse, E.M., 2008. Patterns of anabranching channels: the ultimate end-member adjustment of mega rivers. Geomorphology, v. 101, p. 130-145, doi:10.1016/j.geomorph.2008.05.035

Latrubesse, E.M., Stevaux, J.C. and Sinha, R., 2005. Tropical rivers. Geomorphology, v. 70, p. 187-206, doi:10.1016/j.geomorph.2005.02.005

Le Roux, J.P., 1992. Determining the channel sinuosity of ancient fluvial systems from paleocurrent data: Journal of Sedimentary Petrology, v. 62, p. 283–291, doi: 10.1306/D42678E3-2B26-11D7-8648000102C1865D

Leclair, S.F., 2011. Interpreting fluvial hydromorphology from the rock record: large-river peak flows leave no clear signature. In: From River to Rock Record: the Preservation of Fluvial Sediments and Their Subsequent Interpretation (Eds S.K. Davidson, S. Leleu and C.P. North), SEPM Special Publication, v. 97, p. 113-123, doi:10.2110/sepmsp.097.113

Leclair, S.F., and Bridge, J.S., 2001. Quantitative interpretation of sedimentary structures formed by river dunes. Journal of Sedimentary Research, v. 71, p. 713-716, doi: 10.1306/2DC40962-0E47-11D7-8643000102C1865D

Leopold, L.B., and Wolman, M.G., 1957, River channel patterns: Braided, meandering, and straight: U.S. Geological Survey Professional Paper 282-B, p. 39–84, doi:10.3133/pp282B

Miall, A.D., 2006. How do we identify big rivers? And how big is big? Sedimentary Geology, v. 186, p. 39-50, doi:10.1016/j.sedgeo.2005.10.001

Miall, A.D. 2014. Fluvial Depositional Systems, Springer, New York, 316 pp., doi:10.1007/978-3-319-00666-6

Milliman, J.D., and Meade, R.H., 1983. World-wide delivery of sediment to the oceans. Journal of Geology, v. 91, p. 1-21, doi:10.2307/30060512

Milliman, J., & Farnsworth, K., 2011. River Discharge to the Coastal Ocean: A Global Synthesis. Cambridge: Cambridge University Press. 384 pp., doi:10.1017/CBO9780511781247

NCAR (National Center for Atmospheric Research). Russian River Flow Data by Bodo, Enhanced. Research Data Archive at the National Center for Atmospheric Research, Computational and Information Systems Laboratory. Available at: https://rda.ucar.edu/datasets/ds553.2/

Parsons, D.R., Best, J.L., Orfeo, O., Hardy, R.J., Kostaschuk, R., and Lane, S.N., 2005. Morphology and flow fields of three-dimensional dunes, Rio Parana, Argentina: results from simultaneous multibeam echo sounding and acoustic Doppler current profiling. Journal of Geophysical Research, v. 110, F04S03 1–F04S03 9, doi:10.1029/2004JF000231

Peel, M.C., Finlayson, B.L., Mcmahon, T.A., 2007. Updated world map of the Köppen-Geiger climate classification: Hydrology and Earth System Sciences Discussions, European Geosciences Union, v. 11, p. 1633-1644, doi:10.5194/hess-11-1633-2007

Planet Team, 2020. Planet application program interface: in space for life on earth. San Francisco, CA. https://api.planet.com.

Potter, P.E., 1978, Significance and origin of big rivers: Journal of Geology, v. 86, p. 13-33, doi:10.1086/649653

Potter, P.E., and Hamblin, W.K., 2006. Big rivers worldwide: Part 1 origins: Provo, Utah, Brigham Young University. Geological Studies, 48, 78 pp., doi:10.1086/649653

Reesink, A.J.H., Ashworth, P.H., Sambrook Smith, G.H., Best, J.L., Parsons, D.R., Amsler, M.L., Hardy, R.J., Lane, S.N., Nicholas, A.P., Orfeo, O., Sandbach, S.D., Simpson, C.J., and Szupiany, R.N., 2014. Scales and causes of heterogeneity in bars in a large multichannel river: Rio Parana, Argentina. Sedimentology, v. 61, p. 1055-1085, doi:10.1111/sed.12092

Schumm, S.A., 1981. Evolution and response of the fluvial system sedimentologic implications: SEPM Special Publication, v. 31, p. 19-29, doi:10.2110/pec.81.31.0019

Selley, R.C., 1968. A classification of paleocurrent models: Journal of Geology, v. 76, p. 99–110, doi:10.1086/627311

Slaymaker, O., 2020. Large Arctic rivers. In: Introducing Large Rivers (eds A. Gupta, O. Slaymaker and W.J. Junk). doi:10.1002/9781118451410.ch11

SNHI (Sistema Nacional de Informacion Hidrica). Available at: https://snih.hidricosargentina.gob.ar/

R-ArcticNET. Available at: http://www.r-arcticnet.sr.unh.edu

USGS (United States Geological Survey). Water data available at: https://waterdata.usgs.gov/nwis/rt

II. LITERATURE REVIEW AND INTRODUCTION TO THE FOLLOWING CHAPTERS

This chapter presents a literature review of subjects concerning the present thesis and an introduction to the papers presented in the following chapters, illustrating how they contribute to these areas of research. Topics of the literature review include channel pattern classifications, channel pattern interpretation in fluvial deposits and large rivers modern examples and recognition in the rock record.

II.1 CHANNEL PATTERN CLASSIFICATIONS

Although classifications of channel patterns may date back to as far as the end of the 19th century (e.g. Lokhtin, 1897, *apud* Alabyan & Chalov 1998), the oldest most known publication is the work of Leopold & Wolman (1957), which is commonly appointed as the pioneer of this research branch. Over time, several distinct classifications arose, along with a great amount of misunderstanding between research groups due to non-homogeneous terminology. Leopold & Wolman (1957) classified channel patterns in meandering, braided and straight, although the latter was considered rare, where the meandering are sinuous single channeled rivers and the braided are multichanneled rivers. The authors related the identified channel patterns occurrence in nature to combinations of channel slope and bankfull discharge, in a way that meandering rivers occur at lower slopes and bankfull discharges (i.e. lesser stream power), and braided channels occur as either or both of them increase (i.e. greater stream power). Such association of channel pattern, channel slope and bankfull discharge would become a standard in the research concerning channel pattern classifications, being used by most publications that followed (e.g. Alabyan & Chalov, 1998; Church, 2002) (Fig. 2.1).

Since the work of Leopold & Wolman (1957), it soon became evident that more channel patterns occurred in nature and that other parameters may also exercise influence on channel pattern, such as sediment load, grain size and erodibility (e.g. Schumm, 1985; Ferguson, 1987; Eaton et al., 2010) (Fig. 2.2). The following contributions also acknowledged channel patterns respond to the increase in stream power by displaying a greater number of channels and a decrease in sinuosity (e.g. Schumm, 1981; Bridge, 2003); also highlighting the negative correlation between sinuosity and number of simultaneous channels (Sinha & Friend, 1994; Sinha et al., 2005) (Fig. 2.3).

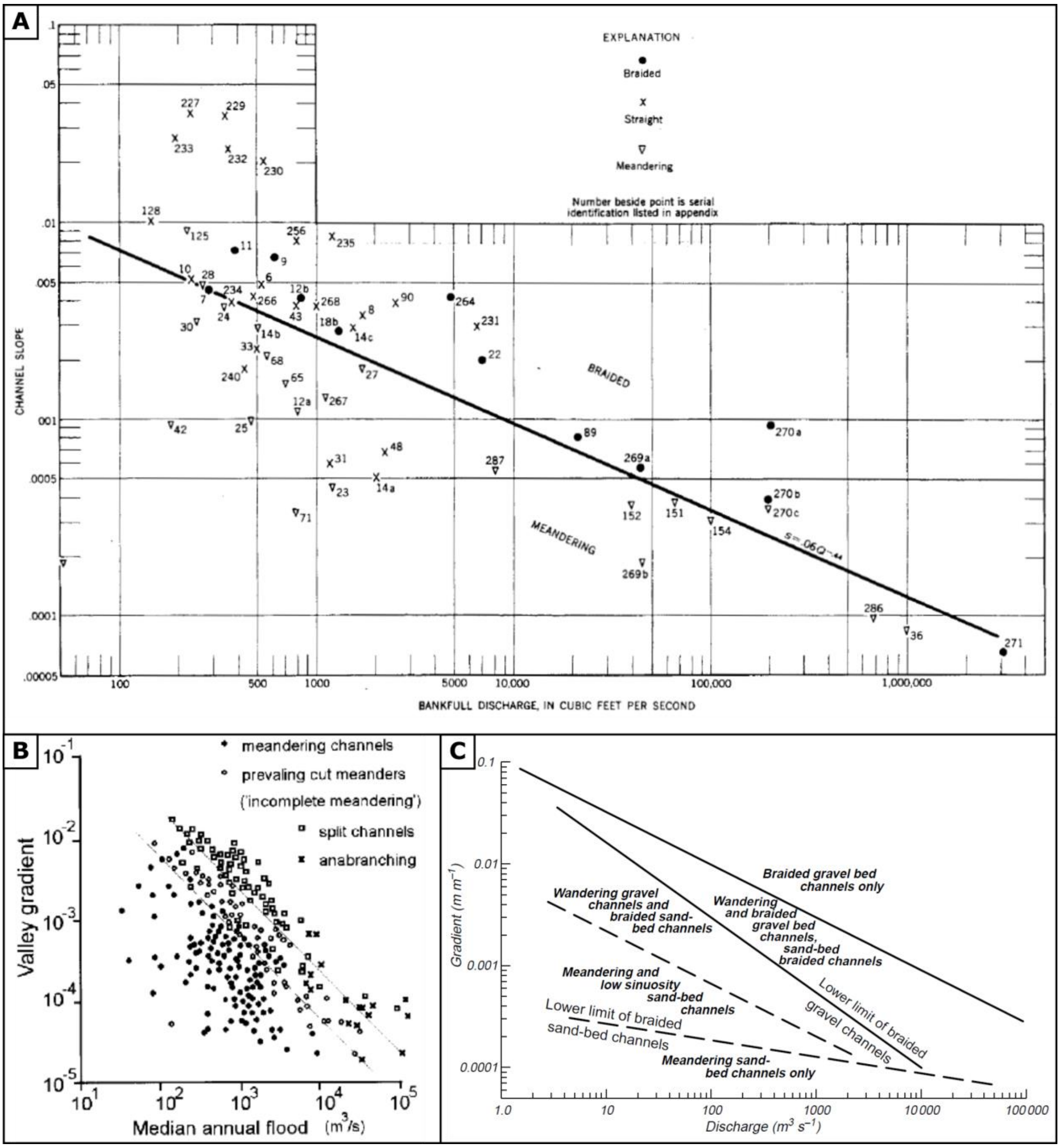

Fig. 2.1 – Discharge-slope diagrams including straight, meandering and braided channels from (a) Leopold & Wolman (1957); and including a greater variety of channel patterns, from (b) Alabyan & Chalov (1998) and (c) Church (2002).

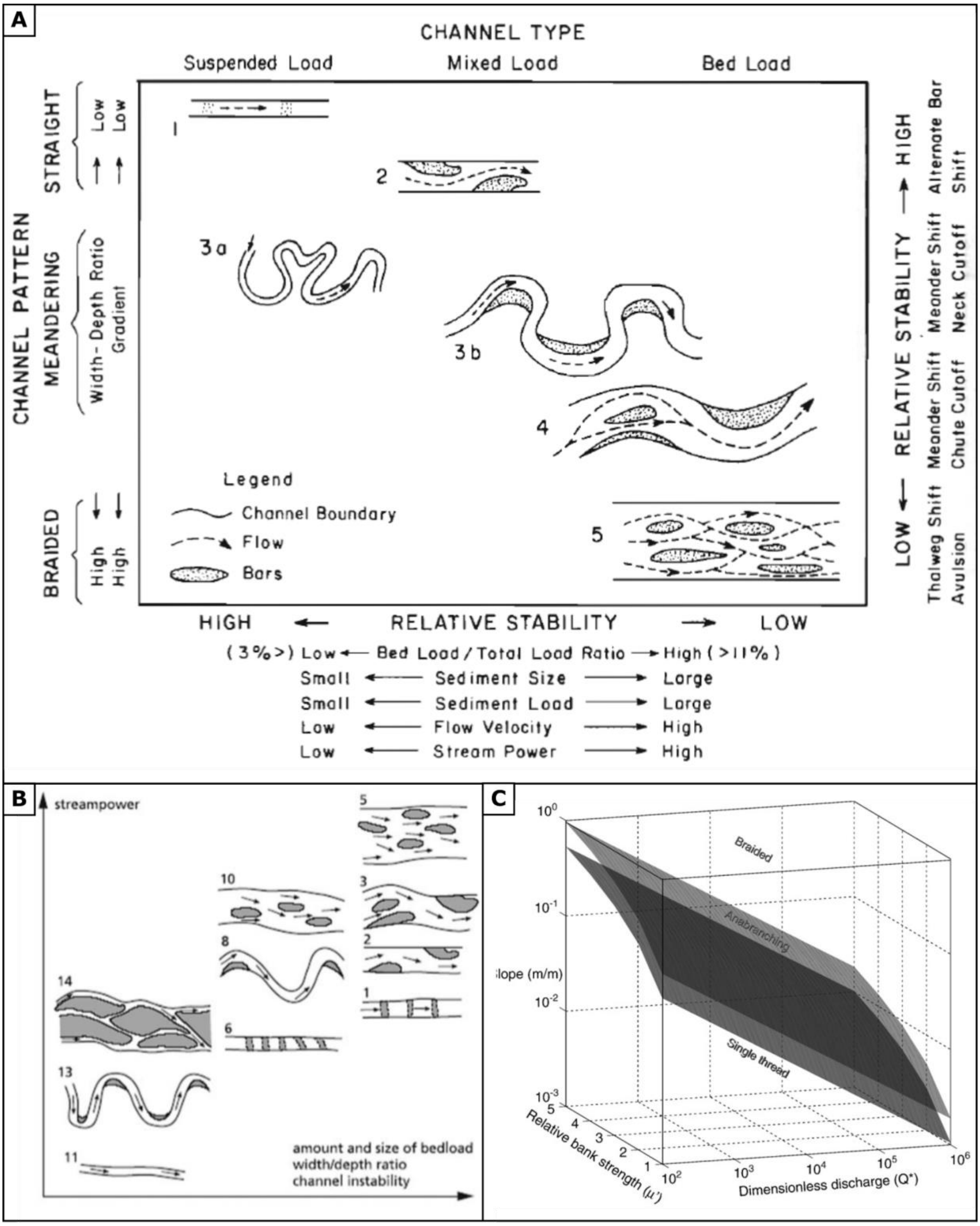

Fig. 2.2 – Diagrams for channel pattern discrimination considering not only channel slope and discharge (stream power), but also sediment load, grain size and-or bank erodibility, from (a) Schumm (1981); (b) Ferguson (1987); and (c) Eaton et al. (2010).

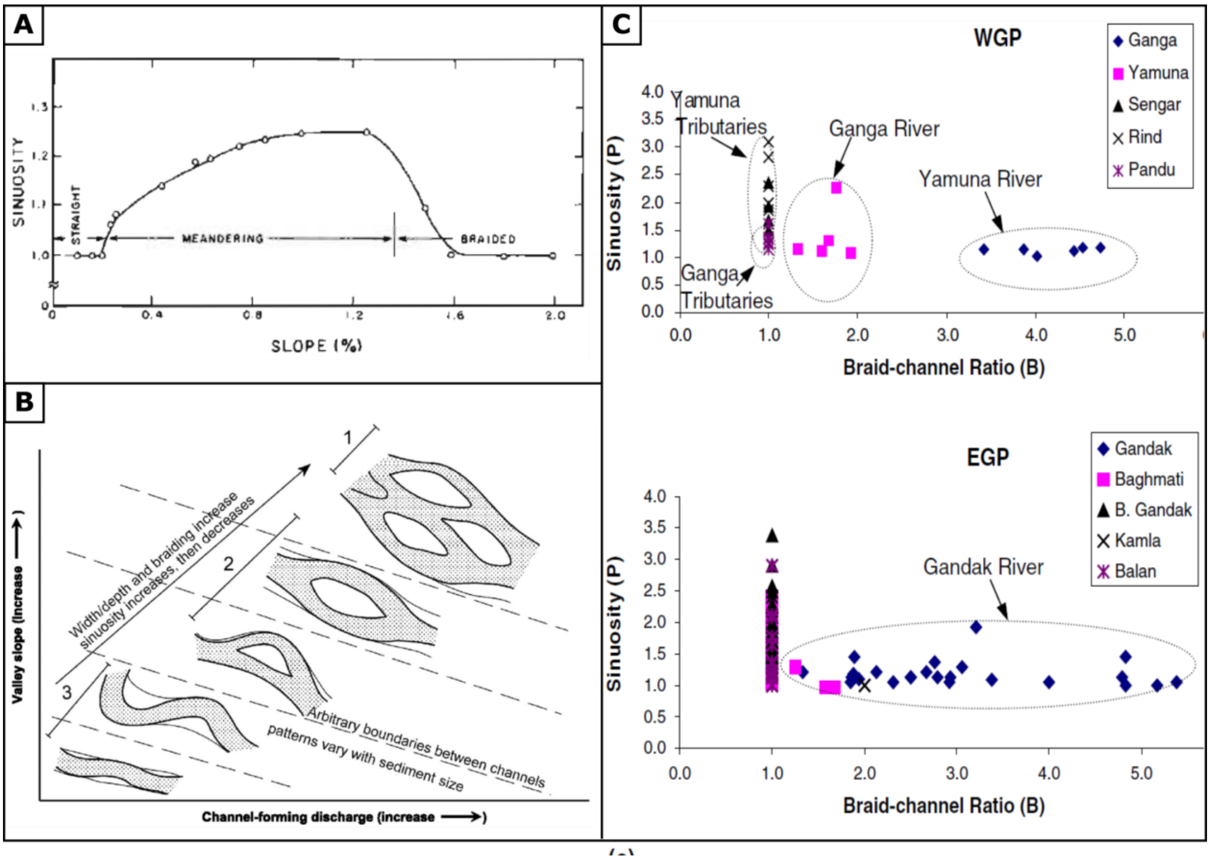

Fig. 2.3 – Controls on channel patterns measured in flume, from Schumm (1981); conceptualized by Bridge (2003); and measured in Indian rivers, from Sinha et al. (2005).

Since the work of Leopold & Wolman (1957), all publications of the following decades documented meandering and braided channels as end members of a continuum of channel patterns, but with no general agreement on nomenclature or class boundaries (a thorough review is presented in Carling et al., 2014), resulting in a great amount of misunderstanding among researchers. In fact, definitions have not been objective (Bridge, 1993), and transition between meandering and braided rivers have been classified in different ways creating conflicting terminology, such as anabranching, wandering, incomplete meandering, meanderthal, among others (e.g. Church, 1983; Nanson & Knighton, 1996; Alabyan & Chalov 1998). To date, besides the meandering and braided, the most common channel pattern classifying terms in use are anastomosing, anabranching and wandering, which are not mutually excludent.

The terms anabranching and anastomosing have assumed more than one meaning since their first appearance. The term anabranching was originated as a contraction of anastomosing branch (Carling et al., 2014), thus being a synonym of anastomosing, which in turn had been used as a synonym of braided rivers (e.g. Leopold et al., 1964). Over time, the term of anastomosing rivers evolved to be considered a system of an interconnected network of low-gradient channels whose stable banks are composed of fine-grained sediment and vegetation (e.g. Schumm, 1968; Smith & Smith, 1980; Makaske, 2001). Whereas the term anabranching rivers was reintroduced by Brice et al. (1978) and Schumm (1985) to describe rivers whose islands width is greater than three times the channel surface width at average discharge. Nanson & Knighton (1996) extended the usage of the term and their work encompassed many different types of multichannel rivers under the definition of anabranching, which they defined as "multiple channels separated by vegetated semi-permanent alluvial islands excised from existing floodplain or formed by within-channel or deltaic accretion". The authors thus considered vastly different types of river patterns as anabranching, ranging from typical anastomosing rivers to the large rivers with alternating single and multichannel reaches, such as the Solimões River (Fig. 2.4). However, since the work has been published, the term anabranching has been used as a channel pattern class (e.g. Jansen & Nanson, 2004; Latrubesse, 2008).

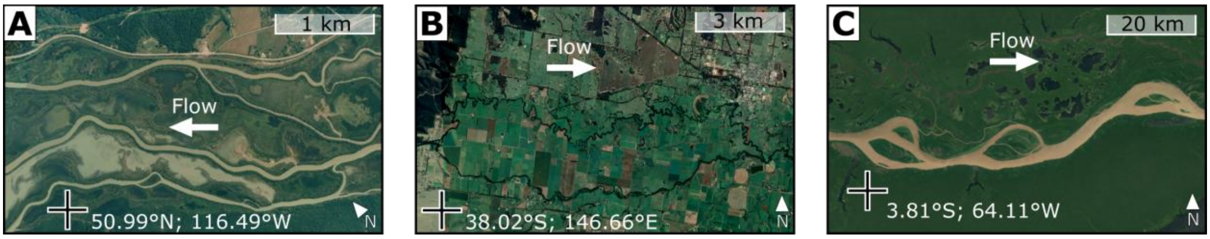

Fig. 2.4 – (a) The anastomosed Columbia River (Canada), (b) Thompson River (Australia) and (c) Solimões River (Brazil): examples of rivers termed anabranching and that strongly differ from each other in their degree of anabranching, braiding index, bar morphology and morphodynamics. Images from Google Earth in collaboration with the Province of British Columbia, CNES Airbus and Maxar Technologies.

Wandering rivers were first defined by Neill (1973) and Church (1983), but also recognized by Brice et al. (1978), as rivers with an alternation of stable single channel reaches and unstable multichannel reaches. The multichannel reaches have their flow separated by often vegetated mid-channel compound bars (also named islands or medial bars) and display low-order braiding. These mid-channel bars are commonly reshaped every year, and yet may be persistent over decades (Wooldridge & Hickin, 2005). Wandering rivers have been commonly recognized in smaller gravel bed rivers located in mountain valleys (e.g. Desloges & Church, 1987; Roberts et al., 1997; Wooldridge & Hickin, 2005) and in large rivers such as in reaches of the Fraser River, in Canada (e.g. Roberts & Morningstar, 1989; Rice & Church, 2010; Ham & Church, 2012), and of the Yellow River, in China (e.g. Jin et al., 2000; Xie et al., 2018). Although these large rivers do not typically display a large proportion of gravel load, they have a strong morphological affinity with wandering rivers: reaches of single channel that branch into two or more channels, separated by often-vegetated, large mid-channel compound bars, and farther rejoin into a single channel (Fig. 2.5).

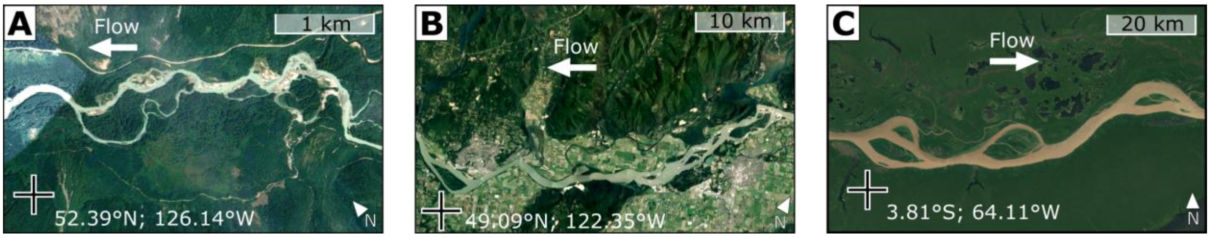

Fig. 2.5 – (a) Bella Coola River (Canada); (b) Fraser River (Canada); (c) Solimões River (Brazil): examples of rivers that fit in the definition of wandering channel pattern. Images from Google Earth in collaboration with Maxar Technologies and CNES Airbus.

As much as definitions of meandering and braided channels seem very straightforward, where meandering rivers are sinuous single channels and braided rivers display multiple parallel simultaneous channels with mid-channel bars that may be overtopped at bankfull, both terms are not free from potential misunderstanding, given their current usage. For instance, the Brahmaputra River, commonly considered a typical braided channel (e.g. Coleman, 1969; Bristow, 1993; Best et al., 2003), has also been considered as anabranching (e.g. Latrubesse, 2008), whereas the Mississippi River, whose lower course mostly presents a great proportion of reaches whose channels are separated by mid-channel bars (Fig. 2.6), has been termed meandering (e.g. Fisk, 1944; Saucier, 1994; Latrubesse, 2008). Whilst the case of the Mississippi River, here used as an example of many similar cases (e.g. Içá and Madeira rivers, among others), may be considered a matter of defining the classification boundary, in terms of channel count index, between mostly single-channel rivers and what must be considered as a separate class, the case of braided rivers may be more challenging. The main difference between braided and anabranching rivers is often attributed to flow division in braided rivers being stage-dependent. That criteria considers braided bars as unstable, ephemeral and overtopped by flow at less than bankfull, whereas anabranching channels would maintain their flow divided at bankfull stage and their often vegetated mid-channel bars would be stable for decades to several millennia (Nanson, 2013). Apart from the fact that even rivers classified as anabranching (e.g. Solimões River) may display whole km-scale vegetated mid-channel bars forming and disappearing in a few years, an additional problem is that stability though time of a barform cannot be accessed in the rock record. The stage-dependent flow division criteria could also present some issues. It is reasonable to presume that such assumptions of flow division were estimated from airborn or satellite imagery, which might be misleading, since vegetated mid-channel bars that seem exposed may be actually overtopped and flooded, with only the tree tops standing above the flow level (Fig. 2.7). The major differences between braided channels and other channel patterns with multiple simultaneous channels, named wandering or anabranching, among others terms, are the greater number of simultaneous and parallel thalwegs of the former compared to the latter, and that the first presents simultaneous thalwegs along the whole or most of their extension, whereas in the second, simultaneous thalwegs are alternated with single channel reaches.

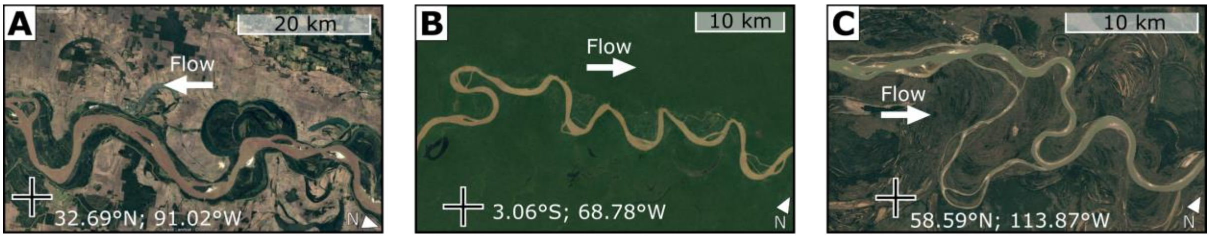

Fig. 2.6 – (a) Mississippi River (United States); Içá River (Brazil); Peace River (Canada): meandering rivers with a high proportion of mid-channel bars. (d) Brahmaputra River; (e) Amazonas River. Images from Google Earth in collaboration with Landsat and Maxar Technologies.

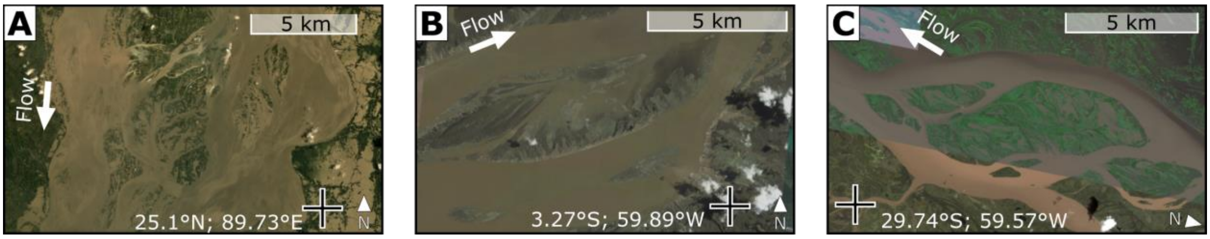

Fig. 2.7 – Details of the (a) Braahmaputra River (Bangladesh); (b) Solimões River (Brazil); (c) Paraná River (Argentina). Images indicate that vegetated mid-channel bars could be flooded at bankfull in all cases, leaving only their treetops emerged. Images from Planet Team (2020) and Google Earth in collaboration with Maxar Technologies.

Summary and open questions:

To date, channel pattern classification has become a complicated concept. Nomenclature has not been homogeneous among research groups and every time a term is used it must be followed by a thorough explanation of its meaning to avoid misunderstandings. Moreover, some of the criteria considered to separate channel patterns may have no direct application to the study of fluvial deposits in the rock record. Research regarding channel pattern classification should address these issues and consider quantitative parameters that may assist interpretation of the rock record.

II.2 INTERPRETATION OF CHANNEL PATTERNS IN FLUVIAL DEPOSITS:

So far, the recognition of channel patterns in the rock record has been mostly based on facies models of meandering and braided channels, whereas other channel types have been overlooked. Important contributions were made over the past decades, yet the established criteria for recognition of channel patterns have not been considered overall effective (e.g. Davidson et al., 2011; Ethridge, 2011; Colombera & Mountney, 2019). Investigations concerned especially the recognition of meandering and braided rivers and included attempts to relate them to distinct vertical facies sequences (e.g. Collinson, 1978; Miall, 1996), to the predominance of a certain type of accretionary element (e.g. Allen, 1993, Bristow, 1987; Miall, 1985; Miall, 1991) or to abundance of sedimentary facies (e.g. Colombera & Mountney, 2019).

Previous works acknowledged the decrease of sinuosity and increase of simultaneous channels following the increase of stream power (e.g. Schumm & Khan, 1971; Begin & Schumm, 1984; Bridge, 2003), as well as the negative correlation between sinuosity and braiding index (Friend & Sinha, 1993; Sinha et al., 2005). Therefore, signatures of sinuosity preserved in floodplains may bring light to channel pattern recognition in the rock record (Bridge, 1985). Paleocurrent analysis has been recognized as a significant tool to interpret sedimentary successions since the 19th century (Sorby, 1859), being popularized a century later after Potter & Pettijohn (1963). Initially used to map marine deposits (e.g. Ruedemann, 1897), it was later employed in the study of continental sandstones (Fig. 2.8) (e.g. Rubey & Bass, 1925) and eventually integrated with statistical and facies analysis (e.g. Brinkmann, 1933; Potter & Olsen, 1958).

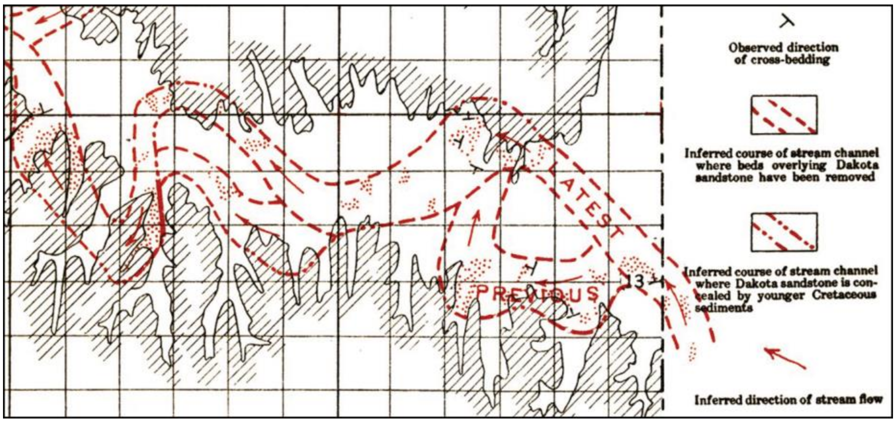

Fig. 2.8 – A cutout depicting part of what could be the first geological map displaying plots of paleocurrent directions, modified from the work of Rubey & Bass (1925), whose investigation of the Cretaceous Dakota sandstone concluded it was formed by a meandering river flowing westward, due to the high dispersion of cross-beddings directions associated with a predominance of measurements to the West.

Spatial variation of paleocurrent in fluvial deposits has been used to interpret paleo-channel patterns of fluvial deposits at the scales of bar deposit and of the channel belt, where the latter has been more successful than the former. Coleman (1969) and Shukla (1999) conducted similar investigations concerning the usage of spatial paleocurrent variance at the bar scale by comparing the cross-strata sets directions in point bars and a braid bars, respectively from meandering and braided reaches of the Brahmaputra and Ganga and rivers. Although restricted to the a few bar tops of both types of bars in a context of an overall braided river, both works show that point bars, characteristic of meandering channels, and braid bars, characteristic of braided channels, display similar dispersion, with a slightly greater dispersions in point bars, therefore hardly distinguishable in ancient fluvial deposits (Fig. 2.9).

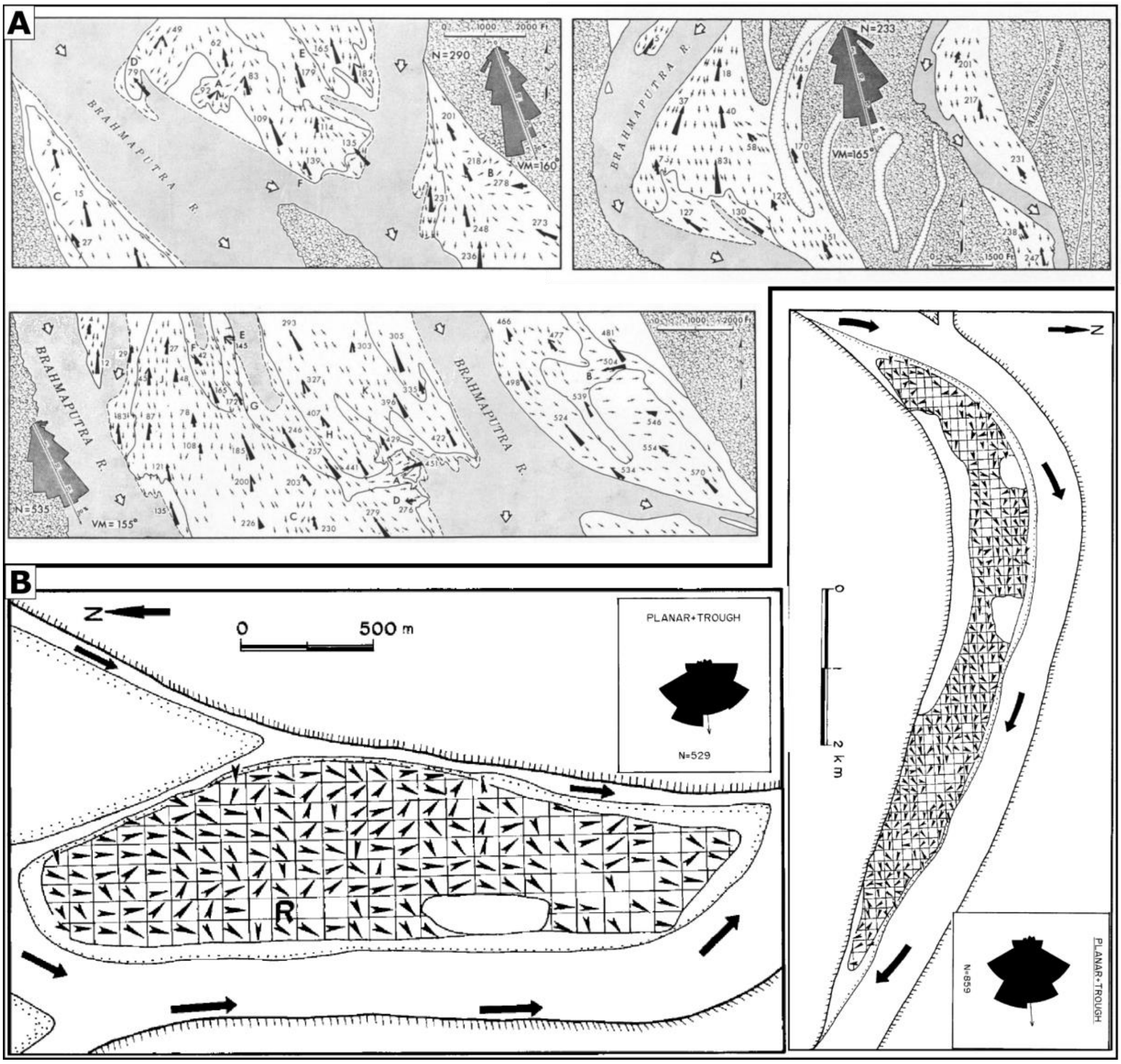

Fig. 2.9 – Comparison of paleocurrent direction from the bar tops of point bars and braid bars. Modified from (a) Coleman (1969) and (b) Shukla (1999).

At the channel belt scale, higher paleocurrent variances were attributed to ancient meandering rivers whereas lower variances were attributed to ancient braided rivers (Fig. 2.10) (e.g. Selley, 1965; Le Roux, 1992; Willis, 1993, Miall, 1994; Khan et al., 1997; Zaleha, 1997; Bataille et al., 2019). Such relation has been considered by geologists at least since the beginning of the 20th century (Fig. 2.8) (Rubey & Bass, 1925). Investigation of modern rivers to quantify the variation of paleocurrent directions and relate it to sinuosity have led to similar results. Ferguson (1977) quantified the variation of directions of several active meandering rivers and related variations to their respective sinuosity. Le Roux (1992) used sedimentary deposits preserved in the floodplain, such as scroll bars and ox-bow lakes, of a few active rivers to establish a relationship between channel sinuosity and variation of flow directions (Fig. 2.10).

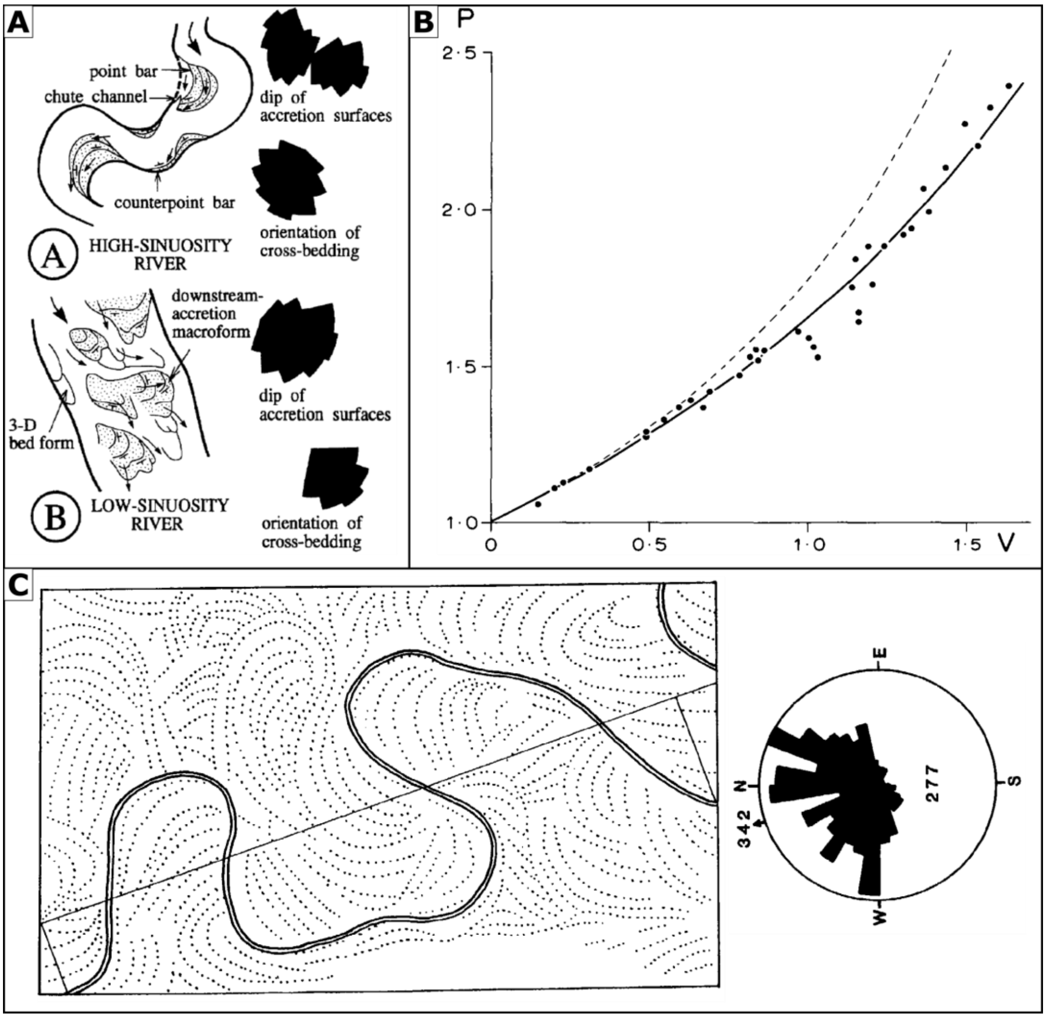

Fig. 2.10 – (a) Hypothetical examples of paleocurrent distribution in high-sinuosity meandering rivers and low-sinuosity braided rivers. From Miall (1994). (b) Relationship between sinuosity (P) and variance of flow direction (V). From Ferguson (1977). (c) Variance of directions inferred from scroll bars preserved in floodplain. Modified from Le Roux (1992).

Summary and open questions:

To date, previous approaches to interpret channel patterns in the rock record have not been considered to be effective. Moreover, research on channel patterns differentiation of fluvial deposits has vastly focused on meandering and braided channels, and criteria to recognize different channel patterns are still lacking. Paleocurrent variance has been mostly used qualitatively to distinguish meandering and braided rivers and a quantitative approach including more channel patterns could assist identification of channel patterns in the rock record.

II.3 LARGE RIVERS: MODERN EXAMPLES AND FACIES MODELS

A growing number of publications has documented large rivers characterized by reaches displaying more than one simultaneous channel, being classified either as anabranching or wandering (e.g. Jin et al., 2000; Jansen & Nanson, 2004; Latrubesse, 2008; Rice & Church, 2010; Ham & Church, 2012; Reesink et al., 2014; Xie et al., 2018). Apart from the nomenclature, many large rivers seem to share a common morphological pattern, exhibiting reaches of a single channel that branches into two or more channels, separated by often-vegetated large mid-channel compound bars, which rejoin into a single channel farther downstream (Fig. 2.11).

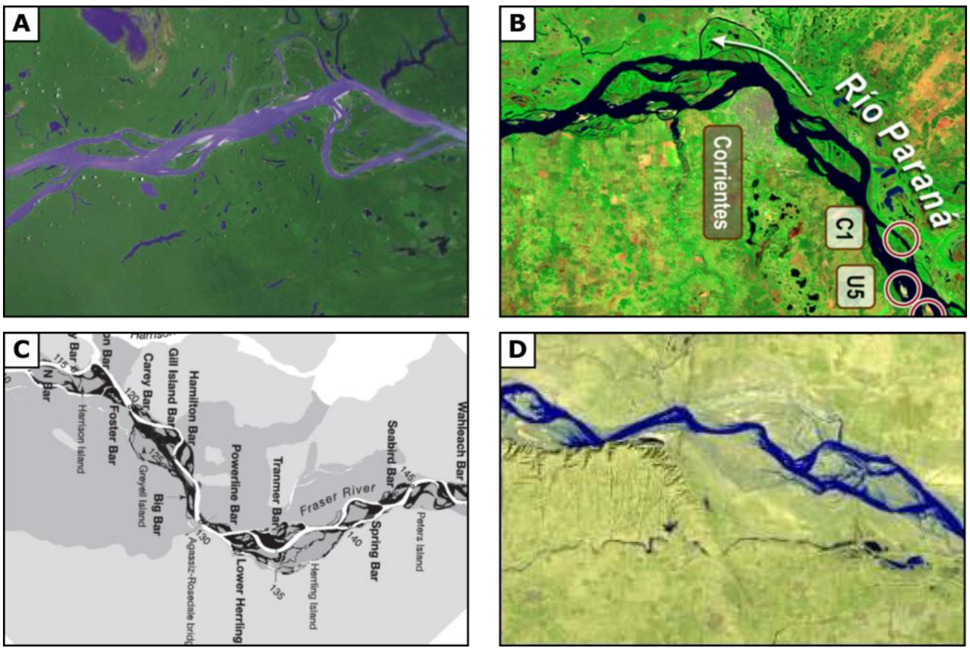

Fig. 2.11 – Many large rivers exhibit a common morphological channel pattern. (a) Solimões River. Modified from Latrubesse (2008). (b) Paraná River. Modified from Reesink et al. (2014). (c) Fraser River. Modified from Rice & Church (2010). (d) Yellow River. Modified from Xie et al. (2018).

In order to build facies models of large rivers, it is mandatory to fully study their bedforms. While bar tops have been successfully studied for decades in regard of both plan view dynamics and internal sedimentary structure (e.g. Coleman, 1969; Bristow, 1987; Best et al., 2003; Sambrook Smith et al., 2009; Rozo et al., 2012; Reesink et al., 2014), riverbeds that comprise the majority of a channel deposit and are more likely of being preserved have been relatively neglected due to intrinsic survey difficulties. Until recently, the investigation of permanently submerged bedforms relied exclusively on two-dimensional bathymetric profiles and plan-view side-scan radar images, thus limiting the understanding of bedform tridimensional morphology and kinematics. Since the beginning of the last decade, Multibeam Echo-Sounder (MBES) surveys have revolutionized current ability to achieve high-resolution quantification of the three-dimensional subsurface bathymetry (Parsons et al., 2005). Previous investigations of large river riverbeds are listed below.

Amazonas River: Available datasets include a MBES survey, longitudinal bathymetric profiles, dune and grain-size data (Fig. 2.12). The MBES image reveals a sandy riverbed with occurrence of exposed bedrock and sediment starved areas. The sandy areas display very large barchanoid compound dunes of more than 10 m with superimposed dunes on both stoss and leeside in the thalweg, and oblique compound dunes with superimposed dunes on stoss and leeside in bank attached bars (Almeida et al., 2016). Longitudinal bathymetric profiles at different locations confirm the recurrent occurrence of lined-up very large-scale dunes of up to 10 m or more (Sioli, 1965; Nordin et al., 1979; Mertes & Meade, 1985; Strasser, 2002) and show that dune height tends to increase with water depth (Mertes & Meade, 1985; Strasser, 2002) and such trend is evidenced by dune data as well (Strasser, 2002). In the many longitudinal profiles, average dune height varied from 1,5 to 7,2 m, while maximum values ranged from 3,5 to 12,7 m. while average wavelength varied from 29 to 314 m, and maximum values ranged from 62 to 453 m. Sediment samples from the Solimões-Amazonas riverbed are composed predominantly by sand, with no significant grain size variation along its course (Nordin et al, 1980; Mertes & Meade, 1985; Strasser, 2008). In contrast, greater grain size variations are described to occur in cross sections, where deeper areas tend to present coarser grain sizes than shallower areas (Mertes & Meade, 1985; Strasser, 2008; Almeida et al., 2016).

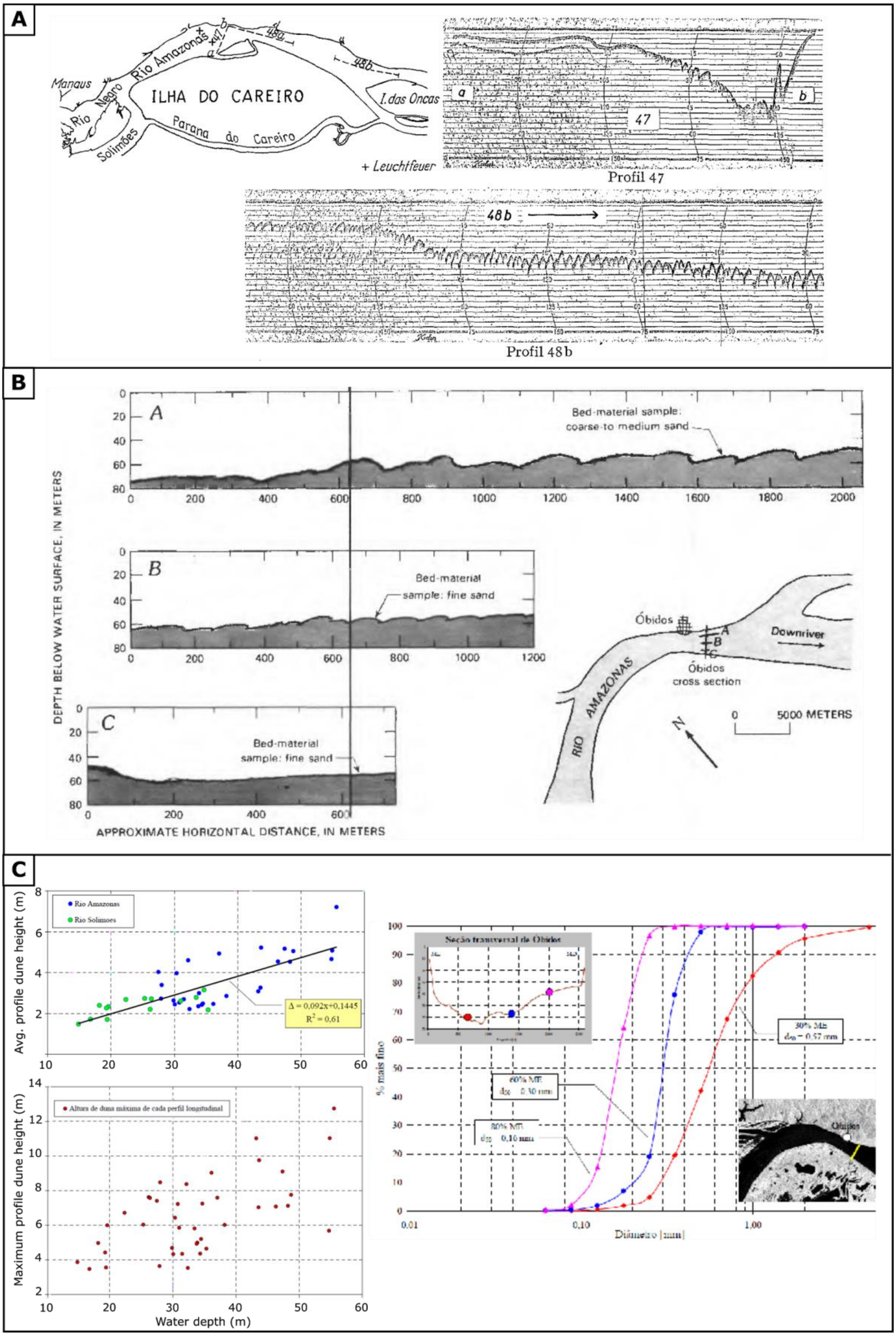

Fig. 2.12 (Next page) – Previous studies in the Amazonas River depict very large dunes scaling in height with increasing water depth in longitudinal bathymetric profiles. Modified from: (a) Sioli (1965); (b) Mertes & Meade (1985); (c) Strasser (2008).

Brahmaputra (Jamuna) River: Available data include longitudinal and transversal bathymetric sections, plan view maps of the riverbed, and dune data, such as height, wavelength and lee angles (Fig. 2.13). The riverbed is dominated by dunes, which occupy from 41 to 100% of the main channels area and occur in thalwegs and superimposed on bars (Roden, 1998; Ashworth et al., 2000). Dunes present straight and sinuous crests and superimposed dunes (Best et al., 2007), implying the occurrence of 2D and 3D compound dunes. Maximum dune height encountered is 6 m and most dunes are around 2 m high (Julien, 1992; Ashworth et al., 2000; Best et al., 2007). Leeside angles range from 2° to 58°, interestingly beyond angle of repose, with a mean angle of 8,6° (Best et al., 2007). Dunes display an increasing range of heights as water depth increases, with a good correlation of maximum dune height and water depth. Generally, dunes are never higher than 37% of the water column (Best et al., 2007). During high stage, dunes are larger compared to low stages, and may increase about 6 to 8 times from one period to another, displaying longer wavelengths and steeper lee angles (Roden, 1998).

Yangtze River: Available data include images of the riverbed in plan view and seismic profiles from a survey of the lowest 1200 km of its course (Fig. 2.14). This course was divided into three regions: the steeper upstream region, which displays a narrow single channel; the downstream lowland, which displays a channel that repeatedly bifurcates and rejoins; and the stretch near the river mouth, which displaying an increasingly wide channel (Wang et al., 2007; Chen et al., 2012). The narrow single channel presents two types of dunes: the steeper area (A) features small (1-3 m of height, 10-60 m of wavelength) and mostly large (height >3 m, wavelength >60m) simple dunes, that can reach up to 4 - 8 m high, with a barchanoid shape (Wang et al, 2007); whereas where the slope decreases (B) the riverbed presents smaller bedforms (<1 m high; <10 m long), named by the authors mega-ripples, with parallel crest (Wang et al, 2007; Chen et al, 2012). In the region where the channel bifurcates and rejoins (C and D) the riverbed is characterized by large sinuous and barchanoid compound dunes (height >3 m, wavelength > 60 m), that can reach up to 8 m of height and 300 m of wavelength, and most of the dunes is higher than 2 m, with 50% ranging from 4 to 8 m, and superimposed dunes can be 2,5 m high and 20 m long (Wang et al, 2007). The wide channel near the river mouth presents small bedforms, with height between 1,6 and 2,4 m and wavelengths of 140 to 155 m (Wang et al, 2007; Chen et al, 2012).

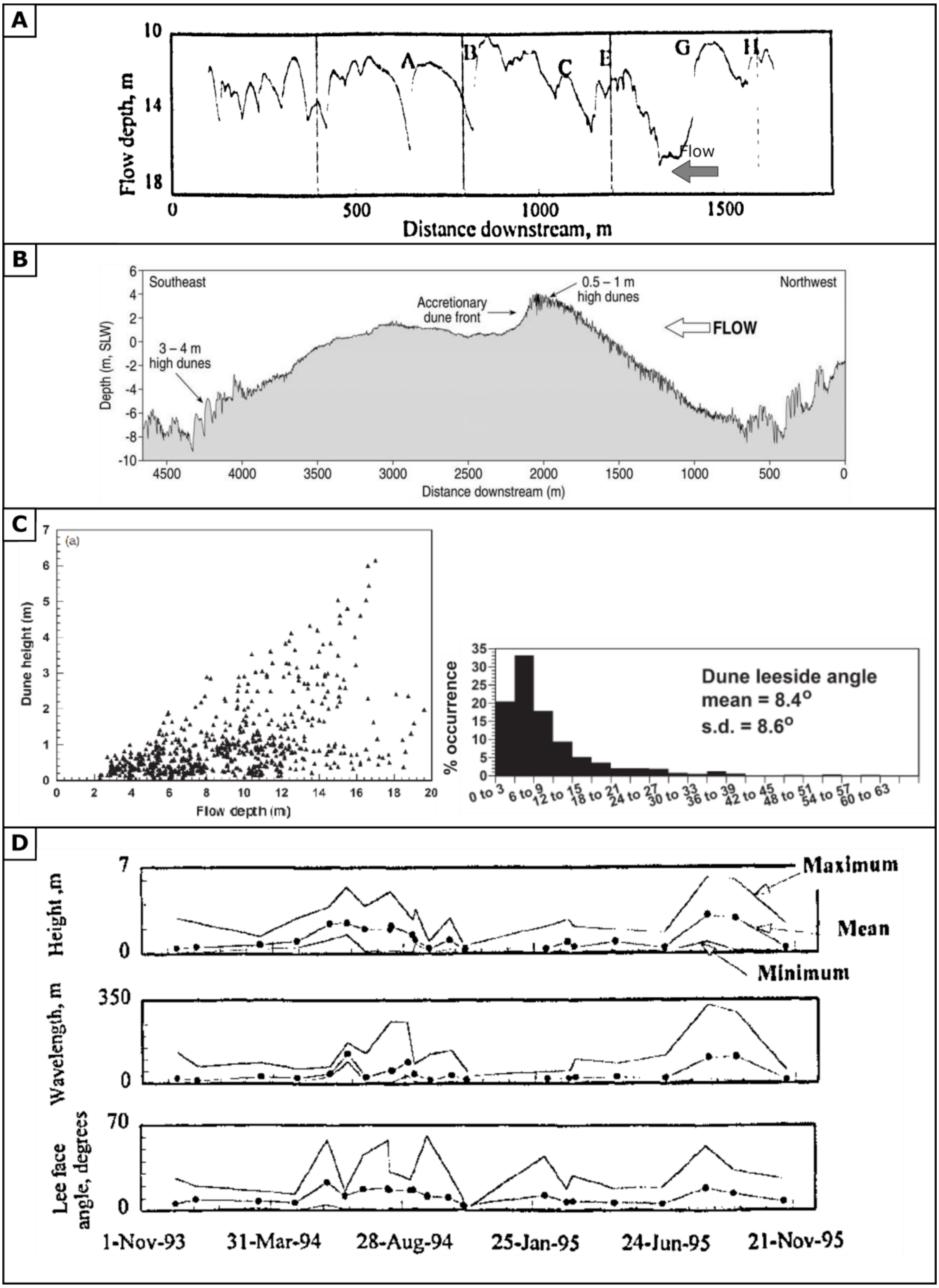

Fig. 2.13 – Longitudinal bathymetric profiles of (a) the tahlweg (modified from Roden, 1998) and (b) mid-channel bar (modified from Ashworth et al., 2000). (c) Dune height and leeside angle data (modified from Best et al., 2007). (d) Different bedform morphologies at different river stages (modified from Roden, 1998).

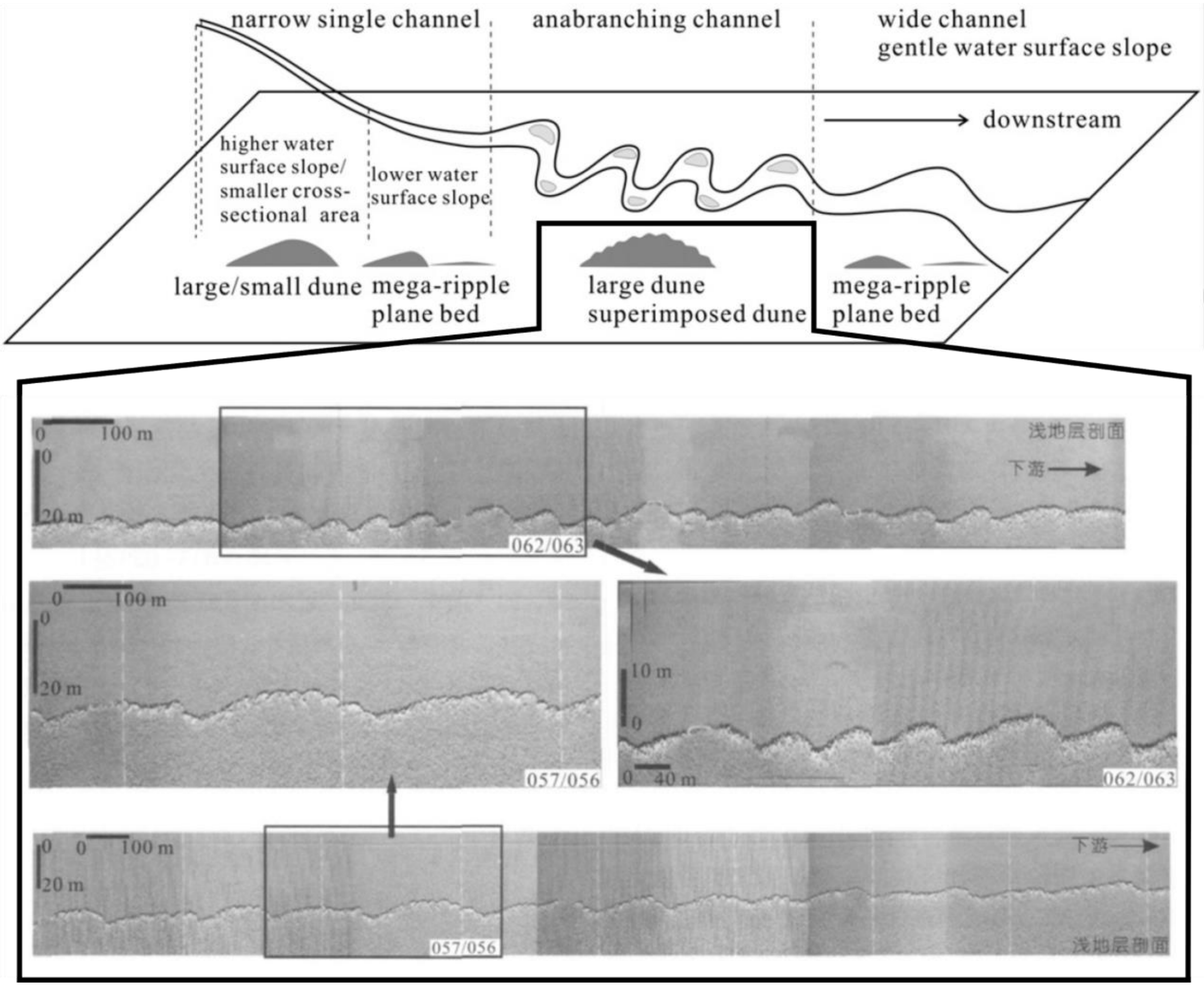

Fig. 2.14 – Simplified schematic map depicting the course of the Yangtze River, with details of the bedforms in the regions where the river is characterized by bifurcating and rejoining channels: large compound dunes, with low leeside angle and superimposed dunes on the stoss and leesides. Modified from Wang et al, (2007) and Chen et al, (2012).

Paraná River: Available dataset comprises riverbed MBES images from the area of the confluence with the Paraguay River and longitudinal sections from the Upper Paraná River (Fig. 2.15). MBES images reveal an overall sandy riverbed predominantly composed of dunes, with large-scale mid-channel bars and some bedrock pinnacles. Unorganized sinuous compound barchanoid dunes of different widths occur in the thalweg, in the region around the confluence (Lane et al., 2008). The mid-channel bar displays sinuous dunes superimposed on the bar head becoming oblique as they are disposed on the bar sides (Sambrook Smith et al., 2009). The shallower area attached to the western margin displays smaller sinuous crested compound dunes (Parsons et al., 2005). Dunes reach up to 3-4 m in height and about 200 m in wavelength in the thalweg, whereas the shallower area attached to the channel margin presents smaller dune heights. Longitudinal profiles from the Upper Parana (Santos & Stevaux, 2000; Martins et al, 2009) show that in dry and rising stages dunes are about 2-3 m high and 100-200 m long whereas during high stage dunes increase in size, and so do the superimposed dunes, with the common occurrence of 5 m high compound dunes. Although there are no riverbed images available in their work, Santos & Stevaux (2000) described dunes as barchans. Dunes have been described to reach 7,5 m and 450 m of wavelength in the Paraná River, with no information about the site of occurrence (Julien, 1992).

Mississippi River: Available dataset comprises MBES images, longitudinal sections and dune morphology data (Fig. 2.16). MBES images reveal a sandy riverbed covered by large sinuous-crested and barchanoid compound dunes nearly as wide as the channel, oblique compound dunes attached at the margins, or small dunes (Abraham & Pratt, 2002; Nittrouer, 2008; Knox & Latrubesse, 2016). Compound dunes with superimposed dunes on their stoss and leesides are a common feature (Harbor, 1998; Leclair, 2011). Dune height greatly varies with water depth (Harbor, 1998) as maximum dune height scales with increasing water depth, reaching up to 10 m at greater depths but also displaying smaller dunes at great depths (Harbor, 1998; Nittrouer, 2008; Knox & Latrubesse, 2016). Dunes also seem to present a stage-dependent morphology, with small dunes occurring during dry season turning into large dunes during flood season (Hider, 1883; Nittrouer, 2008; Leclair, 2011).

Most fluvial facies models have been proposed for meandering and braided rivers, being mostly based on surveys in small rivers (e.g. Cant & Walker, 1978; Mail, 1977) or exposed bar tops of large rivers (e.g. Coleman, 1969; Bristow, 1987; Best et al., 2003). However, more channel patterns occur in nature, and large rivers tend to display neither meandering nor braided patterns (e.g. Latrubesse, 2008). Large rivers, which are likely to leave deposits in the sedimentary record (e.g. Fielding et al., 2012) with their wide floodplains of tens of kilometers (e.g. Lewin et al., 2016), and detailed facies models of large rivers have not been proposed yet. Identification of large rivers in fluvial deposits has mostly relied on the association of cross-strata set thickness with the original dune size (Leclair & Bridge, 2001), which in turn is believed to scale with water depth (Yalin, 1964; Allen, 1984; Ashley, 1990; Paola & Borgman, 1991). In fact, large-scale cross-strata sets have been considered a criterion to identify large rivers (e.g. Miall, 2006; Fielding, 2007) and have been associated to large rivers for decades (Fig. 2.17) (e.g. Conaghan & Jones, 1977; McCabe, 1977; Mossop & Flach, 1983; Fielding et al., 2012).

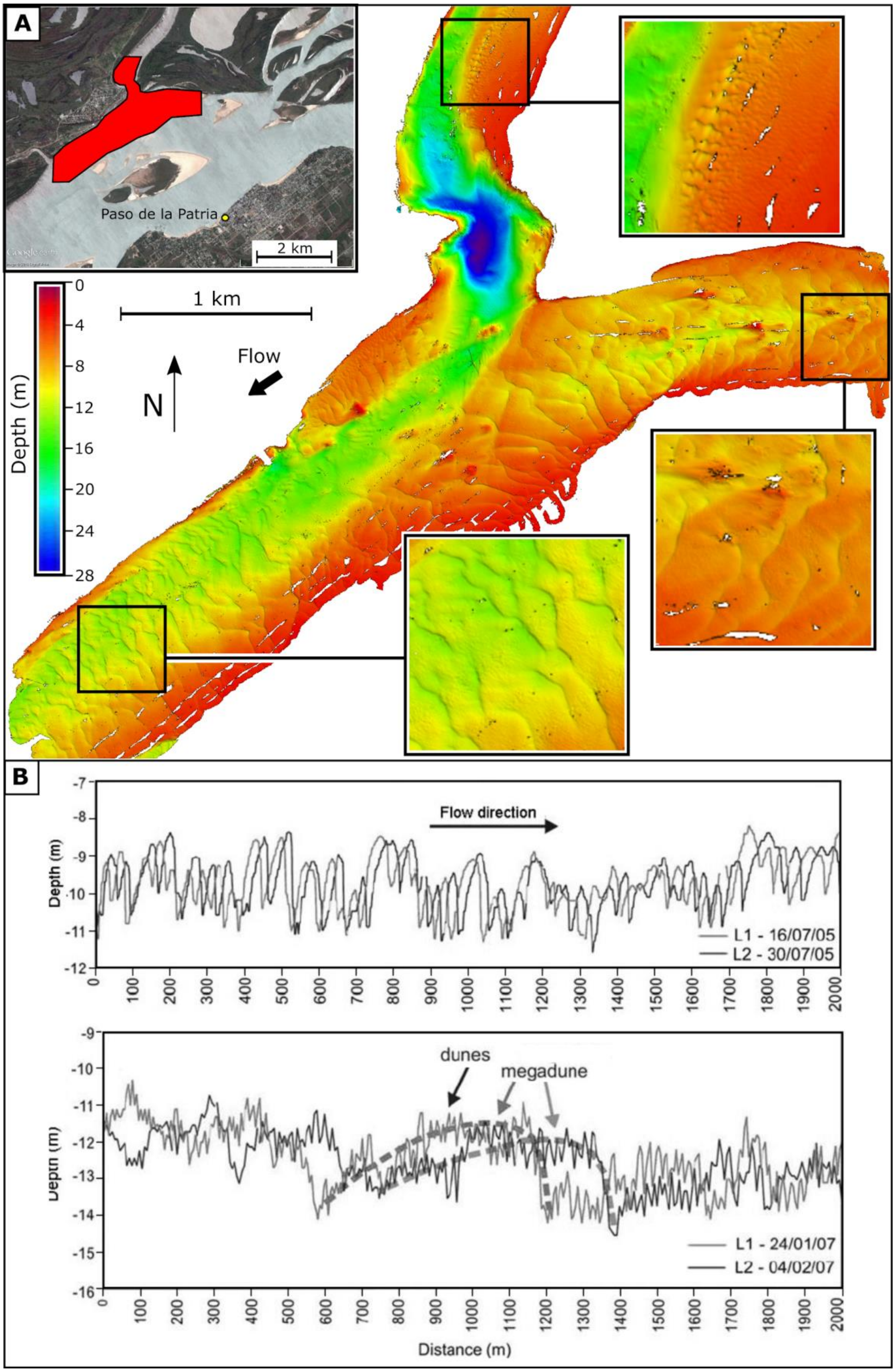

Fig. 2.15 – (a) MBES image of the Paraná River at the confluence with the Paraguay River. From Lane et al. (2008). (b) Longitudinal profiles depict growing dunes during flood stage and the occurrence of large compound dunes, with low leeside angle and superimposed dunes on the stoss and leesides. From Martins et al. (2009).

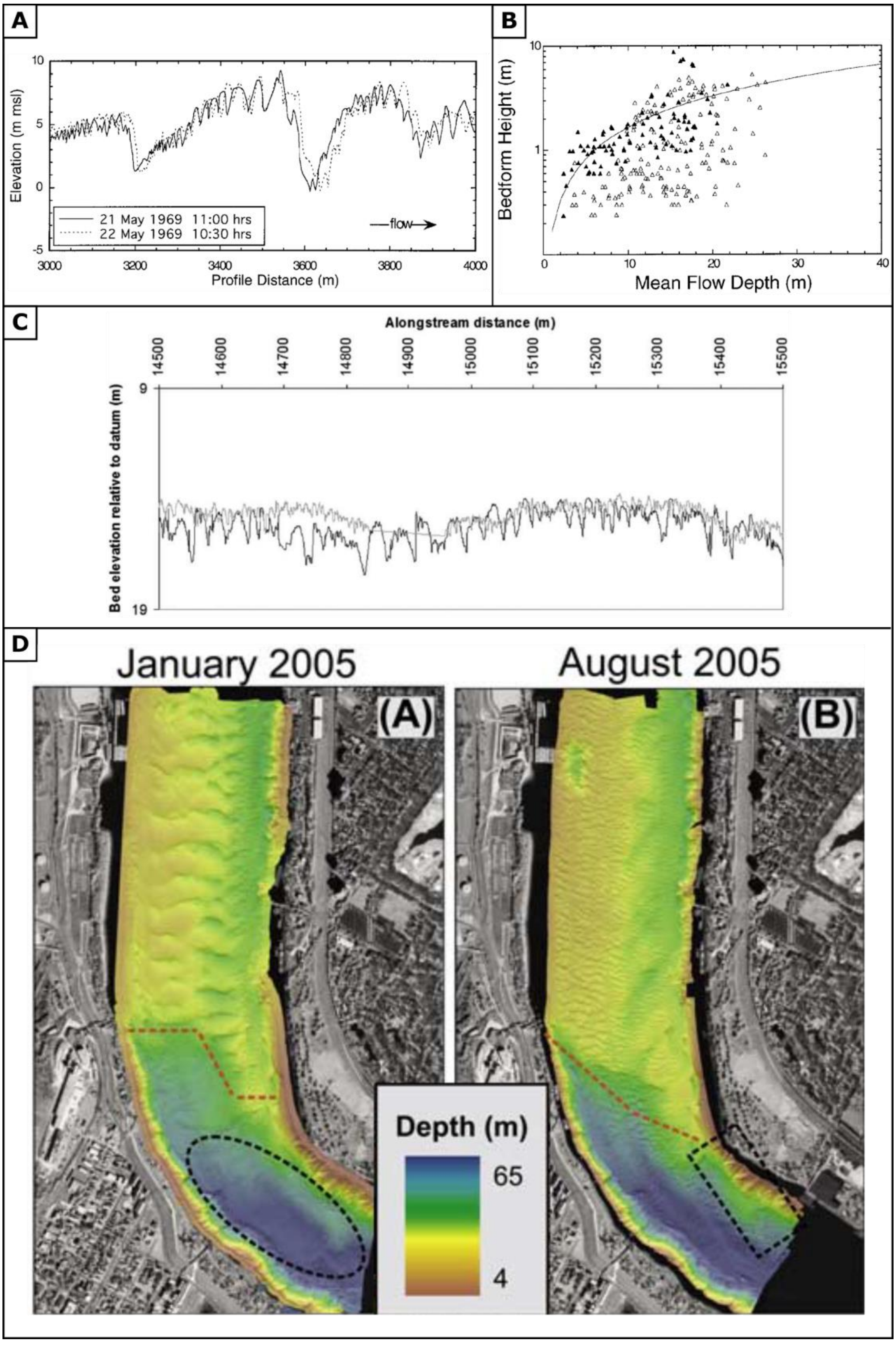

Fig. 2.16 – (a) Longitudinal bathymetric profile indicating the occurrence of large compound dunes with low leeside angles and superimposed dunes on the stoss and leeside. From Harbor (1998). (b) The relationship between dune height data and flow depth. From Harbor (1998). (c) Longitudinal bathymetric profile indicating occurrence of small dunes at greater water depths. Modified from Leclair (2011). (d) MBES image depict growing dunes during flood stage. From Nittrouer (2008).

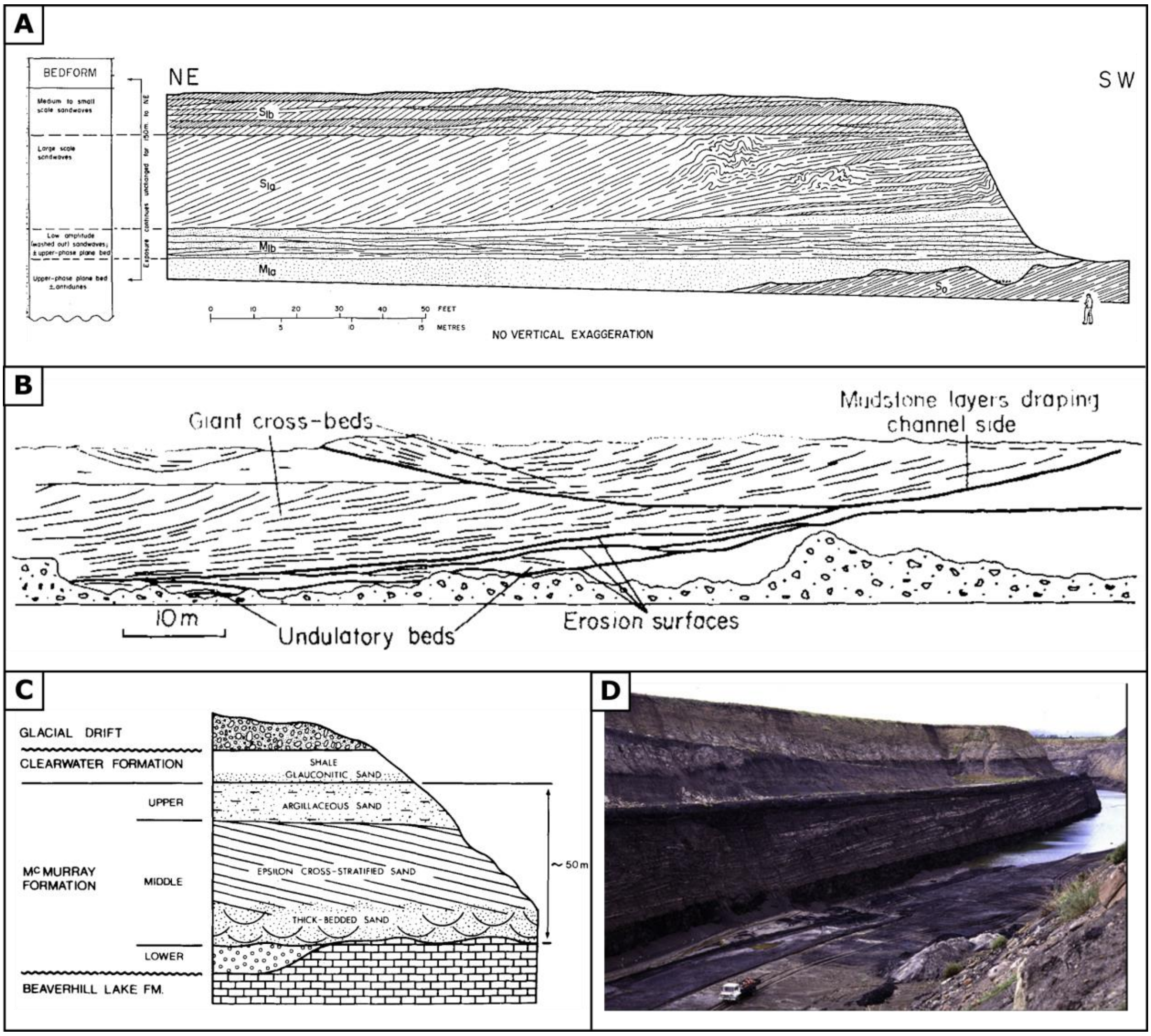

Fig. 2.17 – Examples of interpreted fluvial deposits of large rivers: (a) Triassic Hawkesbury Formation (Australia). Modified from Conaghan & Jones (1977). (b) Carboniferous Millstone Grit Group (England). From McCabe (1977). (c) Cretaceous McMurray Formation (Canada). Modified from Mossop & Flach (1983). (d) Upper Permian Rangal Coal Measures (Australia). Modified from Fielding et al. (2012).

Summary and open questions:

Modern large rivers present similarities regarding channel patterns and bedforms. Their channel pattern exhibits alternating reaches of single and multiple channels, with large mid-channel bars, and their riverbeds commonly display large compound dunes with superimposed dunes on both stoss and leesides, but also present small dunes at great depths. The occurrence of numerous small dunes in deep riverbeds challenges the long-held assumption that dune size is proportional to water depth and question arises as to whether large cross-strata sets must be present within an ancient fluvial deposit for the interpretation of a large channel to be made. Existing facies models, mostly developed for meandering and braided channels, are not able to assist in the recognition of large river deposits, especially because large rivers present different channel patterns. Future research of large rivers should conduct MBES surveys and quantify river dune data at different stages and facies models concerning large rivers should investigate and account for channel patterns different than meandering or braided.

II.4 INTRODUCTION TO THE FOLLOWING CHAPTERS

The results of this work are organized in three manuscripts that address different aspects of large fluvial systems and contribute to the open questions mentioned above. The first manuscript (Chapter III) intends to contribute to channel pattern classification and channel pattern recognition in fluvial deposits by presenting a broad survey of alluvial rivers at a global scale to quantify channel pattern natural variability and by identifying relevant parameters for recognition in the rock record. A channel pattern classification based on quantification of sinuosity and number of channels is presented, along with a method to recognize channel patterns in the rock record based on the quantification of the paleocurrent variance at the channel belt scale.

The second manuscript (Chapter IV) intends to contribute to the recognition of large rivers in the rock record by discussing the relationship of channel scale and water depth with bedform morphology. The work presents MBES high-resolution bathymetric maps of the Solimões-Amazonas River, the quantification of dune data from their riverbeds and riverbed samples. Dune morphology, height and leeside angles, as well as grain size, are related to water depth and these relationships are used to make inferences about how to identify large river in the rock record and are compared with interpreted large river fluvial deposits. The published version of this manuscript is attached at the end of the thesis (Attachment I).

The third manuscript (Chapter V) intends to contribute to the recognition of large rivers in the rock record by presenting the facies models of a channel pattern common to many large rivers and distinct from the meandering or braided channels. Facies model is based on the integration of the Solimões-Amazonas River morphodynamics, MBES bathymetric maps of the riverbed, GPR sections of bar tops and samples from the riverbed and bar tops.

REFERENCES

Abraham, D., and Pratt, T., 2002. Quantification of bed-load transport on the upper Mississippi River using multibeam survey data and traditional methods. US Army Engineer Research and Development Center (ERDC)/Coastal and Hydraulics Laboratory (CHL), Coastal and Hydraulics Engineering Technical Note (CHETN). Available at: http://chl.wes.army.mil/library/publications/chetn.

Alabyan, A.M., and Chalov, R.S., 1998. Types of river channel patterns and their natural controls: Earth Surface Processes and Landforms, v. 23, p. 467-474, doi:10.1002/(SICI)1096-9837(199805)23:5<467::AID-ESP861>3.0.CO;2-T

Allen, J.R.L., 1984. Sedimentary Structures: Their Character and Physical Basis. Elsevier, Amsterdam, 663 pp.

Almeida, R.P., Galeazzi, C.P., Freitas, B.T., Janikian, L., Ianniruberto, M. and Marconato, A. (2016a) Large barchanoid dunes in the Amazon River and the rock record: implications for interpreting large river systems. Earth Planetary Science Letters, v. 454, p. 92-102, doi:10.1016/j.epsl.2016.08.029

Ashley, G.M., 1990. Classification of large-scale subaqueous bedforms: a new look at an old problem. Journal of Sedimentary Petrology, v. 60, p. 160–172, doi:10.2110/jsr.60.160

Ashworth, P.J., Best, J.L., Roden, J.E., Bristow, C.S., and Klaassen, G.J., 2000. Morpohological evolution and dynamics of a large, sand braid-bar, Jamuna River, Bangladesh. Sedimentology, v. 47, p. 533-555, doi:10.1046/j.1365-3091.2000.00305.x

Bataille, C.P., Ridgway, K.D., Colliver, L., and Liu, X.M., 2019. Early Paleogene fluvial regime shift in response to global warming: a subtropical record from the Tornillo Basin, west Texas, USA. GSA Bulletin, v. 131, p. 299-317, doi:10 .1130 /B31872 .1

Begin, Z.B., and Schumm, S.A., 1984. Gradational thresholds and landform singularity: significance for Quaternary studies. Quaternary Research, v. 21, p. 267-274, doi:10.1016/0033-5894(84)90067-X

Best, J.L., Ashworth, P.J., Bristow, C.S. and Roden, J.E., 2003. Three dimensional sedimentary architecture of a large, mid-channel sand braid bar, Jamuna River, Bangladesh. Journal of Sedimentary Research, v. 73, p. 516–530, doi:10.1306/010603730516

Best, J.L., Ashworth, P.J., Sarker, M.H., and Roden, J.E., 2007. The Brahmaputra-Jamuna River, Bangladesh. In: Large Rivers: Geomorphology and Management (Ed. A. Gupta), p. 395–433. Wiley InterScience, Sussex, doi:10.1002/9780470723722.ch19

Brice, J.C., Blodgett, J.C., et al., 1978. Countermeasures for hydraulic problems at bridges. Fed. Highw. Adm. Rep. FHW ARD-78-162, Vols. 1, 2, Washington, DC. 169 pp.

Bridge, J.S., 1993. The interaction between channel geometry, water flow, sediment transport and deposition in braided rivers. In: Braided Rivers (Eds J.L. Best and C.S. Bristow), Geological Society Special Publication, v. 75, p. 13-71.

Bridge, J.S., 1985. Paleochannel patterns inferred from alluvial deposits: a critical evaluation: Journal of Sedimentary Petrology, v. 55, p. 579-589, doi: 10.1306/212F8738-2B24-11D7-8648000102C1865D

Bridge, J.S., 2003. Rivers and Floodplains. Blackwell, Oxford, 491 pp.

Bristow, C.S., 1987. Brahmaputra River: channel migration and deposition. In: Recent Developments in Fluvial Sedimentology (Eds F. G. Ethridge, R.M. Flores and M.D. Harvey), SEPM Special Publication, v. 39, p. 63-74, doi:10.2110/pec.87.39.0063

Bristow, C.S., 1993. Sedimentary structures exposed in bar tops in the Brahmaputra River Bangladesh. In: Braided Rivers (Eds J.L. Best and C.S. Bristow), Geological Society London Special Publication, v. 75, p. 277-289, doi:10.1144/GSL.SP.1993.075.01.17

Cant, D.J., & Walker, R.G., 1978. Fluvial processes and facies sequences in the sandy braided South Saskatchewan River, Canada. Sedimentology, v. 25, p. 625-648, doi:10.1111/j.1365-3091.1978.tb00323.x

Carling, P.A., Jansen, J., and Meshkova, L., 2014. Multichannel rivers: their definition and classification: Earth Surface Processes and Landforms, v. 39, p. 26-37, doi:10.1002/esp.3419

Chen, J., Wang, Z., Li, M., Wei, T., and Chen, Z., 2012. Bedform characteristics during falling flood stage and morphodynamic interpretation of the middle–lower Changjiang (Yangtze) River channel, China. Geomorphology, v. 147-148, p. 18-26, doi:10.1016/j.geomorph.2011.06.042

Church, M., 1983. Pattern of instability in a wandering graveI bed channel. In Modern and Ancient Fluvial Systems, Collinson JD, Lewin J (eds), 2nd International Conference on Fluvial Sedimentology, Proceedings, IAS Special Publication, v. 6. Blackwell Scientific: Oxford; p. 169-180. doi:10.1002/9781444303773.ch13

Church, M., 2002. Geomorphic thresholds in riverine landscapes: Freshwater Biology, v. 47, p. 541-557, doi10.1046/j.1365-2427.2002.00919.x

Coleman, J.M., 1969. Brahmaputra river: Channel processes and sedimentation. Sedimentary Geology, v. 3, p. 129-239, doi:10.1016/0037-0738(69)90010-4

Collinson, J.D., 1978. Alluvial sediments. In: Sedimentary environments and facies, ed. H.G. Reading. Blackwell, Oxford, p. 15-60.

Colombera, L., and Mountney, N.P., 2019. The lithofacies organization of fluvial channel deposits: A meta-analysis of modern rivers. Sedimentary Geology, v. 383, p. 16-40.

Conaghan, P.J., and Jones, J.G., 1977. The Hawkesbury sandstone and the Brahmaputra: a depositional model for continental sheet sandstones. Journal of the Geological Society of Australia, v. 22, p. 275-283, doi:10.1080/00167617508728897

Davidson, S.K., Leleu, S., North, C.P., 2011. From river to rock record: The preservation of fluvial sediments and their subsequent interpretation. In S.K. Davidson, S. Leleu, C.P. North (Eds.), From river to rock record: The Preservation of Fluvial Sediments and Their subsequent Interpretation. SEPM Special Publication, v. 97, p. 3-5, doi: 10.2110/sepmsp.097

Desloges, J.R., & Church, M.A., 1987. Wandering gravel-bed rivers. The Canadian Geographer, v. 33, p. 360-364, doi:10.1111/j.1541-0064.1989.tb00922.x

Eaton, B.C., Millar, R.G., and Davidson, S., 2010, Channel patterns: braided, anabranching, and single-thread: Geomorphology, v. 120, p. 353–364, doi:10.1016/j.geomorph.2010.04.010

Ethridge, F.G. 2011. Interpretation of ancient fluvial channel deposits: review and recommendations. In: Davidson, S.K., Leleu, S., North, C.P. (eds) From River to Rock Record: The Preservation of Fluvial Sediments and their Subsequent Interpretation. SEPM Special Publication, v. 97, p. 9-35, doi:10.2110/sepmsp.097.009

Ferguson, R.I., 1977. Meander sinuosity and direction variance. GSA Bulletin, v. 88, p. 212-214, doi: 10.1130/0016-7606(1977)88<212:MSADV>2.0.CO;2

Ferguson, R.I., 1987. Hydraulic and sedimentary controls of channel patterns, in Richards, K. S. (Ed.), River Channels: Environment and Processes, Blackwell, Oxford, 129-158,

Fielding, C.R., 2007. Sedimentology and stratigraphy of Large River Deposits: recognition in the ancient record, and distinction from 'Incised Valley Fills'. In: Large Rivers: Geomorphology and Management (Ed. A. Gupta), p. 97-113. Wiley InterScience, Sussex, doi:10.1002/9780470723722.ch7

Fielding, C.R., Ashworth, P.J., Best, J.L., Prokocki, E.W., and Sambrook Smith, G.H., 2012. Tributary, distributary and other fluvial patterns: What really represents the norm in the continental rock record? Sedimentary Geology, v. 261-262, p. 15-32, doi:10.1016/j.sedgeo.2012.03.004

Ham, D., & Church, M,, 2012. Morphodynamics of an extended bar complex, Fraser River, British Columbia. Earth Surface Processes and Landforms, v. 37, p. 1074-1089, doi:10.1002/esp.3231

Harbor, D.J., 1998. Dynamics of bedforms in the Lower Mississippi River. Journal of Sedimentary Research, v. 68, p. 750-762, doi:10.2110/jsr.68.750

Hider, A., 1883. Report upon observations at Lake Providence, November 1879 to November 1880: U.S. Army, Chief of Engineers, Annual Report, Part III, p. 2191-2208 (or Report of Mississippi River Commission, Senate Executive Document 32, 47th Congress, 2nd Session, p. 80–98.)

Jansen, J.D., Nanson, G.C., 2004. Anabranching and maximum flow efficiency in Magela Creek, northern Australia. Water Resources Research, v. 40, W04503, doi:10.1029/2003WR002408

Jin D S, Zhang O Y, Chen H, et al. 2000. Analysis of thalweg evolution tendency of the wandering reach in the lower Yellow River after Xiaolangdi Reservoir operation. Journal of Sediment Research, v. 6, p. 52-62. [in Chinese]

Julien, P.Y., 1992. Study of bedform geometry in large rivers. Delft Hydraulics, Colorado State University.

Khan, I.A., Bridge, J.S., Kappelman, J., Wilson, R., 1997. Evolution of Miocene fluvial environments, eastern Potwar plateau, northern Pakistan. Sedimentology, v. 44, p. 221-225, doi:10.1111/j.1365-3091.1997.tb01522.x

Knox, R.L., and Latrubesse, E.M., 2016. A geomorphic approach to the analysis of bedload and bed morphology of the Lower Mississippi River near the Old River Control Structure. Geomorphology, v. 268, p. 35-47, doi:10.1016/j.geomorph.2016.05.034

Lane, S.N., Widdison, P.E., Thomas, R.E., Ashworth, P.J., Best, J.L., Lunt, I.A., Sambrook Smith, G.H., and Simpson, C.J., 2008. Quantification of braided river channel change using archival digital image analysis. Earth Surface Processes and Landforms, v. 35, p. 971-985, doi:10.1002/esp.2015

Latrubesse, E.M., 2008. Patterns of anabranching channels: the ultimate end-member adjustment of mega rivers. Geomorphology, v. 101, p. 130-145, doi:10.1016/j.geomorph.2008.05.035

Le Roux, J.P., 1992. Determining the channel sinuosity of ancient fluvial systems from paleocurrent data: Journal of Sedimentary Petrology, v. 62, p. 283–291, doi: 10.1306/D42678E3-2B26-11D7-8648000102C1865D

Leclair, S.F., 2011. Interpreting fluvial hydromorphology from the rock record: large-river peak flows leave no clear signature. In: From River to Rock Record: the Preservation of Fluvial Sediments and Their Subsequent Interpretation (Eds S.K. Davidson, S. Leleu and C.P. North), SEPM Special Publication, v. 97, p. 113-123, doi:10.2110/sepmsp.097.113

Leclair, S.F., and Bridge, J.S., 2001. Quantitative interpretation of sedimentary structures formed by river dunes. Journal of Sedimentary Research, v. 71, p. 713-716, doi: 10.1306/2DC40962-0E47-11D7-8643000102C1865D

Leopold, L.B., and Wolman, M.G., 1957, River channel patterns: Braided, meandering, and straight: U.S. Geological Survey Professional Paper 282-B, p. 39–84, doi:10.3133/pp282B

Leopold, L.B., Wolman, M.G., and Miller, J.P., 1964. Fluvial processes in geomorphology: San Francisco, W.H. Freeman, 522 pp.

Lokhtin, V. M., 1897. About a Mechanism of River Channel, Sankt-Peterburg, 78 pp. [in Russian]

Lewin, J., Ashworth, P.J., and Strick, R.J.P., 2016. Spillage sedimentation on large river floodplains. Earth Surface Processes and Landforms, v. 42, p. 83-98, doi:10.1002/esp.3996

Makaske, B., 2001. Anastomosing rivers: a review of their classification, origin and sedimentary products: Earth-Science Reviews, v. 53, p. 149–196, doi: 10.1016/S0012-8252(00)00038-6

Martins, D.P., Bravard, J.P., and Steveaux, J.C., 2009. Dynamics of water flow and sediments in the upper Paraná River between Porto Primavera and Itaipu dams, Brazil. Latin American Journal of Sedimentology and Basin Analysis, v. 16, p. 111-118.

McCabe, P.J., 1977. Deep distributary channels and giant bedforms in the Upper Carboniferous of the Central Pennines, northern England. Sedimentology, v. 24, p. 271-290, doi:10.1111/j.1365-3091.1977.tb00257.x

Mertes, L.A.K., and Meade, R., 1985. Particle sizes of sands collected from the bed of the Amazon River and its tributaries in Brazil during 1982-84. Open-File Report 85-333, U.S. Geological Survey, Denver, Colorado.

Miall, A.D., 1977. A review of the braided-river depositional environment. Earth-Science Reviews, v. 13, p. 1-62, doi:10.1016/0012-8252(77)90055-1

Miall, A.D., 1985: Architectural-element analysis: a new method of facies analysis applied to fluvial deposits. Earth Science Reviews, v. 2, p. 261-308, doi:10.1016/0012-8252(85)90001-7

Miall, A.D., 1987: Recent developments in the study of fluvial facies models. In: F.G. Ethridge, R.M. Flores and M.D. Harvey (eds.), Recent developments in fluvial sedimentology, SEPM Special Publication, v. 39, p. 1-9, doi:10.2110/pec.87.39.0001

Miall, A.D., 1994. Reconstructing fluvial macroform architecture from 2- dimensional: examples from the Castlegate sandstone, Book Cliffs, Utah. Journal of Sedimentary Research, v. 64B, p. 146-158, doi:10.1306/D4267F78-2B26-11D7-8648000102C1865D

Miall, A.D. 1996. The Geology of Fluvial Deposits. Springer, Berlin, 582 pp., doi: 10.1007/978-3-662-03237-4

Miall, A.D., 2006. How do we identify big rivers? And how big is big? Sedimentary Geology, v. 186, p. 39-50, doi:10.1016/j.sedgeo.2005.10.001

Mossop, G.D., and Flach, P.D., 1983. Deep channel sedimentation in the Lower Cretaceous McMurray Formation, Athabasca Oil Sands, Alberta. Sedimentology, v. 30, p. 493-509, doi:10.1111/j.1365-3091.1983.tb00688.x

Nanson, G.C., 2013. Anabranching and anastomosing rivers. In John F. Shroder (Ed.), Treatise on geomorphology (Vol. 9, pp. 330 –345). San Diego, CA: Academic Press, doi:10.1016/B978-0-12-374739-6.00244-X

Nanson, G.C., Knighton, A.D., 1996. Anabranching rivers: their cause, character and classification. Earth Surface Processes and Landforms, v. 21, p. 217–239, doi:10.1002/(SICI)1096-9837(199603)21:3<217::AID-ESP611>3.0.CO;2-U

Neill, C.R., 1973. Hydraulic and morphologic characteristics of Athabasca River near Fort Assiniboine. Alberta Research Council, Edmonton. Hway River Engng Div. Rep. REH/73/3, 23 pp.

Nittrouer, J.A., Allison, M.A., and Campanella, R.C., 2008. Bedform transport rates for the lowermost Mississippi River: Journal of Geophysical Research, v. 113, doi:10.1029/2007JF000795

Nordin, C.F., Meade, R.H., Curtis, W.F., Bósio, N.J., Delaney, B.M., 1979. Particle size of sediments collected from the bed of the Amazon River and its tributaries in May and June 1977. Open-File Report 79-329, U.S. Geological Survey, Denver, Colorado.

Paola, C., and Borgman, L., 1991. Reconstructing topography from preserved stratification. Sedimentology, 33, 553–565, doi:10.1111/j.1365-3091.1991.tb01008.x

Parsons, D.R., Best, J.L., Orfeo, O., Hardy, R.J., Kostaschuk, R., and Lane, S.N., 2005. Morphology and flow fields of three-dimensional dunes, Rio Parana, Argentina: results from simultaneous multibeam echo sounding and acoustic Doppler current profiling. Journal of Geophysical Research, v. 110, F04S03 1–F04S03 9, doi:10.1029/2004JF000231

Potter, P.E., and Olsen, J.S., 1954. Variance Components of Cross-Bedding Direction in Some Basal Pennsylvanian Sandstones of the Eastern Interior Basin: Geological Application. Journal of Geology, v. 62, p. 50-73, doi:10.1086/626133

Potter, P.E., and Pettijohn, F.J. Paleocurrents and Basin Analysis. Academic Press Inc, New York, N.Y (1963), 296 pp., doi:10.1007/978-3-662-01020-4

Reesink, A.J.H., Ashworth, P.H., Sambrook Smith, G.H., Best, J.L., Parsons, D.R., Amsler, M.L., Hardy, R.J., Lane, S.N., Nicholas, A.P., Orfeo, O., Sandbach, S.D., Simpson, C.J., and Szupiany, R.N., 2014. Scales and causes of heterogeneity in bars in a large multi-channel river: Rio Parana, Argentina. Sedimentology, v. 61, p. 1055-1085, doi:10.1111/sed.12092

Rice, S.P., and Church, M., 2010. Grain-size sorting within river bars in relation to downstream fining along a wandering channel. Sedimentology, v. 57, p. 232-251, doi:10.1111/j.1365-3091.2009.01108.x

Roberts, M.C., and Morningstar, O.R., 1989. Floodplain formation in a wandering gravel-bed river: Lower Fraser River, British Columbia, Canada. GeoArcheoRhein, v. 2, p. 63-70.

Roberts, M.C., Bravard, J.P., and Jol, H.M., 1997. Radar signatures and structure of an avulsed channel: Rhone River, Aoste, France. Journal of Quaternary Science, v. 12, p. 35-42, doi:10.1002/(SICI)1099-1417(199701/02)12:1<35::AID-JQS290>3.0.CO;2-Z

Roden, J.E., 1998, Sedimentology and dynamics of mega-sand dunes, Jamuna River, Bangladesh [Unpublished. Ph.D. thesis]: University of Leeds, 310 pp.

Rozo, M.G., Nogueira, A.C.R., Truckenbrodt, W., 2012. The anastomosing pattern and the extensively distributed scroll bars in the middle Amazon River. Earth Surface Processes and Landforms, v. 37, p. 1471-1488, doi:10.1002/esp.3249

Ruedemann, R., 1897. Evidence of current action in the Ordovician of New York. American Geologist, v. 19, p. 367-391.

Rubey, W.W., and Bass, N.W., 1925. The geology of Russell County, Kansas, with special reference to oil and gas resources: Kansas Geological Survey, Bulletin 10, pt. 1, p. 1-86.

Sambrook Smith, G.H., Ashworth, P.J., Best, J.L., Lunt, I.A., Orfeo, O. and Parsons, D.R., 2009. The sedimentology and alluvial architecture of a large braid bar, Rio Parana, Argentina. Journal of Sedimentary Research, v. 79, p. 629-642, doi:10.2110/jsr.2009.066

Santos, M.L., and Stevaux, J.C., 2000. Facies and architectural analysis of channel sandy macroforms in the upper Parana river. Quaternary International, v. 72, p. 87-94, doi:10.1016/S1040-6182(00)00024-0

Schumm, S.A., 1968. Speculations concerning paleohydrologic controls of terrestrial sedimentation. GSA Bulletin, v. 79, p. 1573-1588, doi:10.1130/0016-7606(1968)79[1573:SCPCOT]2.0.CO;2

Schumm, S.A., 1981. Evolution and response of the fluvial system sedimentologic implications: SEPM Special Publication, v. 31, p. 19-29, doi:10.2110/pec.81.31.0019

Schumm, S.A.,1985. Patterns of alluvial rivers. Annual Review of Earth and Planetary Sciences, v. 13, p. 5-27, doi:10.1146/annurev.ea.13.050185.000253

Selley, R.C., 1965. Diagnostic characters of fluviatile sediments of the Torridonian Formation (Precambrian) of northwest Scotland. Journal of Sedimentary Petrology, v. 35, p. 366-380, doi:10.1306/74D7127B-2B21-11D7-8648000102C1865D

Shukla, U.K., Singh, I.B., Srivastava, P., Singh, D.S., 1999. Paleocurrent patterns in braid-bar and point-bar deposits: examples from the Ganga river, India. Journal of Sedimentary Research, v. 69, p. 992-1002, doi:10.2110/jsr.69.992

Sioli, H., 1965. Zur Morphologie des FluBbettes des Unteren Amazonas. Die Naturwissenschaften, 52, 104.

Sinha, R., and Friend, P.F., 1994. River systems and their sediment flux, Indo-Gangetic plains, Northern Bihar, India. Sedimentology, v. 41, p. 825-845, doi:10.1111/j.1365-3091.1994.tb01426.x

Sinha, R., Jain, V., Babu, P., and Ghosh, S., 2005. Geomorphic characterization and diversity of the fluvial systems of the Gangetic Plains: Geomorphology, v. 70, p. 207-225, doi:10.1016/j.geomorph.2005.02.006

Smith, D.G., and Smith, N.D., 1980. Sedimentation in anastomosed river systems: examples from alluvial valleys near Banff, Alberta. Journal of Sedimentary Petrology, v. 50, p. 0157-0164, doi:10.1306/212F7991-2B24-11D7-8648000102C1865D

Sorby, H.C., 1859. On the physical geography of the Tertiary estuary of the Isle of Wight. Quarterly Journal of the Geological Society, v. 12, p. 137-138, doi:10.1144/GSL.JGS.1856.012.01-02.18

Strasser, M.A., 2002. Estudo da geometria das formas de fundo no curso médio do rio Amazonas. Dissertação de mestrado, COPPE/UFRJ, 100 p.

Strasser, M.A., 2008. Dunas fluviais no rio Solimões-Amazonas - Dinâmica e transporte de sedimentos. Tese de doutorado, COPPE/UFRJ, 148 p.

Wang, Z., Chen, Z., Shi, Y., Li, M., Zhang, Q., and Wei, T., 2007. Fluvial bedforms and hydrodynamic controls along the Mid-Lower Yangtze channel. Sci. China (Ser. D), v. 37, p. 1223–1234. [in Chinese]

Willis, B. 1993. Ancient river systems in the Himalayan foredeep, Chinji Village area, northern Pakistan. Sedimentary Geology, v. 88, p. 1-76, doi:10.1016/0037-0738(93)90151-T

Wooldridge, C.L., and Hickin, E.J., 2005. Radar architecture and evolution of channel bars in wandering gravel-bed rivers: Fraser and Squamish rivers, British Columbia, Canada. Journal of Sedimentary Research, v. 75, p. 844-860, doi:10.2110/jsr.2005.066

Xie, Z., Huang, H., Yu, G., and Zhang, M., 2018. Quantifying the effects of dramatic changes in runoff and sediment on the channel morphology of a large, wandering river using remote sensing images. Water, v. 10, 1767, doi:10.3390/w10121767

Yalin, M.S., 1964. Geometrical properties of sand waves. Journal of the Hydraul. Division, v. 90, p. 105–119.

Zaleha, M.J., 1997. Fluvial and lacustrine palaeoenvironments of the Miocene Siwalik Group, Khaur area, northern Pakistan. Sedimentology, v. 44, p. 349-368, doi:10.1111/j.1365-3091.1997.tb01529.x

IV. THE SIGNIFICANCE OF SUPERIMPOSED DUNES IN THE AMAZON RIVER: IMPLICATIONS FOR HOW LARGE RIVERS ARE IDENTIFIED IN THE ROCK RECORD

Galeazzi, C.P.[1,*], Almeida, R.P.[1,2], Mazoca, C.E.M.[1], Best, J.L.[3], Freitas, B.T.[4], Ianniruberto, M.[5], Cisneros, J.[6], Tamura, L.N.[1]

[1] Instituto de Geociências, Universidade de São Paulo, Rua do Lago, 562, Cidade Universitária, São Paulo, SP, 05508-900, Brazil (E-mail: cristiano.galeazzi@usp.br)

[2] Instituto de Energia e Ambiente, Universidade de São Paulo, Av. Prof. Luciano Gualberto, 1289, Cidade Universitária, São Paulo, SP, 05508-900, Brazil

[3] Departments of Geology, Geography & GIS, Mechanical Science and Engineering and Ven Te Chow Hydrosystems Laboratory, University of Illinois, 1301 West Green Street, Champaign, IL 61801, USA

[4] Faculdade de Tecnologia, Universidade Estadual de Campinas, R. Paschoal Marmo, 1888, Limeira, SP, 13484-332, Brazil

[5] Universidade de Brasília, Instituto de Geociências, Campus Universitário Darcy Ribeiro, Brasília, DF, 71900-000, Brazil

[6] Department of Geology, University of Illinois, 1301 West Green Street, Champaign, IL 61801, USA

IV.1 INTRODUCTION

Current fluvial facies models are dominated by data and conceptualizations derived mainly from studies of small fluvial systems. Large rivers, defined by large drainage area, channel length and water and sediment discharges (Hovius, 1998; Potter and Hamblin, 2006; Gupta, 2007), have been relatively neglected, largely due to their inaccessibility, deep turbid flows, challenging logistics and often harsh climate, as they are mainly concentrated in the very hot and wet regions of the world (Latrubesse et al., 2005). These conditions have resulted in a comparative paucity of studies that have focused on the description of subaqueous bedforms in such large rivers, whose investigation requires deployment of state-of-the-art geophysical techniques.

Until recently, the investigation of river beds relied exclusively on 2D bathymetric profiles (for instance, see the studies of Strasser, 2002, 2008, in the Amazon River, and Leclair, 2011, in the Mississippi River), thus limiting the understanding of bedform morphology and kinematics. However, since the beginning of the last decade, Multibeam Echo-Sounder (MBES) surveys have revolutionized our ability to achieve high-resolution quantification of the 3D subsurface bathymetry (e.g. Parsons et al., 2005; Nittrouer et al., 2011). This new quantification within large-scale fluvial channels has allowed examination of the relationship between processes and products, and allowed questioning of some long-held assumptions. For instance, dune size has often been proposed to scale with water depth (e.g. Yalin, 1964; Allen, 1984; Ashley, 1990; Paola & Borgman, 1991; Leclair & Bridge, 2001) and proposed facies models for large rivers have related the occurrence of large sets of cross strata to large-scale channels (Wignall & Best, 2000; Miall, 2006; Fielding, 2007). However, the question arises as to if large dunes have to be present within an ancient fluvial deposit for the interpretation of a large channel to be made (Best et al., 2007; Leclair, 2011; Reesink et al., 2014; Bradley & Venditti, 2017). In this respect, the presence of small, within-channel, dunes and superimposed dunes on the leeside of larger dunes has been underappreciated in past work on large rivers, which has focused on the occurrence of very large compound dunes, such as those in the Amazon (Strasser, 2002, 2008; Almeida et al., 2016a), Yangtze (Wang et al., 2007), Jamuna (Best et al., 2007), Mississippi (Harbor, 1998; Abraham & Pratt, 2000; LeClair, 2011), and Paraná (Amsler & Prendes, 2000; Parsons et al., 2005; Sambrook Smith et al., 2009, 2013; Reesink et al., 2014) rivers.

Superimposed dunes on top of host dunes have been previously recognized in diverse depositional settings, such as aeolian (e.g. Rubin & Hunter, 1982), tidal (e.g. Ernstsen et al., 2006) and fluvial (e.g. Coleman, 1969; Allen & Collinson, 1974; Jackson, 1976; Dinehart, 1989) environments, and their preserved counterparts has also been identified in the rock record of these diverse settings (e.g. Brookfield, 1977; Rubin & Hunter, 1982; Haszeldine, 1982; Almeida et al., 2016a). Regarding the fluvial environment, they have been described in flumes and small rivers (e.g Reesink & Bridge, 2007, 2009, 2011; Lunt & Bridge, 2007) and large rivers (e.g. Reesink et al., 2014), being that in these cases the research was related to the effects of the superimposed dunes located on the stoss side of the host dunes. Although the surveyed areas in the Amazon River also display compound dunes with superimposed dunes restricted to the stoss side, this work focuses on the large dunes with superimposed dunes migrating down their leeside, which largely dominate the riverbed. This setting is also observed in the images of previously published works of large rivers in the world (see references above). From the point of view of the sedimentary record, superimposed dunes on the leeside of compound dunes are of great significance since processes taking place in the leeside have greater preservation potential than those on the usually erosional stoss side.

The present paper examines the scale of dunes within the Amazon River, Brazil, in order to quantify the occurrence of different dune sizes within the main channel. The Amazon River ranks first in water discharge, drainage basin area, and suspended sediment discharge, amongst the world's great rivers, and is an ideal system in which to examine dune morphometrics and scaling. In this paper, high-resolution MBES images are presented from two reaches of the Amazon River, highlighting the importance of the presence of small, superimposed dunes on the leeside of very large compound dunes migrating within the channel. The dunes of the river bed are described using a range of quantitative parameters, which allow examination of their relationship with large, low-angle compound dunes, and their potential importance in the ancient fluvial record.

IV.2 LOCATION

In Brazil, the Amazon River is named the Solimões River from the Peruvian border to its confluence with the Rio Negro, near Manaus (Fig. 4.1), after which it is called the Amazon. The reaches studied herein are located in the Lower Solimões River, just before the confluence with the Rio Negro, and in the Upper Amazon River, about 33 km downstream of the confluence (Fig. 4.1). In the Lower Solimões River, a bathymetric survey was conducted downstream of Marchantaria Island (Fig. 4.1), and covered an area of *c.* 10 km², where maximum flow depths were 45 m. In the Upper Amazon River, the area surveyed is located near the northern bank of the Careiro Island (Fig. 4.1), and covered an area of *c.* 8 km², with a maximum flow depth of 66 m.

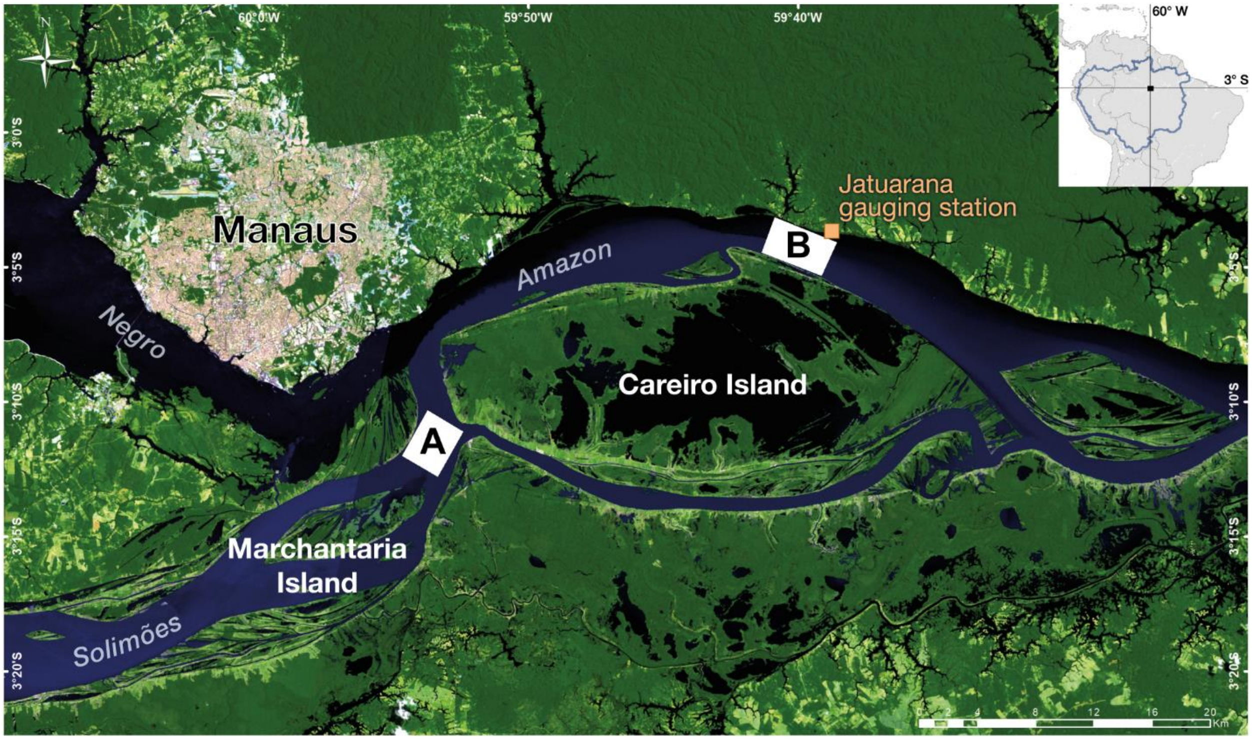

Fig. 4.1. Location of the surveyed areas in the Lower Solimões (A) and Upper Amazon (B) rivers.

The hydraulic characteristics of these two localities are given by two gauging stations maintained by the Brazilian Water Agency (ANA), which reflect a large variation in water discharge between low (October to December) and high (May to July) flow stage. For the Lower Solimões River, the Manacapuru gauging station, located about 85 km upstream of the surveyed area, shows an average water discharge ranging from *c.* 67,000 (low) to 138,000 m^3s^{-1} (high stage). In the Upper Amazon River, water discharge increases significantly due to the input from the Rio Negro, and at the Jatuarana gauging station, located at the margin of the surveyed area, the average water discharge varies from *c.* 80,000 to 174,000 m^3s^{-1}. The surveys reported herein were undertaken in July 2015, when the river was at flood stage. Discharge of the precise date or month of when the surveys were conducted is not available, however the historical mean discharge in July at the Manacapuru (available data ranging from January of 1972 to July of 2013) and Jatuarana (from October of 1977 to January of 2015) gauging stations are *c.* 133,000 and 167,000 m^3s^{-1} respectively (Fig. 4.2).

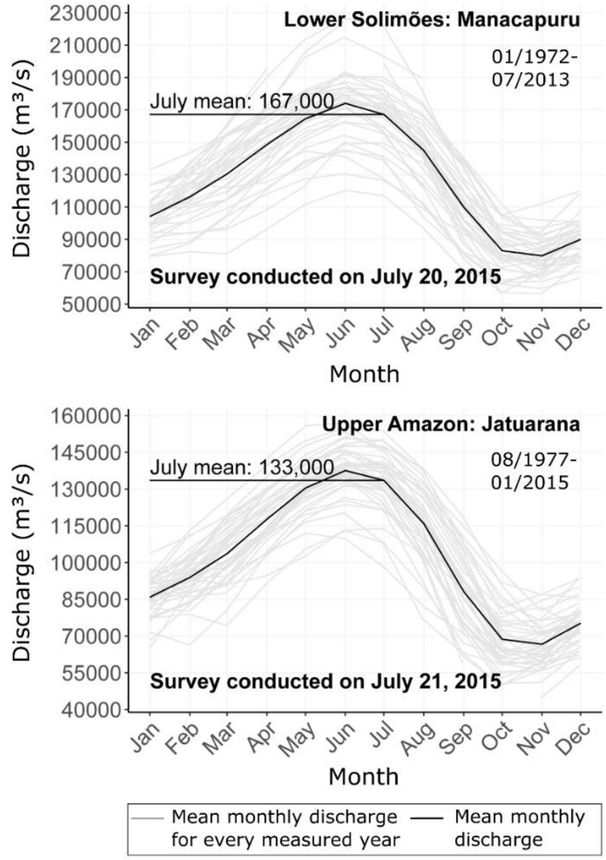

Fig. 4.2. Monthly discharge for each measured year (gray curves) and mean monthly discharge (black curves) for the Manacapuru (Lower Solimões) and Jatuarana (Upper Amazon) gauging stations.

IV.3 METHODS

High-resolution 3D bathymetry of the river bed was obtained using a Teledyne-Reson Seabat 7101 Multibeam Echo Sounder (MBES), operating at a frequency of 240kHz, with 511 equi-angle beams achieving a maximum vertical measurement resolution of 12.5 mm. The MBES was pole-mounted over the side of the vessel, with positioning and motion reference provided by an SBG Ekinox-E inertial system and Vector VS330 GNSS Receiver with Atlas L-band differential correction service. In order to attain better beam forming, an AML Micro-X probe equipped with a SV-Xchange sound velocity sensor was installed close to the MBES sonar head. All sensors were interfaced with the PDS2000 navigation and data acquisition suite. MBES calibration was carried out following a standard patch test protocol, to compensate for residual installation offsets, and sound velocity profiling of the water column was undertaken on a daily basis using a Valeport Mini sound velocity probe. All soundings were reduced to the water reference level of the Port of Manaus fluviometric station.

The MBES surveys yielded high-resolution digital elevation models (DEM), which were used to quantify dune height, wavelength and leeside angles, as well as the area occupied by different types of bedforms, using GIS software. The area occupied by the leesides of the dunes was identified by producing aspect maps that highlighted surfaces dipping in the direction of the river flow. The aspect map of simple and superimposed dunes was computed directly from the original DEM, whereas the leeside of compound dunes was computed using a 33x33 pixel moving average window to filter the superimposed dunes. The distinction between leesides of compound dunes with or without superimposed dunes was accomplished manually.

All dune heights and the leeside angles of compound dunes were measured manually on longitudinal sections in the direction of flow, parallel to the river banks, spaced laterally *c.* 30-60 m apart: this yielded 1233 and 1550 measurements of primary and secondary dunes respectively. Bedform height was defined as the vertical distance from the crest to the trough of the dunes. Wavelength was defined as the horizontal distance between consecutive throughs. The leeside angles of compound dunes were measured from the base of the leeside to the lowest brinkpoint, excluding low angles related to the asymptotic portions of the leeside at the base of the dune.

The leeside angles of simple and superimposed dunes were obtained using slope maps produced from the DEM, by quantifying pixels with slope values in the leeside area of the dunes. In order to avoid measuring pixels from the low-angle upper and lower parts of the leesides, the morphometric algorithm DEV, or deviation from mean elevation (Gallant & Wilson, 2000; De Reu et al., 2013) was applied with a DEV range of 0.2-0.5. Dunes with amplitudes smaller than 0.45 m were excluded from the dataset, since their wavelengths were too close to the horizontal resolution of the DEM to allow accurate slope measurements.

Bed material samples were collected at 12 sites in the Upper Amazon River (Almeida et al., 2016a) and 14 sites in the Lower Solimões River during low flow stage, 3 months after the MBES survey, using a 10 kg Van Veen grab sampler. Grain size analyses were performed with a Malvern Mastersizer 2000 (size fractions <1 mm) and mechanical sieves (>1 mm).

IV.4 BEDFORMS IN THE SOLIMÕES AND AMAZON RIVERS

Bedforms quantified from the MBES images were classified into two groups: (i) primary bedforms, represented by simple and compound dunes, and (ii) secondary bedforms, represented by simple superimposed dunes on the stoss *and* lee sides of the compound dunes, which are the primary, or host, dunes for these secondary bedforms. The term ‘simple dune’ is herein restricted to describe dunes with no superimposed dunes, i.e. contrary to a compound dune. In extent, the superimposed dunes described herein, with quantitative measurements and statistics, are those located in the leeside of the compound dunes.

Both survey areas in the Lower Solimões and Upper Amazon rivers display a thalweg and bank-attached bars on the right channel margin (Fig. 4.3A,C). The beds largely comprise sand, which forms simple and compound dunes, but also locally possesses bedrock outcrops. Compound dunes always possess superimposed dunes on their stoss side, but also very often on their leeside. The shaded areas in Figs. 4.3B and 4.3.D represent the leesides of compound dunes with (blue) and without (red) superimposed bedforms. Superimposed dunes cover *c.* 94% of the total area of the compound dune leesides, and thus only *c.* 6% possess slopes at, or near, the angle-of-repose. The surveyed reaches show similar patterns in their bedform distribution with regards to water depth: i) shallower areas on the bar tops are characterized by simple dunes, with visual observations at low flow also showing minor upper-stage plane bed or ripples in the shallowest regions; and ii) deeper areas, represented by the thalwegs and the base of bars, which are dominated principally by very large compound dunes. In deeper areas, the occurrence of simple dunes as primary bedforms is restricted to specific locations that determine the local sediment supply, such as downstream of bedrock pinnacles or downstream of confluence scours. Otherwise, the deeper areas of the channel exhibit only compound dunes. In this way, simple dunes occur as primary bedform from 10 to 36 m water depth (Fig. 4.4A), but are present at greater flow depths as a secondary bedform, in the shape of superimposed dunes (Fig. 4.4B), which are of one order of magnitude smaller the host dunes (Fig. 4.4C). Compound dunes develop from 22 m to greater depths, and largely dominate the areas of sedimentation at this depth interval, occupying *c.* 90% of the area.

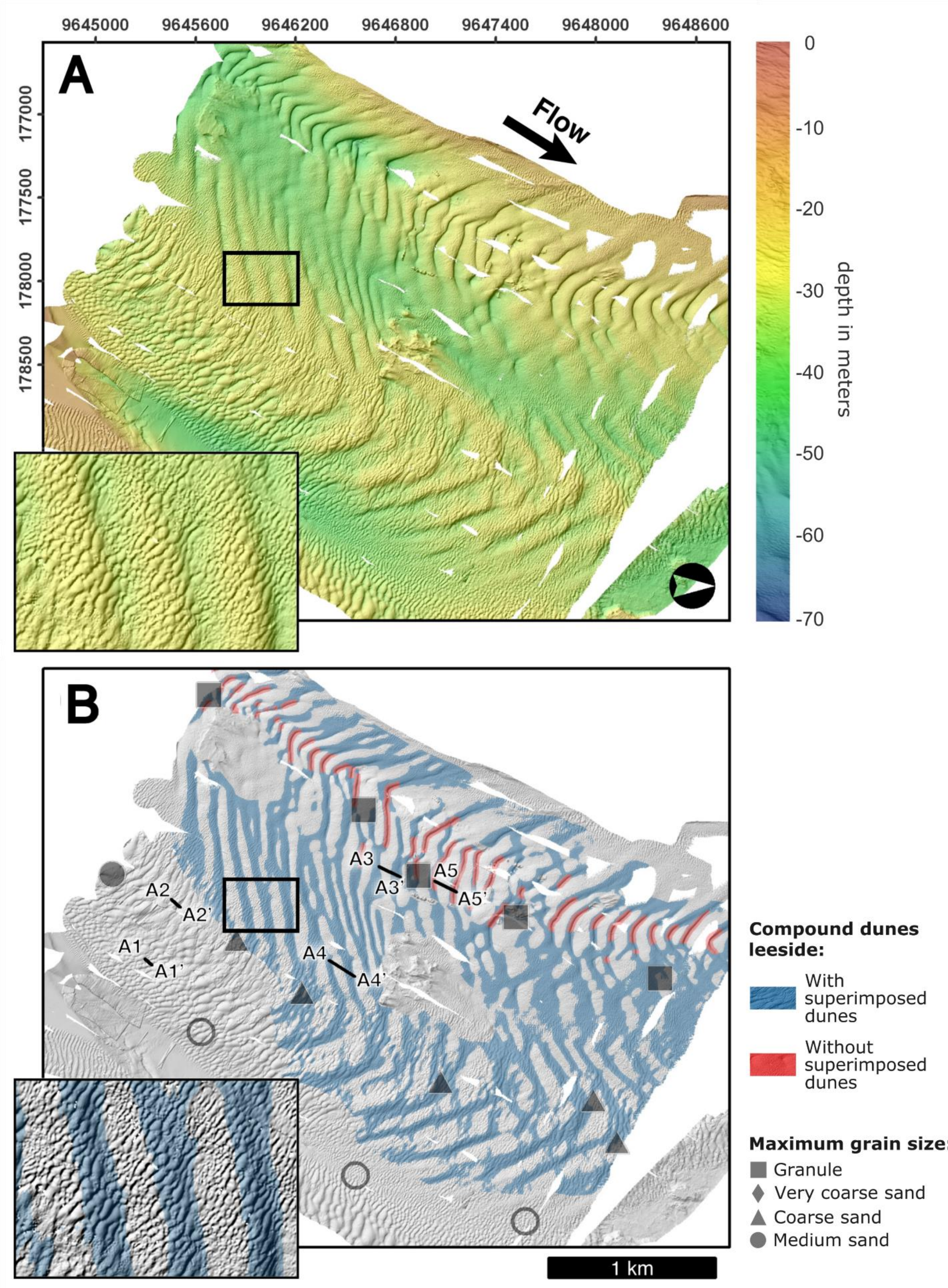

A
B
9645000
9645600
9646200
9646800
9647400
9648000
9648600
177000
177500
178000
178500
Flow
0
-10
-20
-30
-40
-50
-60
-70
depth in meters
A1
A1'
A2
A2'
A3
A3'
A4
A4'
A5
A5'
Compound dunes leeside:
With superimposed dunes
Without superimposed dunes
Maximum grain size:
Granule
Very coarse sand
Coarse sand
Medium sand
1 km

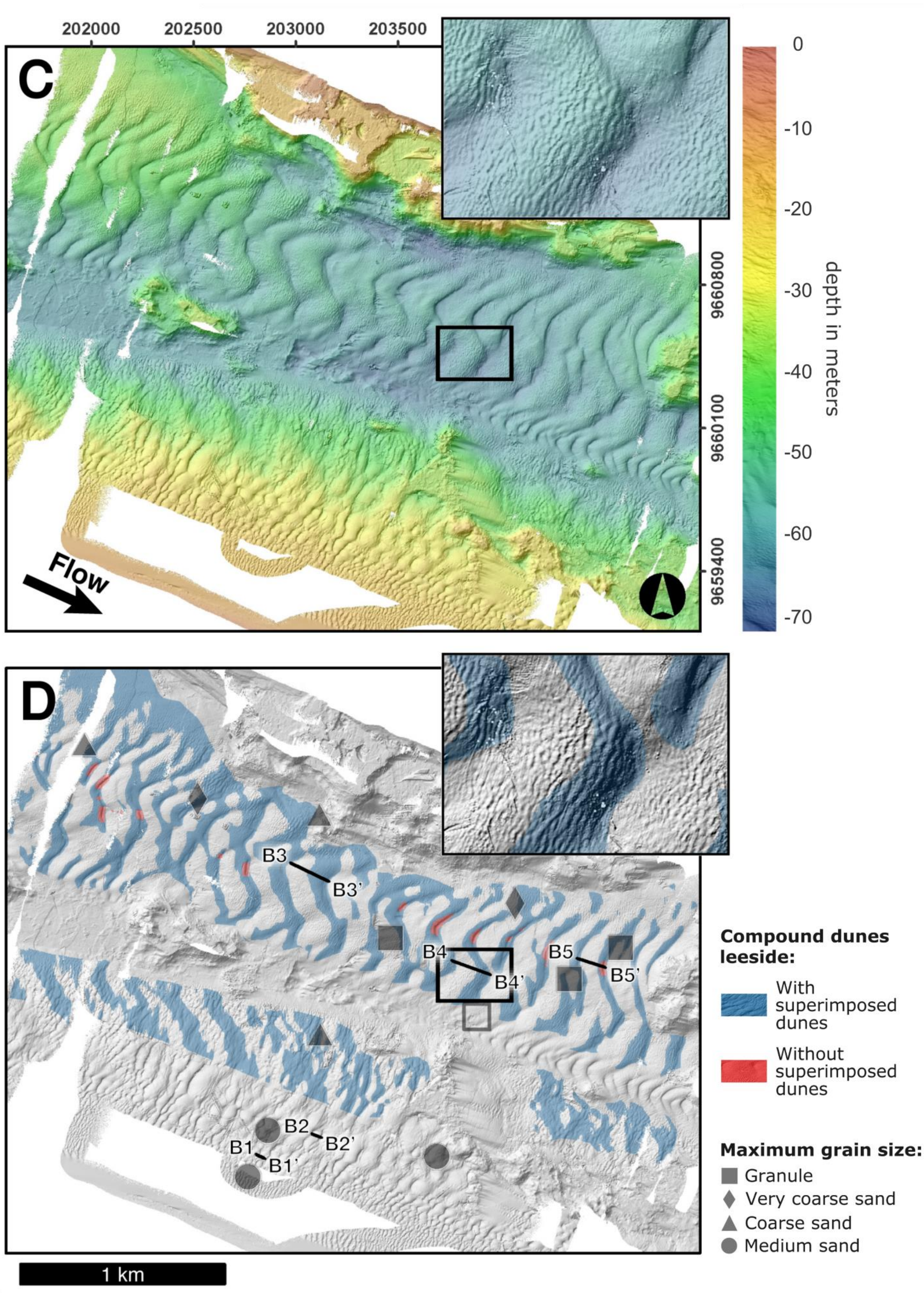

202000
202500
203000
203500
C
0
-10
-20
-30
-40
-50
-60
-70
depth in meters
9660800
9660100
9659400
Flow
D
B3
B3'
B4
B4'
B5
B5'
B2
B2'
B1
B1'
Compound dunes leeside:
With superimposed dunes
Without superimposed dunes
Maximum grain size:
Granule
Very coarse sand
Coarse sand
Medium sand
1 km

Fig. 4.3 (previous pages). Multibeam Echosounder (MBES) bathymetric map of survey areas in (A) Lower Solimões River, and (C) Upper Amazon River. In the detail inset boxes, large compound dunes are highlighted, which possess superimposed dunes on their leesides. (B) and (D) highlight the leesides of compound dunes with (blue), or without (red), superimposed dunes, and indicate the location of the longitudinal sections shown in Fig. 4.4 as well as bed sediment sampling areas. Empty symbols indicate samples collected from downstream of scours or bedrock protrusions. The inset boxes illustrate the same compound dunes as shown in (A) and (B).

Both survey areas in the Lower Solimões and Upper Amazon rivers display a thalweg and bank-attached bars on the right channel margin (Fig. 4.3A,C). The beds largely comprise sand, which forms simple and compound dunes, but also locally possesses bedrock outcrops. Compound dunes always possess superimposed dunes on their stoss side, but also very often on their leeside. The shaded areas in Figs 4.3B and D represent the leesides of compound dunes with (blue) and without (red) superimposed bedforms. Superimposed dunes cover *c.* 94% of the total area of the compound dune leesides, and thus only *c.* 6% possess slopes at, or near, the angle-of-repose. The surveyed reaches show similar patterns in their bedform distribution with regards to water depth: i) shallower areas on the bar tops are characterized by simple dunes, with visual observations at low flow also showing minor upper-stage plane bed or ripples in the shallowest regions; and ii) deeper areas, represented by the thalwegs and the base of bars, which are dominated principally by very large compound dunes. In deeper areas, the occurrence of simple dunes as primary bedforms is restricted to specific locations that determine the local sediment supply, such as downstream of bedrock pinnacles or downstream of confluence scours. Otherwise, the deeper areas of the channel exhibit only compound dunes. In this way, simple dunes occur as primary bedform from 10 to 36 m water depth (Fig. 4.4A), but are present at greater flow depths as a secondary bedform, in the shape of superimposed dunes (Fig. 4.4B), which are of one order of magnitude smaller the host dunes (Fig. 4.4C). Compound dunes develop from 22 m to greater depths, and largely dominate the areas of sedimentation at this depth interval, occupying *c.* 90% of the area.

In terms of morphology, compound dunes commonly display greater dune heights in the central sections, which significantly decrease towards the sides, whereas simple and superimposed dunes show a greater continuity in dune height along their width. In planform, simple dunes commonly possess straight to sinuous crests, mostly perpendicular to the flow, whilst compound dunes display barchanoid, sinuous and straight crests, the latter being oblique or perpendicular to the flow. Superimposed dunes mainly exhibit straight crests that are perpendicular to the flow. In a profile view, compound dunes are flatter than simple dunes, as expressed by a lower dune form index (height/wavelength), being 0.03 for compound and 0.05 for simple dunes (Fig. 4.4D). Simple and compound dunes commonly exhibit convex shapes with an average of 39% of the wavelength occupied by the leeside. Superimposed dunes display convex shapes or planar tops, with an average of 58% of the wavelength occupied by the leeside (Fig. 4.5).

Bedform data from both reaches were analyzed to determine dune height, wavelength, leeside angle and grain size using a classification split into three water depth intervals: shallower than 20 m, between 20 and 40 m and deeper than 40 m. Statistics regarding superimposed dunes relate to those located in the leeside of compound dunes. Dunes whose sediment supply was affected by bedrock pinnacles or confluent flows were not included in this statistical analysis.

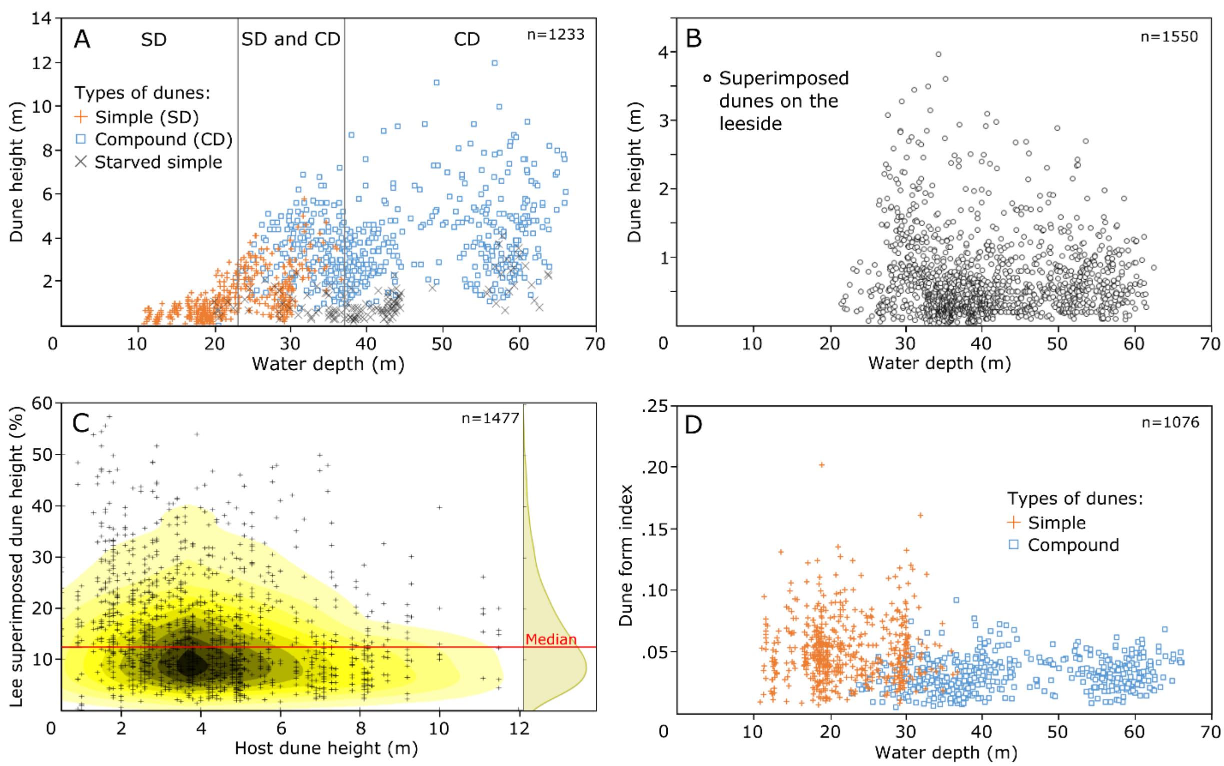

Fig. 4.4. Dune height vs. water depth for: (A) primary dunes, including simple dunes from the shallow channel and compound dunes from the deep channel, and (B) secondary bedforms, which include superimposed dunes on the leeside of the compound dunes. (C) Height of superimposed dunes in relation to the height of their respective host dunes, with contours representing the 2D density plot and a median (red line). To the right, the frequency density for the y-axis. (D) Relationship between dune form index (height/wavelength) and water depth for the primary bedforms.

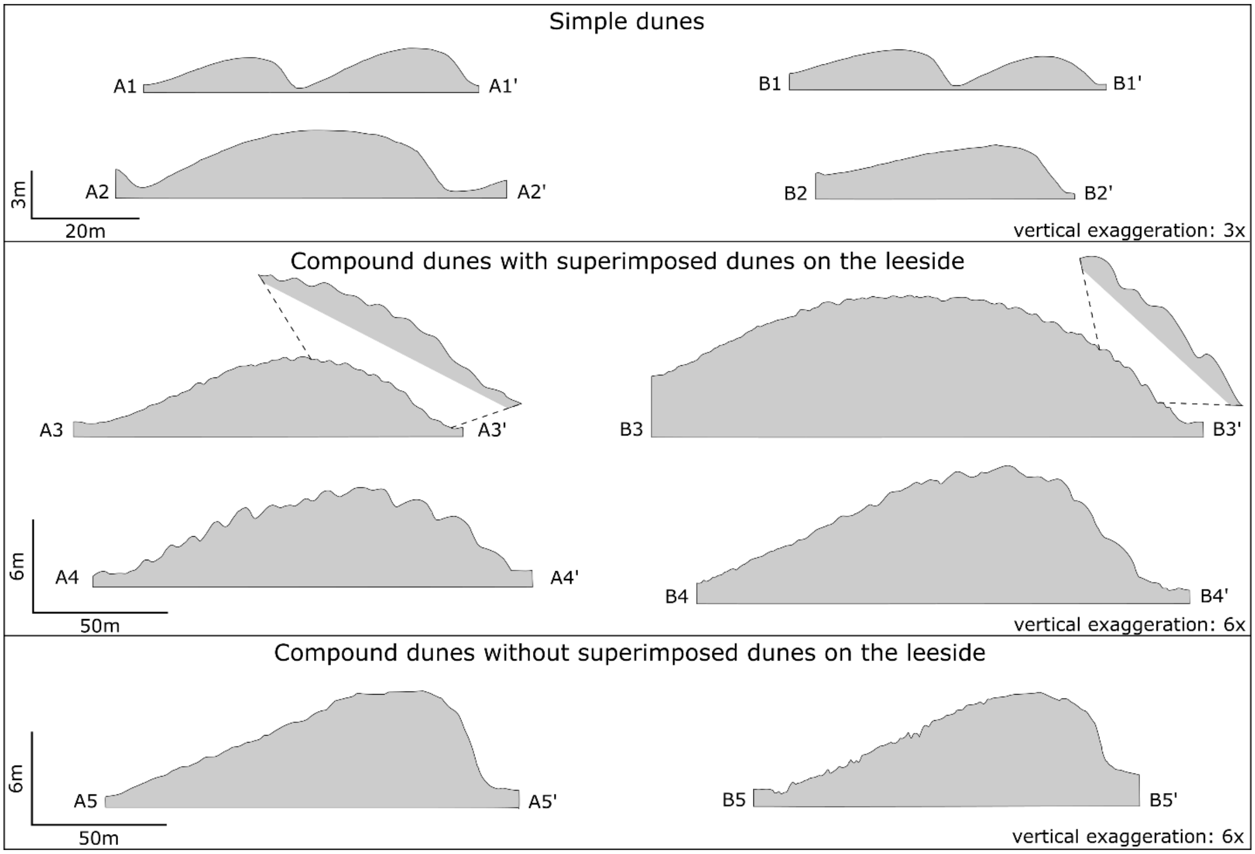

Fig. 4.5. Longitudinal sections of simple and compound dunes. Location of the sections is shown in Fig. 4.3.

Dune height

The dune height data for the primary simple and compound bedforms show that maximum dune height increases at greater water depths (Fig. 4.6A, note that outliers are not included, for maximum dune heights see Fig. 4.3). However, the minimum dune height does not increase with water depth, thus yielding a wider scatter in the data at greater water depths. At flow depths shallower than 20 m, only primary simple dunes occur, and are limited to a maximum height of 1.4 m, with a mean of 0.5 m. From 20 to 40 m flow depth, the primary simple dunes become larger, as shown by mean and maximum dune heights of 1.7 m and 4.7 m, respectively. At this same depth interval, compound (and therefore superimposed) dunes are also present, with mean and maximum heights of 3.3 m and 8.7 m respectively. At water depths deeper than 40 m, compound dunes reach a mean height of 4.4 m and maximum amplitude of 12.2 m.

These data also show that, contrary to the size of the primary bedforms, the size of superimposed dunes on the leeside of the compound dunes does not change significantly with water depth, and that they exhibit a contrasting height compared to their host compound dunes (Fig. 4.6A). From 20 to 40 m in depth, superimposed dunes show a mean height of 0.6 m, reaching a maximum value of 4 m, whereas at depths greater than 40 m, the mean dune height is 0.7 m, with a maximum of 3.1 m. At both depth intervals, 70% of these dunes are smaller than 1 m in height, averaging about 15% of the height of the host dune. From 20 to 40 m in depth, average is of about 18%, varying from 1 to 57%, whereas below 40 m, average is of about 12%, varying from 2 to 56%.

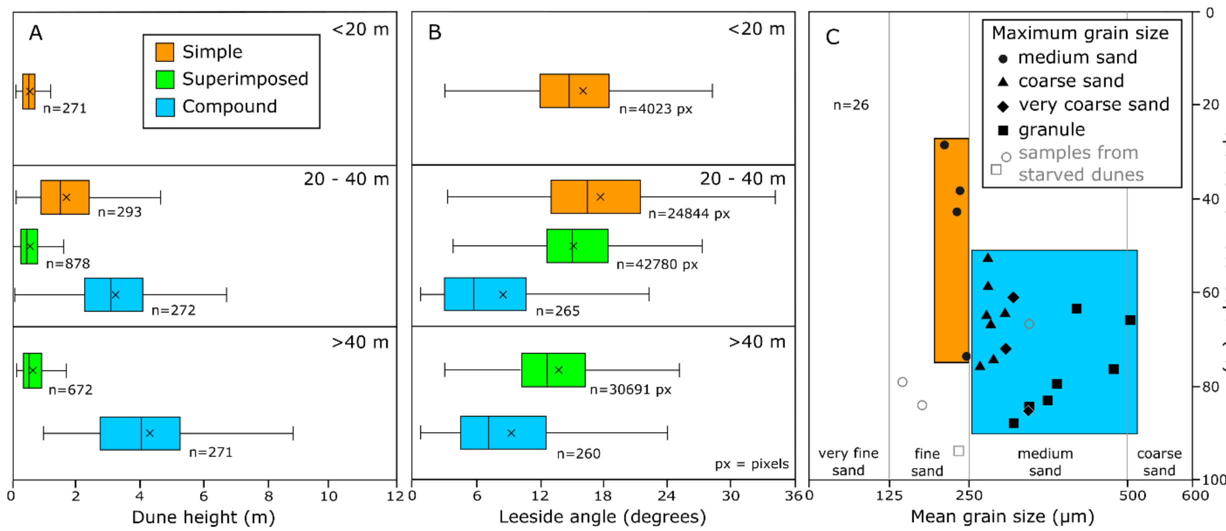

Fig. 4.6. Distribution of (A) dune height, (B) leeside angle and (C) mean and maximum grain size at different water depth intervals for simple, compound and superimposed dunes. Boxplots in (A) and (B) do not include outliers. Open symbols in (C) indicate samples from starved dunes downstream of confluence or bedrock outcrops.

Leeside angle

The leeside angles of primary bedforms show different values, with simple dunes being characterized by steeper leeside angles than compound dunes (Fig. 4.6B). At water depths shallower than 20 m, simple dunes possess mean leeside angles of 16°, with 48% and 15% of values being steeper than 15° and 21° respectively. Between 20 and 40 m flow depth, simple dunes show a mean angle of 18°, with 60% and 27% of values being steeper than 15° and 21° respectively. However, at flow depths between 20 and 40 m, compound dunes show a mean leeside angle of 9°, with 78% of values below 15°. At flow depths deeper than 40 m, compound dunes possess a mean leeside angle of 10°, with 79% of these slopes being below 15°.

The leeside angle of superimposed dunes is also steeper compared to the host compound dunes, although it is more gentle than the primary simple dunes. At water depths between 20 and 40 m, dunes display a mean leeside angle of 16°, with 51% and 14% of values steeper than 15° and 21° respectively. At flow depths greater than 40 m, the superimposed dunes have a mean leeside angle of 14°, with 33% of slopes steeper than 15° and 9% greater than 21°.

Compound dunes of all morphologies display superimposed dunes on their leeside at any given height and grain size, but the leeside angle of compound dunes is nearly always below 15-18° when leeside bedform superimposition is present (Fig. 4.7). At greater leeside angles, superimposed dunes are rarely present, and here the leesides are probably dominated by avalanching. In the present data, such steeper-angled leesides with sediment avalanching occur almost exclusively associated with barchanoid compound dunes. Low leeside angles are very common in compound dunes, thus implying these possess abundant superimposed dunes downclimbing their lee faces (Fig. 4.3).

Grain size

The mean grain size of both surveyed reaches (see Fig. 4.3 for location) ranges from 0.148 to 0.505 mm (Fig. 4.6C). Mean and maximum grain sizes show a strong relationship with the type of primary bedform, with simple dunes possessing a mean grain size from 0.148 to 0.247 mm (fine sand), reaching a maximum size of medium sand, whereas compound dunes have mean grain sizes of 0.271 to 0.505 mm (medium to coarse sand), reaching a maximum size of granules. Coarser grain sizes are also related to greater water depths within the channels, particularly regarding maximum grain size.

IV.5 DISCUSSION

Since bedform height controls the thickness of the resulting cross-strata sets as a partial preservation of the original foreset (e.g. Paola & Borgman, 1991; Leclair & Bridge, 2001; Leclair, 2011; Reesink et al., 2015), the results presented herein imply there may be predictable trends in the distribution of cross-strata set thickness for the deposits of large rivers in the rock record. The basic assumption of previous research that recognized large river deposits in the rock record is that the abundance of large dunes is reflected in a high proportion of large-scale cross-strata sets in the rock record (e.g. Miall, 2006; Fielding, 2007). However, a previous work by Reesink et al. (2014) challenged this view, showing large river deposits from the Rio Paraná dominated by small dunes and ripples. The here presented results from the world's largest fluvial channel show that even in the thalweg of an exceedingly larger and deeper river the dominant bedforms are smaller than what would be expected, since superimposed dunes are remarkably common on both stoss and leesides of large compound dunes in the deep channels of the Amazon and Solimões rivers (Fig. 4.3). The implications of this finding are important for the interpretation of channel size based on cross-strata set thickness in the rock record, since the preserved sets would be formed by the migration of these superimposed bedforms down the leeside of host dunes, resulting in low-angle cosets instead of single large-scale cross-strata sets (e.g. Brookfield, 1977; Haszeldine, 1982; Almeida et al., 2016a, 2016b).

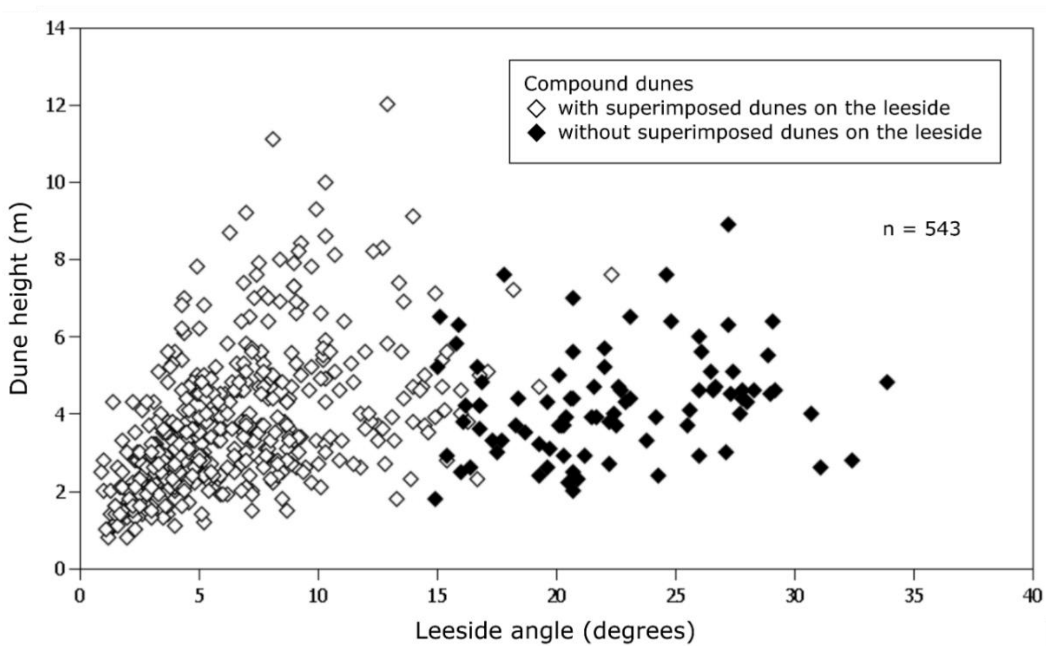

Fig. 4.7. Relationship between compound dune height, leeside angle and the occurrence of superimposed dunes on the leeside.

Recent works have shown that paleodepth estimations from cross-strata sets thickness in outcrops, based on the assumption that dune height scales with water depth, may be problematic (e.g. Best et al., 2007; LeClair, 2011; Reesink et al., 2014; Bradley & Venditti, 2017). The data presented herein confirm that at any depth, there is a wide range of possible dune heights (Fig.

4.4A,B). The relationship of dune height and water depth in the Amazon River is particularly similar to the one observed in the Jamuna River (Best et al., 2007): despite a wide range of dune heights at any water depth, there is an evident scaling of the maximum dune height, which is about 20 and 30% of the water depth, in the case of the Amazon and Jamuna rivers, respectively.

The dominance of superimposed dunes on the leeside of the compound dunes is of great significance for the sedimentary record. Previous works on compound dunes in both aeolian and fluvial deposits have shown the effects on the sedimentary structures of superimposed dunes located on the stoss (e.g. Reesink & Bridge, 2007, 2009, 2011) and leeside (e.g. Brookfield, 1977; Haszeldine, 1982; Almeida et al., 2016a, 2016b) of larger host dunes, resulting respectively in higher- and lower-angle inclined cosets. These sedimentary structures have been identified in sedimentary deposits of active rivers (e.g. Reesink & Bridge, 2011; Reesink et al., 2014) and the rock record (e.g. Brookfield, 1977, Haszeldine, 1982; Almeida et al., 2016a). Note that both "higher-" and "lower-angle inclined cosets" are low-angle dipping surfaces below the angle-of-repose of a dune (Reesink & Bridge, 2007, 2009; Almeida et al., 2016a) and the terms "higher" and "lower" are given to distinguish them. According to these previous works, and considering the MBES data presented here, the following sedimentary structures can be inferred from the studied bedforms of the Amazon River (Fig. 4.8): simple cross-strata sets in the shallow channel, formed by the simple dunes, and inclined cosets in the deep channel, formed by the compound dunes. Furthermore, the compound dunes would thus display two types of inclined cosets: (i) lower-angle inclined cosets, related to the occurrence of superimposed dunes on the leeside, and (ii) higher-angle inclined cosets, related to the effects of stoss side superimposed dunes on the host bedform leeside. In most of the surveyed areas of the deep channel, compound dunes present superimposed dunes on the leeside (Fig. 4.3), which would produce lower-angle inclined cosets, with individual cross-strata sets scaled to the height of the superimposed dunes. Only in the rare case compound dunes with superimposed dunes restricted to the stoss side, foresets would be produced at the scale of the large host dune, laterally transitioning to higher-angle inclined cosets.

Since the size of the bedform defines the maximum possible thickness of the preserved cross-strata sets, and the thickness of cross-stratal sets is a fraction of the formative dune height (e.g. Paola & Borgman, 1991; Leclair & Bridge, 2001; Leclair, 2011; Reesink et al., 2015), sedimentary structures formed by the superimposed bedforms described herein would be relatively small, at any flow depth (Fig. 4.6A). Apart from rarer, larger, deep channel compound dune avalanche leesides (6% of the total area in the reaches studied herein) that would result in meter-scale cross-strata sets and higher-angle inclined cosets, the dominant deep channel superimposed dunes and smaller shallow channel simple dunes would produce centimeter-to-decimeter-scale thick cross-strata sets (Fig. 4.8).

These latter thicknesses are usually expected in deposits of small rivers, where dunes are limited to a few meters in height (e.g. Van den Berg, 1987; Julien & Klaassen, 1995; Wilbers & Ten Brinke, 2003). Similarity of the set thicknesses occurs since published works searched by the authors of this work from small rivers deposits suggest that the compound dunes with superimposed dunes on the leeside are not the dominant feature in those settings. On the contrary, their dunes are characterized by avalanche foresets (e.g. Carling, 2000; Dinehart, 2002; Wilbers & Ten Brinke, 2003; Huizinga, 2010; Eilertsen et al., 2013), and superimposed dunes occur on the stoss side of the host dunes (e.g. Carling, 2000; Reesink et al., 2011). The presence of superimposed dunes upon compound dune leesides in the deep channel, as well as the wide scatter of dune height at any given water depth, also reveals that inferences of paleo-water depth based on cross-strata set thickness may be misleading (Reesink et al., 2015).

The leeside angle results (Fig. 4.6) reveal that both shallower and deeper areas of the channel covered by mobile sediment show dunes with leeside angles steeper than 15°, which has not been recognized to date in large rivers (Hendershot et al., 2016). In shallower flows, these higher-angle dunes are primary simple dunes, whereas in deeper areas, these higher-angle dunes are superimposed on compound dunes with leeside angles below 15°. These results also show a threshold leeside angle at which compound dunes display superimposed dunes on their leesides of *c.* 15-18°, and above which the leeside faces may be ascribed to avalanche slopes (Fig. 4.7), matching the value of leeside angles that control the onset of permanent flow separation (e.g. Kostaschuck & Villard, 1996; Best & Kostaschuck, 2002; Hendershot et al., 2016). It is interesting to note that a similar relationship of higher dune form index in shallow areas, with higher leeside angles, and lower dune form index in deep areas, with lower leeside angles (Fig. 4.4C), was also described in a work by Bradley & Venditti (2017), although at a very different scale. In this work, the split occurs at around 30 m of water depth, whereas Bradley & Venditti (2017) found this difference to occur at 2,5 m of water depth.

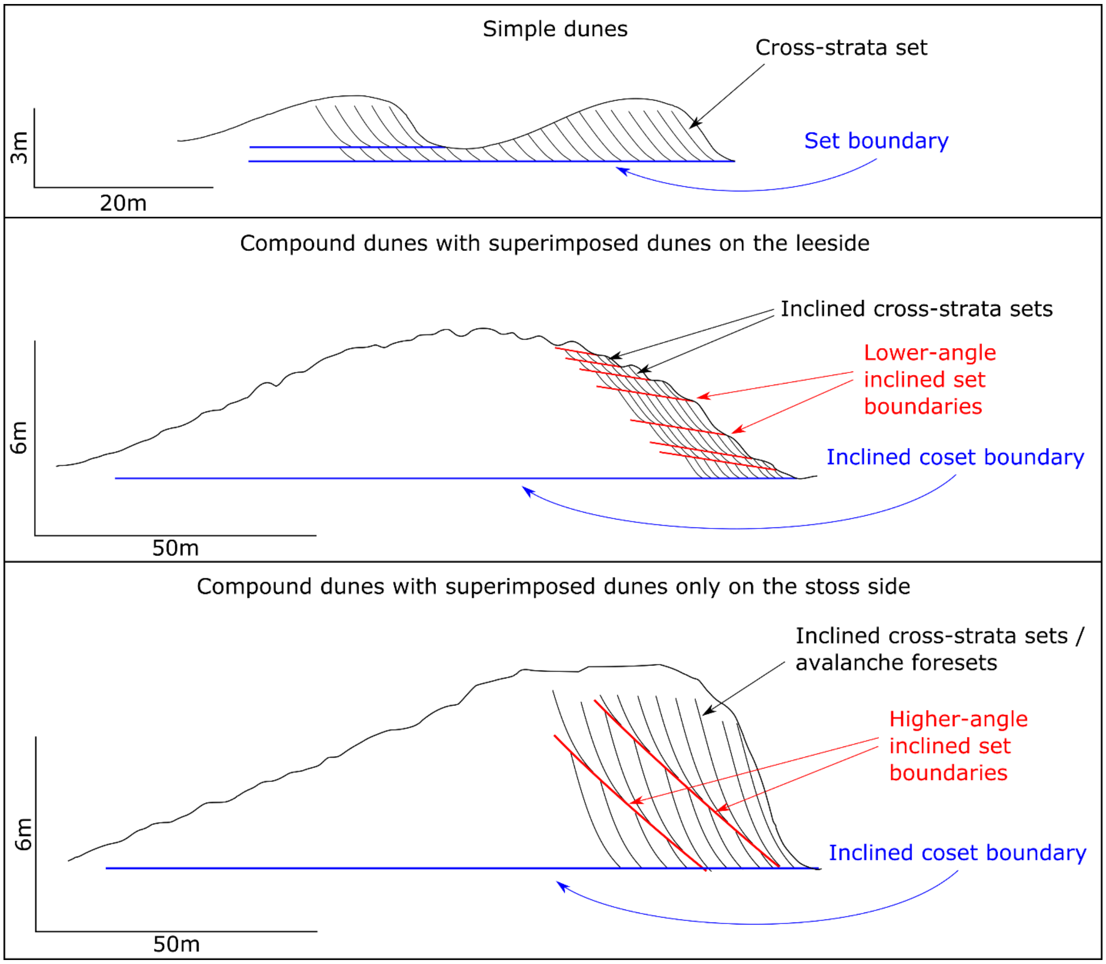

Fig. 4.8. Expected sedimentary structures for the simple dunes, in the shallow channel, and for the compound dunes with and without superimposed dunes on the leeside, in the deep channel.

Successions dominated by centimeter-to-decimeter-scale cross-strata sets could be formed in channels as deep as several tens of meters, and therefore independent criteria must be used to recognize channel scale. These superimposed dunes are also migrating on much lower angle surfaces (Fig. 4.8), and suggests the need for careful evaluation of such low-angle surfaces in the rock record, which may be very difficult to infer with limited exposures, or impossible in core. Given the data presented herein (Fig. 4.6), it may be possible to recognize the deposits of deep fluvial channels based on the identification of coarse sandstones with meter-scale thick cross-stratified cosets (formed by the migration of large compound dunes) composed of centimiter-to-decimiter scale thick inclined cross-strata sets (formed by the migration of the superimposed dunes) with foreset dip angles ranging from 12° to 21°. The recognition of compound dune cosets is thus key to the interpretation of river scale, since compound dunes are a main element in large river channels (e.g. Wang et al., 2007; Best et al., 2007), and the maximum height of these large bedforms appears better correlated with water depth (Fig. 4.4).

Given the lack of sequential MBES surveys at different river stages in the studied locations, the origin of conspicuous smaller bedforms both on the stoss and leesides of larger host dunes cannot be directly interpreted from our data. The low-angle leeside surfaces of the large compound dunes might be attributed to changes in flow stage, with the large bedform being progressively deformed by an increase in sediment accumulation on the leeside (e.g. Kostaschuk & Villard, 1996) or by erosion of the host dune crest. It is possible that the weakening of flow separation resulting from the low-angle leeside enables the active migration of smaller bedforms also on the lee surface, giving rise to the observed morphology of compound dunes.

The rock record of large rivers

Despite the great contribution of modern day large rivers to the global sediment transport and their common occurrence in subsiding areas related to active tectonic environments, the recognition of large rivers in the rock record is relatively scarce. Examples of interpreted large river deposits are the Cretaceous McMurray Formation in western Canada (e.g. Hubbard et al., 2011) the Triassic Hawkesbury Sandstone in southeastern Australia (e.g. Miall, 2006; Fielding, 2007), and the Pleistocene deposits in central-western Amazonia (e.g. Rossetti et al., 2005, Horbe et al., 2013). Two main types of criteria are often used to infer river scale: (1) thickness of preserved channel-forms, channel-fill successions or bar-forms scaled to channel depth, and (2) average or maximum thickness of preserved cross-strata sets, considered to be a function of channel depth.

The Middle McMurray Formation exhibits 30-40 m thick point-bar deposits, interpreted from large-scale inclined heterolithic strata (IHS) and related to kilometer-scale scoll-bars imaged in 3D seismic surveys (e.g. Hubbard et al., 2011; Jablonski & Darlrymple, 2016). Despite the thick channel-fill elements, ripple cross-laminated sandstones and heterolithic strata are more abundant than the 0.5 to 2 m thick cross-bedded sandstones even close to the channel bases (Jablonski & Darlrymple, 2016). Previous models to explain this apparent discrepancy are grain-size controls on bedform development and tidal influence (Jablonski & Darlrymple, 2016, and references therein). Our data suggests the possibility of the actual larger bedforms on the deeper parts of the channel being preferably preserved as cross-strata cosets resulting from smaller bedforms, ripples in the McMurray case, migrating on their leedides. It is important to note that in the absence of well-developed large-scale IHS or available seismic images, similar successions would hardly be interpreted as deep channel deposits based on the cross-strata set size distribution alone.

Another example of interpreted large river deposits are the Pleistocene sands exposed at up to 30 m tall river banks in central-western Amazonia. These sands are genetically related to the largest active rivers on Earth and compose large scale finning upward cycles dominated by tabular and trough cross-bedded medium to fine sands, with the local occurrence of coarse sand near the base of the fining-upward cycles and frequent intercalated silts and muds near their tops (Rossetti et al., 2005, Horbe et al., 2013). Again, the preserved 0.1 to 0.3 m thick cross-strata sets do not differ significantly from what is found in much smaller river deposits, and the low-angle cross-strata set bounding surfaces hamper the recognition of the 0.6 to 1.5 m thick cross-strata cosets, which are locally concave upward and downstream (Almeida et al., 2016a). In fact, the preserved cross-strata set thicknesses are compatible with the partial preservation of bedforms with a size comparable to those found as superimposed dunes on larger bedforms in the modern Amazonas and Solimões rivers.

An example of large river deposits interpreted based on cross-strata set thickness is the Triassic Hawkesbury Formation of southeastern Australia, where 2-3 m and up to 8 m thick, often concave upward and downstream, cross-strata sets abound (Conaghan & Jones, 1975; Rust & Jones, 1987; Miall & Jones, 2003). Closer inspection reveals cosets with internal smaller cross-strata sets within these structures, more frequent away from the axis of the concave forms. These deposits have been interpreted as large thalweg dunes (Almeida et al., 2016a). Some of the large-scale cross-strata sets may be locally interpreted as bar foresets (see discussion in Almeida et al., 2016a). Therefore, even in the best-known case of large-scale cross-strata in large river deposits, the sedimentary product of bedform superposition indicating the dominance of compound dunes is remarkable. In the three examples above, the reinterpretation of centimeter-scale cross-strata sets as formed by smaller bedforms migrating on the lee-surfaces of larger bedforms can be reconciled with an origin in deep-channels.

IV.6 CONCLUSIONS

High-resolution multibeam echo sounder bathymetric maps of two reaches of the Amazon River were surveyed during peak flood, and reveal that small dunes can be frequent in large rivers, suggesting significant implications for interpretations of the rock record. Despite being dominated by large-scale compound dunes at greater flow depths, these data show how small dunes can be widespread, both in shallower (as primary bedforms) and deeper (as secondary) flows in the world's largest river (Fig. 4.6A).

The presence of large sets of cross-strata has been thought to be the most common attribute needed to recognize the deposits of large rivers (e.g. Miall, 2006; Fielding, 2007). However, the very common presence of small dunes in both shallow and deep channel indicates that large river deposits may principally comprise bedform elements that are found within small rivers. Although very large compound dunes do occur in the deeper areas of the channel, their morphology, characterized by very low leeside angles with downclimbing superimposed dunes, suggests that large meter-scale cross-strata sets might be rare or absent. Given that the bedform height is the possible maximum thickness of the resulting cross-strata set, the maximum preserved cross-strata set thickness must be significantly smaller than what is expected for dunes deprived of superimposed dunes on their leesides.

Low leeside angle dunes are a common feature among large rivers (Hendershot et al., 2016) and are indeed present in the surveyed reaches of the present work, being represented by large compound dunes. However, the compound dunes generally display superimposed dunes on their leeside at angles lower than 15-18° (Fig. 4.7), corresponding to 94% of the area of the leesides of compound dunes. Steeper leeside angles with no superimposed dunes, interpreted as avalanche slopes, were thus limited in area. The superimposed dunes possess higher leeside angles, commonly steeper than 15° (Fig. 4.6B), which have rarely been recognized in large rivers (Hendershot et al., 2016). This relationship of large, low-angle, compound dunes and superimposed bedforms is present in other large rivers whose data resolution allows visualization, such as the Yangtze (Wang et al., 2007), Paraná (Amsler & Prendes, 2000; Parsons et al., 2005) and Mississippi (Abraham & Pratt, 2000).

Previous studies of the morphology of compound dunes in the Amazon River (Strasser, 2002, 2008) and other large rivers in the world, such as the Yangtze (Wang et al., 2007), Jamuna

(Best et al., 2007), Paraná (Reesink et al., 2014) or Mississippi (Harbor, 1998), suggest decimeter-scale cross-strata sets are much more likely to be preserved and found in the rock record than larger meter-scale cross-sets. In this work, a collection of shallow and deep channel bedform examples is provided, indicating how ubiquitous are small dunes in the largest river of the world, and even there where the largest dunes are observed, they possess smaller superimposed dunes on the leeside that might be misleading when interpreting rock record. The size of the superimposed dunes on the large compound dunes is comparable to dunes formed in small rivers, and criteria to differentiate between them should thus be considered in interpretation of ancient alluvium, such as coset recognition, leeside angle, facies association and grain size. Therefore, successions dominated by decimeter-scale cross-strata sets superimposed on larger, low-angle surfaces, but showing rarer preservation of large-scale avalanche foresets near the base of fining-upward cycles that are tens of meters thick, may be characteristic of the deposits of large sand-bed river channels.

REFERENCES

Abraham, D. and Pratt, T. (2002) Quantification of bed-load transport on the upper Mississippi River using multibeam survey data and traditional methods. US Army Engineer Research and Development Center (ERDC)/Coastal and Hydraulics Laboratory (CHL), Coastal and Hydraulics Engineering Technical Note (CHETN), http://chl.wes.army.mil/library/publications/chetn.

Allen, J.R.L. (1984) *Sedimentary structures: their character and physical basis*. Elsevier, Amsterdam, 663 pp.

Allen, J.R.L. and Collinson, J.D. (1974) The superimposition and classification of dunes formed by unidirectional aqueous flows. *Sed. Geol.,* 12, 169–178.

Almeida, R.P., Galeazzi, C.P., Freitas, B.T., Janikian, L., Ianniruberto, M. and Marconato, A. (2016a) Large barchanoid dunes in the Amazon River and the rock record: implications for interpreting large river systems. *Earth Planet. Sci. Lett.*, 454, 92–102.

Almeida, R.P., Freitas, B.T., Turra, B.B., Figueiredo, F.T., Marconato, A. and Janikian, L. (2016b) Reconstructing fluvial bar surfaces from compound cross-strata and the interpretation of bar accretion direction in large river deposits. *Sedimentology*, 63, 609–628.

Amsler, M.L. and Prendes, H.H. (2000) Transporte de sedimentos y processes fluviales associados. In: *El Río Paraná em su trama médio, Contribuicíon al conocimiento y practicas ingenieriles en un gran río de llanura* (Eds. C. Paoli and M. Schreider), pp. 233–305. Santa Fé, Universidad Nacional del Litoral.

AGÊNCIA NACIONAL DE ÁGUAS (ANA) – Brazilian Water Agency. HidroWeb: sistemas de informações hidrológicas. At: http://hidroweb.ana.gov.br/HidroWeb (October 2016).

Ashley, G.M. (1990) Classification of large-scale subaqueous bedforms: a new look at an old problem. *J. Sed. Petrol.*, 60, 160–172.

Best, J.L. and Kostaschuck, R. (2002) An experimental study of turbulent flow over a low-angle dune. *J. Geophys. Res.*, 107, 18-1–18-19.

Best, J.L., Ashworth, P.J., Sarker, M.H., and Roden, J.E. (2007) The Brahmaputra-Jamuna River, Bangladesh. In: *Large rivers: Geomorphology and management* (Ed. A. Gupta), pp. 395–433. Sussex, Wiley InterScience.

Bradley, R.W. and Venditti, J.G. (2017) Reevaluating dune scaling relations. *Earth-Sci. Rev.*, 165, 356–376.

Brookfield, M.E. (1977) The origin of bounding surfaces in ancient aeolian sandstones. *Sedimentology*, 24, 303–332.

Carling, P.A., Williams, J.J., Gölz, E. and Kelsey, A.D. (2000) The morphodynamics o fluvial sand dunes in the River Rhine, near Mainz, Germany. II. Hydrodynamics and sediment transport. *Sedimentology*, 47, 253–278.

Coleman, J.M. (1969) Brahmaputra river: Channel processes and sedimentation. *Sed. Geol.*, 3, 129–239.

Conaghan, P.J. and Jones, J.G. (1975) The Hawkesbury Sandstone and the Brahmaputra: a depositional model for xontinental sheet sandstones. *J. Geol. Soc. Aust.*, 22, 275–283.

De Reu, J., Bourgeois, J., Bats, M., Zwertvaegher, A., Gelorini, V., De Smedt, P., Chu, W., Antrop, M., De Maeyer, P., Finke, P., Van Meirvenne, M., Verniers, J. and Crombé, P. (2013) Application of the topographic position index to heterogeneous landscapes. *Geomorphology*, 186, 39–49.

Dinehart, R.L. (1989) Dune migration in a steep, coarse-bedded stream. *Water Resour. Res.*, 25, 911–923.

Ernstsen, V.B., Noormets, R., Winter, C., Hebbeln, D., Bartholomä, A., Flemming, B.W., Bartholdy, J. (2006) Quantification of dune dynamics during a tidal cycle in an inlet channel of the Danish Wadden Sea. *Geo Mar. Lett.*, 26, 151–163.

Fielding, C.R. (2007) Sedimentology and stratigraphy of Large River Deposits: recognition in the ancient record, and distinction from 'Incised Valley Fills'. In: *Large Rivers: Geomorphology and Management* (Ed. A. Gupta), pp. 97–113. Sussex, Wiley InterScience.

Gallant, J.C. and Wilson, J.P. (2000) Primary topographic attributes. In: *Terrain Analysis: Principles and Applications* (Eds. J.P. Wilson and J.C. Gallant), pp. 51–86. New York, John Wiley and Sons.

Gupta, A. (2007) Introduction. In: *Large rivers: geomorphology and management*. (Ed. A. Gupta), pp. 1–5. Sussex, Wiley InterScience.

Harbor, D.J. (1998) Dynamics of bedforms in the Lower Mississippi River. *J. Sed. Res.*, 68, 750–762.

Haszeldine, R.S. (1982) Descending tabular cross-bed sets and bounding surfaces from a fluvial channel in the Upper Carboniferous of North-East England. *J. Sed. Petrol.*, 53, 1233–1247.

Hendershot, M.L., Venditti, J.G., Bradley, R.W., Kostaschuck, R.A., Church, M. and Allison, M.A. (2016) Response of low-angle dunes to variable flow. *Sedimentology*, 63, 743–780.

Horbe, A.M.C., Motta, M.B., Almeida, C.M., Dantas, E.L. and Vieira, L.C. (2013) Provenance of Pliocene and recent sedimentary deposits in western Amazonia, Brazil: consequences for the paleodrainage of the Solimões-Amazonas River. *Sed. Geol.*, 296, 9–20.

Hovius, N. (1998) Controls of sediments supply by large rivers. In: *Relative Role of Eustasy Climate and Tectonism in Continental Rocks* (Eds. K. Shanley and P. McCabe). *SEPM Spec. Publ.*, 59, 3–16.

Hubbard, S.M., Smith, D.G., Nielsen, H., Leckie, D.A., Fustic, M., Spencer, R.J. and Bloom, L. (2011) Seismic geomorphology and sedimentology of a tidally influenced river deposit, Lower Cretaceous Athabasca oil sands, Alberta, Canada. *AAPG Bull.*, 95, 1123–1145.

Huizinga, R.J. (2010) Bathymetric surveys at highway bridges crossing the Missouri River in Kansas City, Missouri, using a multibeam echo sounder, 2010. *U.S. Geol. Surv. Scientific Investigations Report*, 2010–5207, 61 pp.

Jackson, R.G. II (1976) Largescale ripples of the lower Wabash River. *Sedimentology*, 23, 593–623.

Jablonski, B.V.J. and Dalrymple, R.W. (2016) Recognition of strong seasonality and climatic cyclicity in an ancient, fluvially dominated, tidally influenced point bar: Middle McMurray Formation, Lower Steepbank River, north-eastern Alberta, Canada. *Sedimentology*, 63, 552–585.

Julien, P.Y. and Klaassen, G.J. (1995) Sand-dune geometry of large rivers during floods. *J. Hydraul. Eng.*, 121, 657–663.

Kostaschuck, R.A. and Villard, P.V. (1996) Flow and sediment transport over large subaqueous dunes: Fraser River, Canada. *Sedimentology*, 30, 727–742.

Latrubesse, E.M., Stevaux, J.C. and Sinha, R. (2005) Tropical rivers. *Geomorphology*, 70, 187–206.

Leclair, S.F. (2011) Interpreting fluvial hydromorphology from the rock record: large-river peak flows leave no clear signature. In: *From River to Rock Record: the Preservation of Fluvial*

Sediments and Their Subsequent Interpretation (Eds. S.K. Davidson, S. Leleu and C. P. North), *SEPM Spec. Publ.*, 97, 113–123.

LeClair, S.F. and Bridge, J.S. (2001) Quantitative interpretation of sedimentary structures formed by river dunes. *J. Sed. Res.*, 71, 713–716.

Leclair, S.F. and Bridge, J.S. (1997) Preservation of cross-strata due to migration of subaqueous dunes over aggrading and non-aggrading beds: comparison of experimental data and theory. *Geosci. Can.*, 24, 55–66.

Lunt, I.A. and Bridge, J.S. (2007) Formation and preservation of open-framework gravel strata in unidirectional flows. *Sedimentology*, 54, 71–87.

Miall, A.D. (2006) How do we identify big rivers? And how big is big? *Sed. Geol.*, 186, 39–50.

Miall, A.D. and Jones, B.G. (2003) Fluvial architecture of the Hawkesbury Sandstone (Triassic), near Sydney, Australia. *J. Sed. Res.*, 73, 531–545.

Nittrouer, J.A., Mohrig, D., and Allison, M.A. (2011) The lowermost Mississippi River: a mixed bedrock-alluvial channel. *Sedimentology*, 58: 1914–1934.

Paola, C. and Borgman, L. (1991) Reconstructing topography from preserved stratification. *Sedimentology*, 33, 553–565.

Parsons, D.R., Best, J.L., Orfeo, O., Hardy, R.J., Kostaschuk, R. and Lane, S.N. (2005) Morphology and flow fields of three-dimensional dunes, Rio Paraná, Argentina: results from simultaneous multibeam echo sounding and acoustic Doppler current profiling. *J. Geophys. Res.*, 110, F04S03 1–9.

Potter, P.E. and Hamblin, W.K. (2006) Big Rivers Worldwide: Part 1 Origins: Provo, Utah, Brigham Young University, *Geology Studies*, 48, 78 pp.

Reesink, A.J.H., and Bridge, J.S. (2007) Influence of superimposed bedforms and flow unsteadiness on formation of cross strata in dunes and unit bars. *Sed. Geol.*, 202, 281–296.

Reesink, A.J.H., and Bridge, J.S. (2009) Influence of bedform superimposition and flow unsteadiness on the formation of cross strata in dunes and unit bars—Part 2, further experiments. *Sed. Geol.*, 222, 274–300.

Reesink, A.J.H., and Bridge, J.S. (2011) Evidence of bedform superimposition and flow unsteadiness in unit-bar deposits, South Saskatchewan River, Canada. *J. Sed. Res.*, 81, 814–840.

Reesink, A.J.H., Ashworth, P.H., Sambrook Smith, G.H., Best, J.L., Parsons, D.R., Amsler, M.L., Hardy, R.J., Lane, S.N., Nicholas, A.P., Orfeo, O., Sandbach, S.D., Simpson, C.J., Szupiany, R.N. (2014) Scales and causes of heterogeneity in bars in a large multi-channel river: Río Paraná, Argentina. *Sedimentology*, 61, 1055–1085.

Reesink, A.J.H., Van den Berg, J.H., Parsons, D.R., Amsler, M.L., Best, J.L., Hardy, R.J., Orfeo, O., Szupiany, R.N. (2015) Extremes in dune preservation: controls on the completeness of fluvial deposits. *Earth-Sci. Rev.*, 150, 652–665.

Rossetti, D.F., Toledo, P.M. and Góes, A.M. (2005) New geological framework for Western Amazonia (Brazil) and implications for biogeography and evolution. *Quatern. Res.*, 63, 78–89.

Rubin, D.M. and Hunter, R.E. (1982) Bedform climbing in theory and nature. *Sedimentology*, 29, 121–138.

Rust, B.R. and Jones, B.G. (1987) The Hawkesbury Sandstone south of Sydney, Australia: Triassic analogue for the deposit of a large, braided river. *J. Sed. Petrol.*, 57, 222–233.

Sambrook Smith, G.H., Ashworth, P.J., Best, J.L., Lunt, I.A., Orfeo, O., and Parsons, D.R. (2009) The sedimentology and alluvial architecture of a large braid bar, Río Paraná, Argentina. *J. Sed. Res.*, 79, 629–642.

Sambrook Smith, G.H., Best, J.L., Orfeo, O., Vardy, M.E., and Zinger, J.A. (2013) Decimeter-scale in situ mapping of modern cross-bedded dune deposits using parametric echo sounding: A new method for linking river processes and their deposits. *Geophys. Res. Lett.*, 40, 3883–3887.

Strasser, M.A. (2002) Estudo da geometria das formas de fundo no curso médio do Rio Amazonas. MSc. Dissertation, Universidade Federal do Rio de Janeiro, Rio de Janeiro, 100 pp.

Strasser, M.A. (2008) Dunas fluviais no rio Solimões–Amazonas – dinâmica e transporte de sedimentos. Ph.D. Thesis, Universidade Federal do Rio de Janeiro, Rio de Janeiro, 148 pp.

Van den Berg, J.H. (1987) Bedform migration and bedload transport in some rivers and tidal environments. *Sedimentology*, 34, 681–698.

Wang Z., Chen, Z., Shi, Y., Li, M., Zhang, Q. and Wei, T. (2007) Fluvial bedforms and hydrodynamic controls along the Mid-Lower Yangtze channel. *Science in China (Series D)*, 37, 1223–1234. (in Chinese)

Wilbers, A.W.E. and Ten Brinke, W.B.M. (2003) The response of subaqueous dunes to floods in sand and gravel bed reaches of the Dutch Rhine. *Sedimentology*, 50, 1013–1034.

Wignall, P.B. and Best, J.L. (2000) The Western Irish Namurian Basin reassessed. *Basin Res.*, 12, 59–78.

Yalin, M.S. (1964) Geometrical properties of sand waves. *Proc Am. Soc. Civ. Engnrs., J. Hydraulics Division*, HY5, 105–119.

VI. CONCLUSIONS

The present work aimed at contributing to two challenging subjects in fluvial sedimentology: the recognition of channel pattern and of large river deposits in the rock record. Although both subjects have been studied for decades, there is still a significant margin for improvement with many gaps to be filled. Despite the numerous works, criteria for the recognition of channel patterns in fluvial deposits have been considered by some researchers to be overall ineffective; such difficulties are also attributable to the current stage of works on channel pattern classification, marked by a lack of consensus among different research groups concerning terminology. Difficulties concerning large rivers are of different nature, being mainly related to the intrinsic difficulties of studying these large depositional systems; only recently geophysics provided tools that allow detailed studies of such large water bodies and their respective riverbeds. The mentioned challenges were addressed in the present work by conducting a survey of alluvial river at a global scale to quantify the natural variability of rivers and by surveying the Solimões-Amazon River, the largest river in the world, with state-of-the-art geophysical methods.

By surveying more than 350 reaches of alluvial rivers with available water discharge data at a global scale, this work presents an improved channel pattern classification developed to be applicable to the rock record, based on quantitative parameters of sinuosity and channel count index. Channel patterns are here organized in four groups: high-sinuosity single channel (meandering); high-sinuosity moderately-braided channels; low-sinuosity moderately-braided channels; and low-sinuosity multichannels (braided), where the moderately-braided channels occur at intermediate stream power compared to meandering (low stream power) and braided (high stream power) channels. Meandering rivers are the most frequent channel pattern in Earth’s surface, but they are mostly small rivers with catchment areas, large rivers commonly present moderately-braided channels (Chapter III).

Sedimentologists studying the rock record have mainly recognized fluvial deposits of meandering and braided channels, with a clear majority of braided channel occurrence. The fact that meandering channels are ubiquitous in the world but mostly occur in small rivers might explain the apparent contradiction of the relative lack of documentation of meandering rivers compared to braided rivers in the rock record in spite of their frequency and also indicate a bias towards preservation of larger rivers. However, the extensive interpretation of braided channel deposits contrasts with the apparent scarcity of braided rivers in modern setting, and with the fact that their occurrence is restricted to conditions of high stream power, high slopes, and smaller drainage basin areas, being also the only channel pattern restricted to a specific discharge regime of high seasonality. The extensive interpretation of braided channel patterns for these deposits could thus indicate a bias of preservation towards braided channel forming conditions, but it could also indicate that moderately-braided rivers, which are dominant among modern large rivers, have been severely under-reported. Given the frequency of the moderately-braided channel pattern in large rivers with large drainage basins areas, and the extensive occurrence of large rivers in the rock record we advocate towards a reevaluation of the many fluvial deposits interpreted of braided and meandering river deposits (Chapter III).

A classification based on sinuosity and channel count index allows to establish criteria of recognition applicable to the rock record that rely on quantitative paleocurrent variance at the scale of the channel belt. Preserved barforms in the floodplains of more than 100 modern rivers were used to infer and quantify paleoflow directions at the channel belt scale, which resulted in ranges of paleocurrent variance that may lead to channel pattern identification in the rock record. Braided channels have the lowest paleocurrent variances, whereas meandering channels have the highest; in between are the variances of moderately braided channels, the high-sinuosity type displaying higher values than the low-sinuosity type. The continuum of channel patterns trends of increase in stream power matched by decrease in sinuosity and increase in channel count index are also successfully revealed by the method. (Chapter III).

Geophysical surveys of the Amazon River resulted in important contributions for the recognition of large rivers in the rock record. High-resolution multibeam echo sounder bathymetric maps of the riverbed reveal that small dunes are frequent in large rivers, suggesting significant implications for interpretations of fluvial deposits, since the presence of large sets of cross-strata has been thought to be the most common attribute needed to recognize the deposits of large rivers. Although very large dunes do occur in the riverbed, such dunes commonly present low leeside angles covered by a great number of small dunes on both stoss and leesides. These bedforms also occur in other large rivers, and the common presence of small dunes in both shallow and deep channels indicates that large river deposits may principally comprise bedform elements that are similar to those found within small rivers, which may be misleading when interpreting the rock record, ushering the need for additional criteria (Chapter IV).

Associated with the analysis of satellite imagery, geophysical surveys of the Amazon River allow the proposition of a facies model for large rivers, since many large rivers share a similar channel patterns here named moderately braided. Through high-resolution bathymetric maps and shallow seismic and GPR profiles, the examples of different parts of the depositional system were detailed, leading to inferences of their preservation as fluvial deposits and additional criteria for recognition of large rivers, such as vertical trends of cross-strata set and coset thickness, cross-strata leeside angle and grainsize (Chapter V).

This work reinforces the need for studying the transitional channel patterns and encourages researchers to take a step beyond the meandering-braided channel dichotomy when studying fluvial deposits and investigate the greater complexity and sedimentological outcomes of the other channel types. Moderately-braided channels are the most likely to represent the greatest transcontinental fluvial systems, being also the most significant agent of sediment transport and mass movement on Earth. Results of this work put at stake research on fluvial sedimentology, who so far has explored meandering and braided channels with a great amount of valuable details, but has left aside the other types.

ATTACHMENTS

Sedimentology (2018) doi: 10.1111/sed.12471

The significance of superimposed dunes in the Amazon River: Implications for how large rivers are identified in the rock record

CRISTIANO P. GALEAZZI*, RENATO P. ALMEIDA*†, CARLOS E. M. MAZOCA*, JIM L. BEST‡, BERNARDO T. FREITAS§, MARCO IANNIRUBERTO¶, JULIA CISNEROS** and LARISSA N. TAMURA*

**Instituto de Geociências, Universidade de São Paulo, Rua do Lago, 562, Cidade Universitária, São Paulo, SP 05508-900, Brazil (Email: cristiano.galeazzi@usp.br)*

†Instituto de Energia e Ambiente, Universidade de São Paulo, Av. Prof. Luciano Gualberto, 1289, Cidade Universitária, São Paulo, SP 05508-900, Brazil

‡Departments of Geology, Geography & GIS Mechanical Science and Engineering, Ven Te Chow Hydrosystems Laboratory, University of Illinois, 1301 West Green Street, Champaign, IL 61801, USA

§Faculdade de Tecnologia, Universidade Estadual de Campinas, R. Paschoal Marmo, 1888, Limeira, SP 13484-332, Brazil

¶Instituto de Geociências, Universidade de Brasília, Campus Universitário Darcy Ribeiro, Brasília, DF 71900-000, Brazil

***Department of Geology, University of Illinois, 1301 West Green Street, Champaign, IL 61801, USA*

ABSTRACT

The recognition of large fluvial channels in the geological record is of great importance for regional palaeohydraulic and palaeogeographical reconstructions, inputs to reservoir modelling, and estimating the input of sediment to sedimentary basins, with consequent larger-scale implications for modelling basin fill. However, available criteria for the interpretation of the scale of ancient fluvial systems are still poorly tested, particularly the widely-adopted assumption that the abundance of large-scale dunes in some deep channels implies that abundant large-scale cross-strata sets will be preserved in similar palaeochannels. To test this hypothesis, high-resolution multibeam echo-sounding imaging of two reaches in the Amazon River where large dunes are common were investigated, yielding an extensive dataset concerning dune geometry, position within the channel and, most importantly, the presence and distribution of smaller superimposed dunes on their lee sides. These results show that despite 90% of the bedforms at water depths >20 m being constituted by up to 12·2 m high compound dunes, 94% of the lee sides of these dunes are covered by smaller superimposed dunes. These results suggest that steep avalanche foresets that are several metres in height may be rare in the preserved stratigraphic record of these large channels, which are instead more commonly represented by decimetre-scale cross-stratified cosets formed by superimposed dunes migrating down the lee side of the large-scale host bedforms. This observation thus suggests that the recognition of compound dune cosets is key to the interpretation of river-channel scale, since compound dunes are the principal bedform in most large river channels. Consequently, successions dominated by decimetre-scale thick cross-strata sets, but that show rarer preservation of outsized metre-scale avalanche foresets, and abundant similar-sized cosets near the base of fining-upward cycles are probably the most common bedform record of large-river channels.

Keywords Amazon River, large river bedforms, large river deposits, low-angle compound dunes, MBES, superimposed dunes.

INTRODUCTION

Current fluvial facies models are dominated by data and conceptualizations derived mainly from studies of small fluvial systems. Large rivers, defined by large drainage area, channel length and water and sediment discharges (Hovius, 1998; Potter & Hamblin, 2006; Gupta, 2007), have been relatively neglected, largely due to their inaccessibility, deep turbid flows, challenging logistics and often harsh climate, because they are mainly concentrated in the very hot and wet regions of the world (Latrubesse *et al.*, 2005). These conditions have resulted in a comparative paucity of studies that have focused on the description of subaqueous bedforms in such large rivers, whose investigation requires deployment of 'state of the art' geophysical techniques.

Until recently, the investigation of river beds relied exclusively on two-dimensional bathymetric profiles (for instance, see the studies of Strasser, 2002, 2008, in the Amazon River; and Leclair, 2011, in the Mississippi River), thus limiting the understanding of bedform morphology and kinematics. However, since the beginning of the last decade, Multibeam Echo-Sounder (MBES) surveys have revolutionized current ability to achieve high-resolution quantification of the three-dimensional subsurface bathymetry (Parsons *et al.*, 2005; Nittrouer *et al.*, 2011). This new quantification within large-scale fluvial channels has allowed examination of the relationship between processes and products, and enabled questioning of some long-held assumptions. For instance, dune size has often been proposed to scale with water depth (Yalin, 1964; Allen, 1984; Ashley, 1990; Paola & Borgman, 1991; LeClair & Bridge, 2001), and proposed facies models for large rivers have related the occurrence of large sets of cross-strata to large-scale channels (Wignall & Best, 2000; Miall, 2006; Fielding, 2007). However, the question arises as to whether large dunes have to be present within an ancient fluvial deposit for the interpretation of a large channel to be made (Best *et al.*, 2007; Leclair, 2011; Reesink *et al.*, 2014; Bradley & Venditti, 2017). In this respect, the presence of small, within-channel, dunes and superimposed dunes on the lee side of larger dunes has been underappreciated in past work on large rivers, which has focused on the occurrence of very large compound dunes, such as those in the Amazon, in northern South America (Strasser, 2002, 2008; Almeida *et al.*, 2016a), Paraná, in southern South America (Amsler & Prendes, 2000; Parsons *et al.*, 2005; Sambrook Smith *et al.*, 2009, 2013; Reesink *et al.*, 2014), Yangtze, in eastern Asia, (Wang *et al.*, 2007), Jamuna, in southern Asia, (Best *et al.*, 2007) and Mississippi, in North America, (Harbor, 1998; Abraham & Pratt, 2002; Leclair, 2011).

Superimposed dunes on top of host dunes have been previously recognized in diverse depositional settings, such as aeolian (Rubin & Hunter, 1982), tidal (Ernstsen *et al.*, 2006) and fluvial (Coleman, 1969; Allen & Collinson, 1974; Jackson, 1976; Dinehart, 1989) environments, and their preserved counterparts have also been identified in the rock record of these diverse settings (Brookfield, 1977; Haszeldine, 1982; Rubin & Hunter, 1982; Almeida *et al.*, 2016a). Regarding the fluvial environment, they have been described in flumes and small rivers (Lunt & Bridge, 2007; Reesink & Bridge, 2007, 2009, 2011) and large rivers (Reesink *et al.*, 2014), being that in these cases the research was related to the effects of the superimposed dunes located on the stoss side of the host dunes. Although the surveyed areas in the Amazon River also display compound dunes with superimposed dunes restricted to the stoss side, this work focuses on the large dunes with superimposed dunes migrating down their lee side, which largely dominate the riverbed. This setting is also observed in the images of previously published works of large rivers in the world (see references above). From the point of view of the sedimentary record, superimposed dunes on the lee side of compound dunes are of great significance since processes taking place in the lee side have greater preservation potential than those on the usually erosional stoss side.

The present paper examines the scale of dunes within the Amazon River, Brazil, in order to quantify the occurrence of different dune sizes within the main channel. The Amazon River ranks first in water discharge, drainage basin area and suspended sediment discharge, amongst the world's great rivers, and is an ideal system in which to examine dune morphometrics and scaling. In this paper, high-resolution MBES images are presented from two reaches of the Amazon River, highlighting the importance of the presence of small, superimposed dunes on the lee side of very large compound dunes migrating within the channel. The dunes of the river bed are described using a range of quantitative parameters, which allow examination of their relationship with large, low-angle compound dunes, and their potential importance in the ancient fluvial record.

LOCATION

In Brazil, the Amazon River is named the Solimões River from the Peruvian border to its confluence with the Rio Negro, near Manaus (Fig. 1), after which it is called the Amazon. The reaches studied herein are located in the Lower Solimões River, just before the confluence with the Rio Negro, and in the Upper Amazon River, about 33 km downstream of the confluence (Fig. 1). In the Lower Solimões River, a bathymetric survey was conducted downstream of Marchantaria Island (Fig. 1) and covered an area of *ca* 10 km^2, where maximum flow depths were 45 m. In the Upper Amazon River, the area surveyed is located near the northern bank of Careiro Island (Fig. 1), and covered an area of *ca* 8 km^2, with a maximum flow depth of 66 m.

The hydraulic characteristics of these two localities are given by two gauging stations maintained by the Brazilian Water Agency (ANA) , which reflect a large variation in water discharge between low (October to December) and high (May to July) flow stages. For the Lower Solimões River, the Manacapuru gauging station, located about 85 km upstream of the surveyed area, shows an average water discharge ranging from *ca* 67 000 (low stage) to 138 000 m^3 s^{-1} (high stage). In the Upper Amazon River, water discharge increases significantly due to the input from the Rio Negro, and at the Jatuarana gauging station, located at the margin of the surveyed area, the average water discharge varies from *ca* 80 000 to 174 000 m^3 s^{-1}. The surveys reported herein were undertaken in July 2015, when the river was at flood stage. Discharge of the precise date or month of when the surveys were conducted is not available; however the historical mean discharge in July at the Manacapuru (available data ranging from January 1972 to July 2013) and Jatuarana (from October 1977 to January 2015) gauging stations are *ca* 133 000 m^3 s^{-1} and 167 000 m^3 s^{-1}, respectively (Fig. 2).

METHODS

High-resolution three-dimensional bathymetry of the river bed was obtained using a Teledyne-Reson Seabat 7101 Multibeam Echo Sounder (MBES; Teledyne RESON A/S, Slangerup, Denmark), operating at a frequency of 240 kHz, with 511 equi-angle beams achieving a maximum vertical measurement resolution of 12·5 mm. The MBES was pole-mounted over the side of the vessel, with positioning and motion reference provided by an SBG Ekinox-E inertial system (SBG Systems S.A.S., Carrières-sur-Seine, France) and Vector VS330 GNSS Receiver with Atlas L-band differential correction service (Hemisphere GNSS Inc., Scottsdale, AZ, USA). In order to attain better beam forming, an AML Micro-X probe equipped with a SV-Xchange sound velocity sensor (AML Oceanographic, Sidney, BC, Canada) was installed close to the MBES sonar head. All sensors were interfaced with the PDS2000 navigation and data acquisition suite (Teledyne RESON). The MBES calibration was carried out following a standard patch test protocol, to compensate for residual installation offsets, and sound velocity profiling of the water column was undertaken on a daily basis using a Valeport Mini sound velocity probe (Valeport Limited, Devon, UK). All soundings were reduced to the water reference level of the Port of Manaus fluviometric station.

The MBES surveys yielded high-resolution digital elevation models (DEM), which were used to quantify dune height, wavelength and lee-side angles, as well as the area occupied by different types of bedforms, using GIS software. The area occupied by the lee sides of the dunes was identified by producing aspect maps that highlighted surfaces dipping in the direction of the river flow. The aspect map of simple and superimposed dunes was computed directly from the original DEM, whereas the lee side of compound dunes was computed using a 33 × 33 pixel moving average window to filter the superimposed dunes. The distinction between lee sides of compound dunes with or without superimposed dunes was accomplished manually.

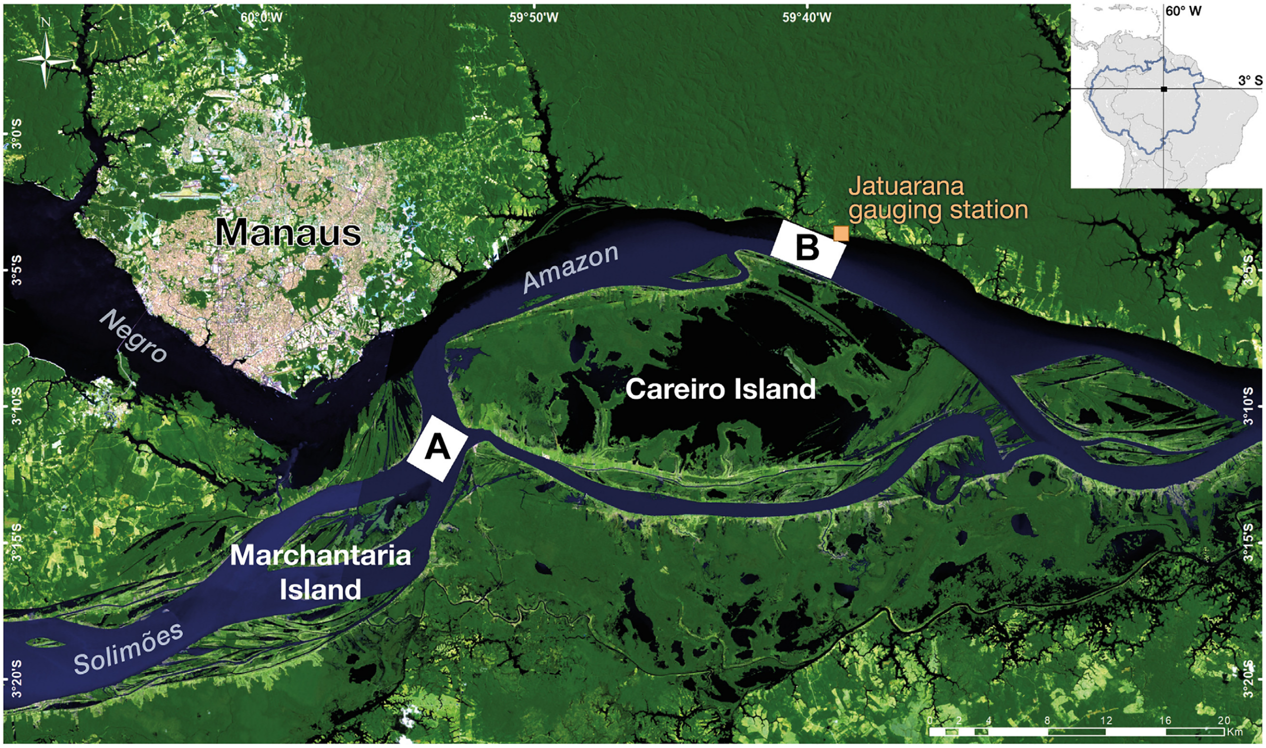

Fig. 1. Location of the surveyed areas in the Lower Solimões (A) and Upper Amazon (B) rivers.

All dune heights and the lee-side angles of compound dunes were measured manually on longitudinal sections in the direction of flow, parallel to the river banks, spaced laterally *ca* 30 to 60 m apart: this yielded 1233 and 1550 measurements of primary and secondary dunes, respectively. Bedform height was defined as the vertical distance from the crest to the trough of the dunes. Wavelength was defined as the horizontal distance between consecutive troughs. The lee-side angles of compound dunes were measured from the base of the lee side to the lowest brinkpoint, excluding low angles related to the asymptotic portions of the lee side at the base of the dune.

The lee-side angles of simple and superimposed dunes were obtained using slope maps produced from the DEM, by quantifying pixels with slope values in the lee-side area of the dunes. In order to avoid measuring pixels from the low-angle upper and lower parts of the lee sides, the morphometric algorithm DEV, or deviation from mean elevation (Gallant & Wilson, 2000; De Reu *et al.*, 2013) was applied with a DEV range of 0·2 to 0·5. Dunes with amplitudes smaller than 0·45 m were excluded from the dataset, since their wavelengths were too close to the horizontal resolution of the DEM to allow accurate slope measurements.

Bed material samples were collected at 12 sites in the Upper Amazon River (Almeida *et al.*, 2016a) and 14 sites in the Lower Solimões River during low flow stage, three months after the MBES survey, using a 10 kg Van Veen grab sampler. Grain-size analyses were performed with a Malvern Mastersizer 2000 (size fractions <1 mm; Malvern Instruments Limited, Malvern, UK) and mechanical sieves (>1 mm).

BEDFORMS IN THE SOLIMÕES AND AMAZON RIVERS

Bedforms quantified from the MBES images were classified into two groups: (i) primary bedforms, represented by simple and compound dunes; and (ii) secondary bedforms, represented by simple superimposed dunes on the stoss and lee sides of the compound dunes, which are the primary, or host, dunes for these secondary bedforms. The term ‘simple dune’ is herein restricted to describe dunes with no superimposed dunes, i.e. contrary to a compound dune. In extent, the superimposed dunes described

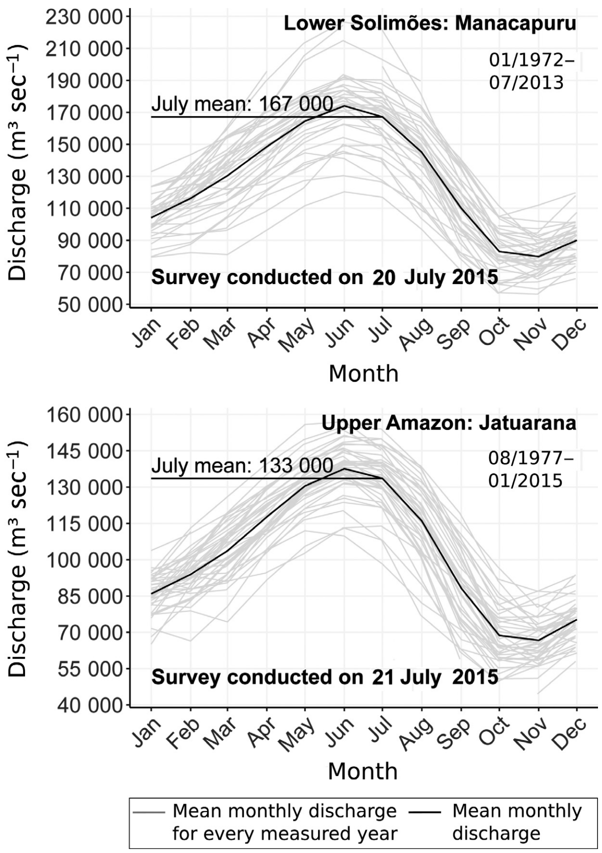

Fig. 2. Monthly discharge for each measured year (grey curves) and mean monthly discharge (black curves) for the Manacapuru (Lower Solimões) and Jatuarana (Upper Amazon) gauging stations.

herein, with quantitative measurements and statistics, are those located in the lee side of the compound dunes.

Both survey areas in the Lower Solimões and Upper Amazon rivers display a thalweg and bank-attached bars on the right channel margin (Fig. 3A and C). The beds largely comprise sand, which forms simple and compound dunes, but also locally possesses bedrock outcrops. Compound dunes always possess superimposed dunes on their stoss side, but also very often on their lee side. The shaded areas in Fig. 3B and D represent the lee sides of compound dunes with (blue) and without (red) superimposed bedforms. Superimposed dunes cover *ca* 94% of the total area of the compound dune lee sides, and thus only *ca* 6% possess slopes at, or near, the angle of repose. The surveyed reaches show similar patterns in their bedform distribution with regard to water depth: (i) shallower areas on the bar tops are characterized by simple dunes, with visual observations at low flow also showing minor upper-stage plane bed or ripples in the shallowest regions; and (ii) deeper areas, represented by the thalwegs and the base of bars, which are dominated principally by very large compound dunes. In deeper areas, the occurrence of simple dunes as primary bedforms is restricted to specific locations that determine the local sediment supply, such as downstream of bedrock pinnacles or downstream of confluence scours. Otherwise, the deeper areas of the channel exhibit only compound dunes. In this way, simple dunes occur as a primary bedform from 10 to 36 m water depth (Fig. 4A), but are present at greater flow depths as a secondary bedform, in the shape of superimposed dunes (Fig. 4B), which are of one order of magnitude smaller than the host dunes (Fig. 4C). Compound dunes develop from 22 m to greater depths, and largely dominate the areas of sedimentation at this depth interval, occupying *ca* 90% of the area.

In terms of morphology, compound dunes commonly display greater dune heights in the central sections, which significantly decrease towards the sides, whereas simple and superimposed dunes show a greater continuity in dune height along their width. In planform, simple dunes commonly possess straight to sinuous crests, mostly perpendicular to the flow, whilst compound dunes display barchanoid, sinuous and straight crests, the latter being oblique or perpendicular to the flow. Superimposed dunes mainly exhibit straight crests that are perpendicular to the flow. In a profile view, compound dunes are flatter than simple dunes, as expressed by a lower dune form index (height/wavelength), being 0·03 for compound dunes and 0·05 for simple dunes (Fig. 4D). Simple and compound dunes commonly exhibit convex shapes with an average of 39% of the wavelength occupied by the lee side. Superimposed dunes display convex shapes or planar tops, with an average of 58% of the wavelength occupied by the lee side (Fig. 5).

Bedform data from both reaches were analyzed to determine dune height, wavelength, lee-side angle and grain size using a classification split into three water depth intervals: shallower than 20 m, between 20 m and 40 m, and deeper than 40 m. Statistics regarding superimposed dunes relate to those located in the lee side of compound dunes. Dunes whose sediment supply was affected by bedrock pinnacles or confluent flows were not included in this statistical analysis.

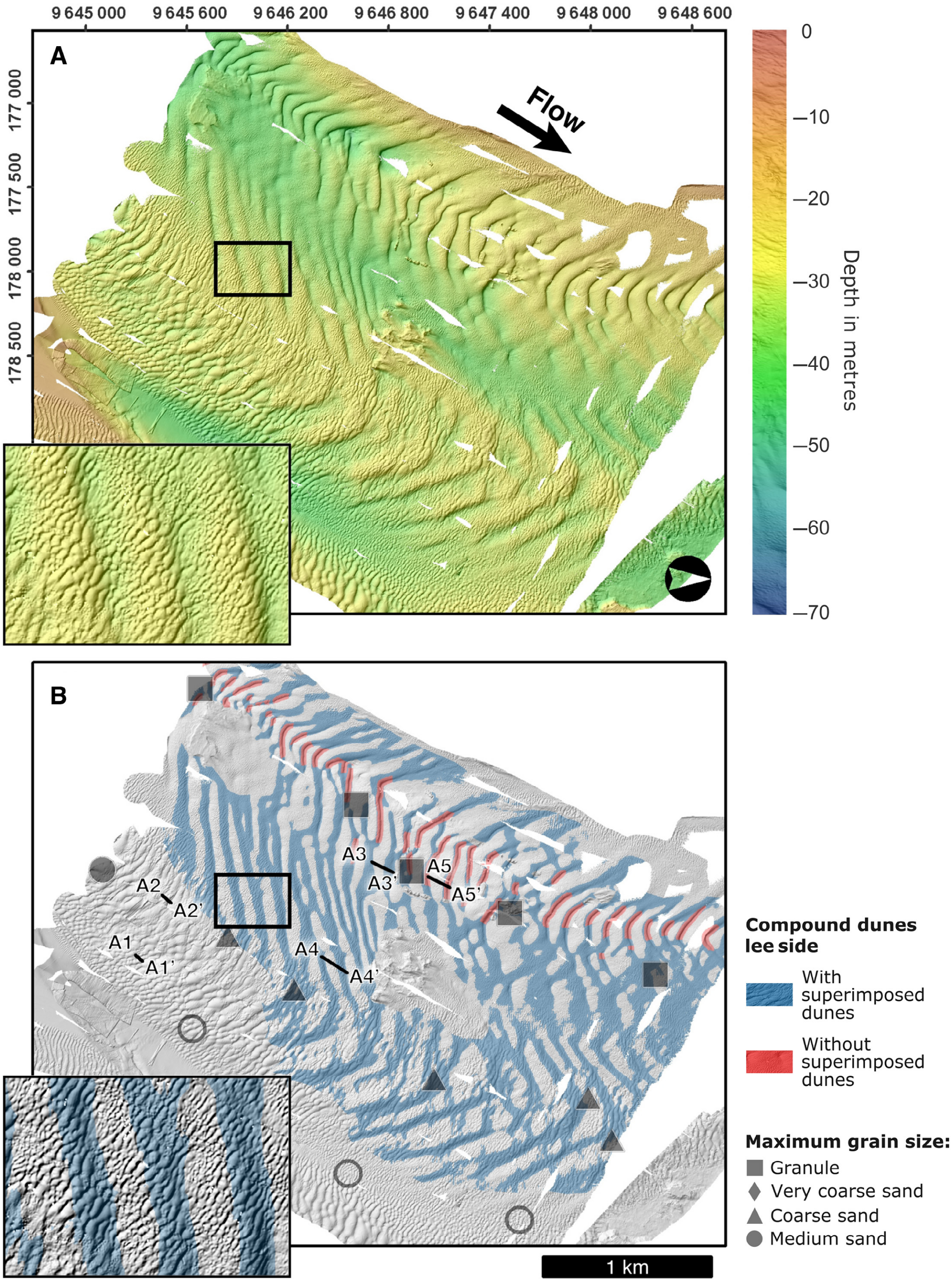

Fig. 3. Multibeam Echosounder (MBES) bathymetric map of survey areas in: (A) Lower Solimões River; and (C) Upper Amazon River. In the detailed inset boxes, large compound dunes are highlighted, which possess superimposed dunes on their lee sides; (B) and (D) highlight the lee sides of compound dunes with (blue), or without (red), superimposed dunes, and indicate the location of the longitudinal sections shown in Fig. 4 as well as bed sediment sampling areas. Empty symbols indicate samples collected from downstream of scours or bedrock protrusions. The inset boxes illustrate the same compound dunes as shown in (A) and (B).

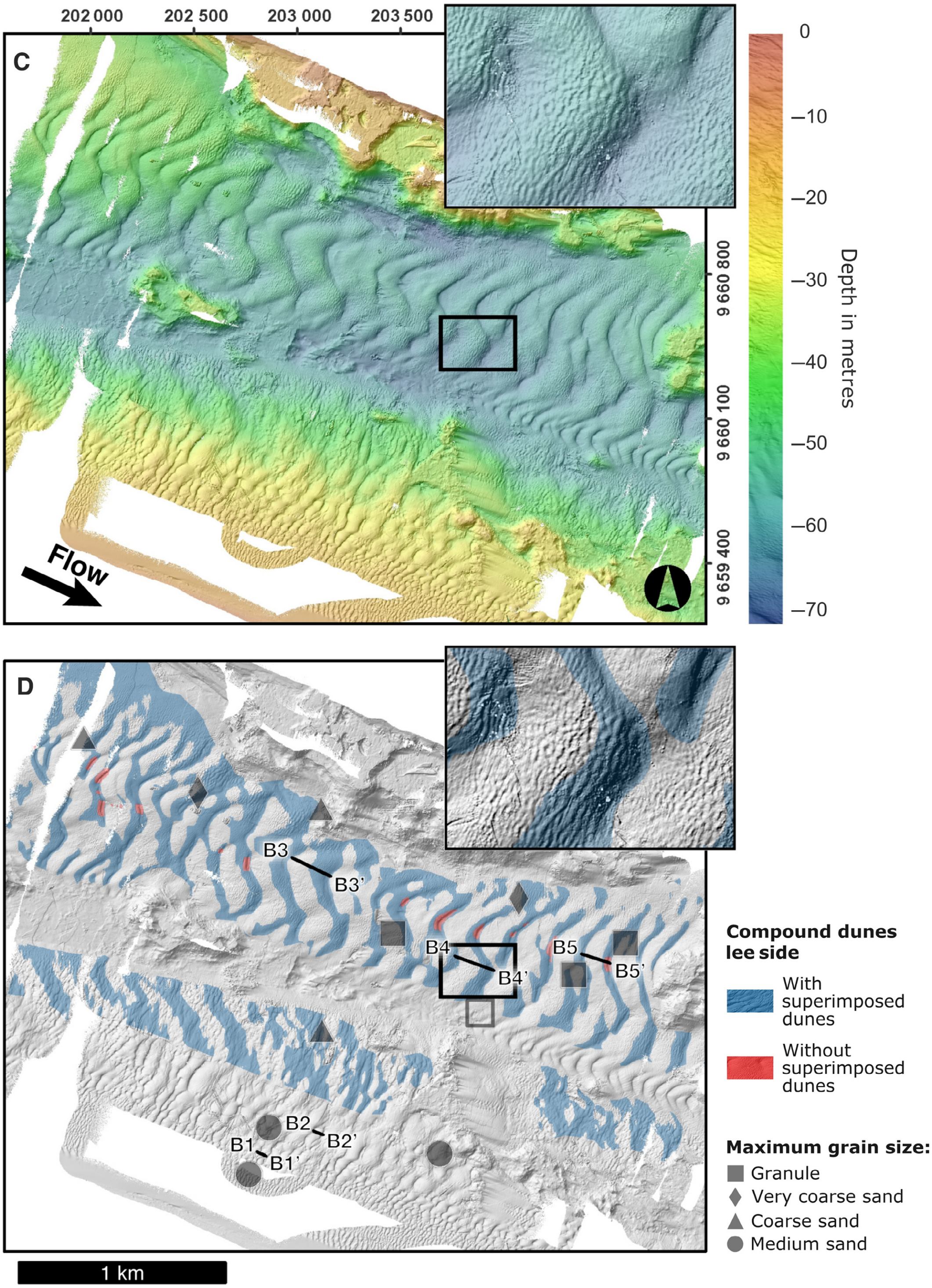

Fig. 3. Continued.

Dune height

The dune height data for the primary simple and compound bedforms show that maximum dune height increases at greater water depths (Fig. 6A, note that outliers are not included; for maximum dune heights see Fig. 3). However, the minimum dune height does not increase with water depth, thus yielding a wider scatter in the data at greater water depths. At flow depths shallower than 20 m, only primary simple dunes occur, and are limited to a maximum height of 1·4 m, with a mean of 0·5 m. From 20 to 40 m flow depth, the primary simple dunes become larger, as shown by mean and maximum dune heights of 1·7 m and 4·7 m, respectively. At this same depth interval, compound (and therefore superimposed) dunes are also present, with mean and maximum heights of 3·3 m and 8·7 m, respectively. At water depths deeper than 40 m, compound dunes reach a mean height of 4·4 m and maximum amplitude of 12·2 m.

These data also show that, contrary to the size of the primary bedforms, the size of superimposed dunes on the lee side of the compound dunes does not change significantly with water depth, and that they exhibit a contrasting height compared to their host compound dunes (Fig. 6A). From 20 to 40 m in depth, superimposed dunes show a mean height of 0·6 m, reaching a maximum value of 4 m, whereas at depths >40 m, the mean dune height is 0·7 m, with a maximum of 3·1 m. At both depth intervals, 70% of these dunes are smaller than 1 m in height, averaging about 15% of the height of the host dune. From 20 to 40 m in depth, the average is of about 18%, varying from 1 to 57%, whereas below 40 m, average is of about 12%, varying from 2 to 56%.

Lee-side angle

The lee-side angles of primary bedforms show different values, with simple dunes being characterized by steeper lee-side angles than compound dunes (Fig. 6B). At water depths shallower than 20 m, simple dunes possess mean lee-side angles of 16°, with 48% and 15% of values being steeper than 15° and 21°, respectively. Between 20 m and 40 m flow depth, simple dunes show a mean angle of 18°, with 60% and 27% of values being steeper than 15° and 21°, respectively. However, at flow depths between 20 m and 40 m, compound dunes show a mean lee-side angle of 9°, with 78% of values below 15°. At flow depths deeper than 40 m, compound dunes possess a

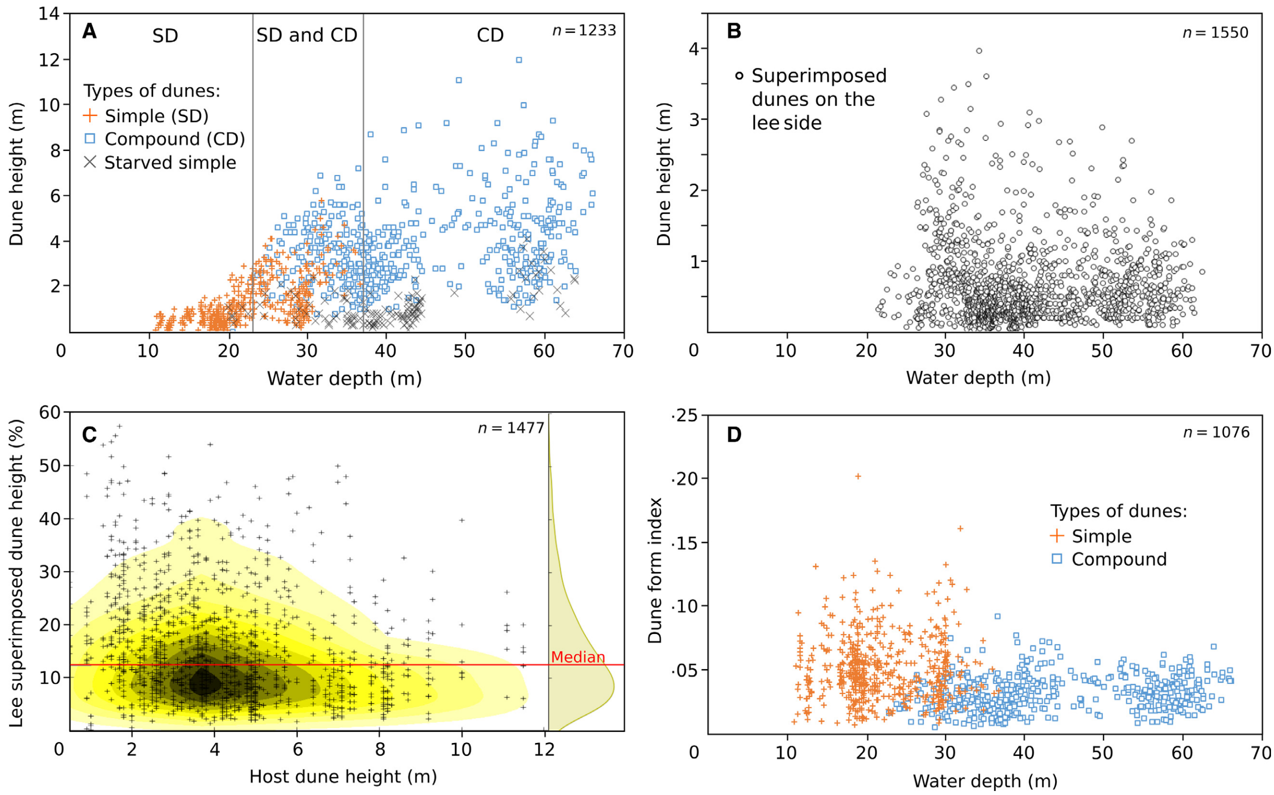

Fig. 4. Dune height versus water depth for: (A) primary dunes, including simple dunes from the shallow channel and compound dunes from the deep channel; and (B) secondary bedforms, which include superimposed dunes on the lee side of the compound dunes. (C) Height of superimposed dunes in relation to the height of their respective host dunes, with contours representing the two-dimensional density plot and a median (red line). To the right, the frequency density for the *y*-axis. (D) Relationship between dune form index (height/wavelength) and water depth for the primary bedforms.

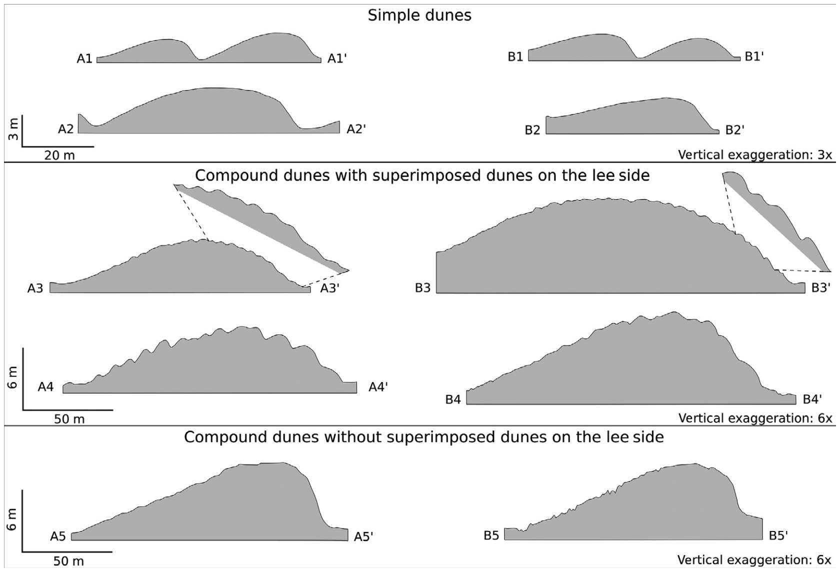

Fig. 5. Longitudinal sections of simple and compound dunes. Location of the sections is shown in Fig. 3.

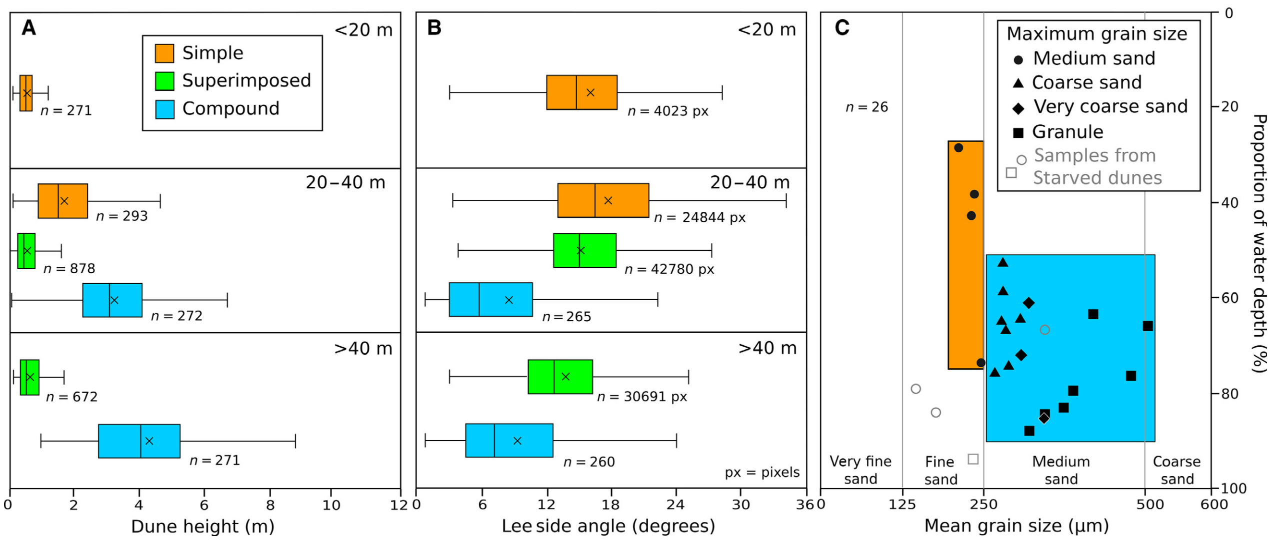

Fig. 6. Distribution of: (A) dune height; (B) lee-side angle; and (C) mean and maximum grain size at different water depth intervals for simple, compound and superimposed dunes. Boxplots in (A) and (B) do not include outliers. Open symbols in (C) indicate samples from starved dunes downstream of confluence or bedrock outcrops.

mean lee-side angle of 10°, with 79% of these slopes being below 15°.

The lee-side angle of superimposed dunes is also steeper compared to the host compound dunes, although it is more gentle than the primary simple dunes. At water depths between 20 m and 40 m, dunes display a mean lee-side angle of 16°, with 51% and 14% of values steeper than 15° and 21°, respectively. At flow depths >40 m, the superimposed dunes have a mean lee-side angle of 14°, with 33% of slopes steeper than 15° and 9% greater than 21°.

Compound dunes of all morphologies display superimposed dunes on their lee side at any given height and grain size, but the lee-side angle of compound dunes is nearly always below 15 to 18° when lee side bedform superimposition is present (Fig. 7). At greater lee-side angles, superimposed dunes are rarely present, and here the lee sides are probably dominated by avalanching. In the present data, such steeper-angled lee sides with sediment avalanching occur almost exclusively associated with barchanoid compound dunes. Low lee-side angles are very common in compound dunes, thus implying that these possess abundant superimposed dunes downclimbing their lee faces (Fig. 3).

Grain size

The mean grain size of both surveyed reaches (see Fig. 3 for location) ranges from 0·148 to 0·505 mm (Fig. 6C). Mean and maximum grain sizes show a strong relationship with the type of primary bedform, with simple dunes possessing a mean grain size from 0·148 to 0·247 mm (fine sand), reaching a maximum size of medium sand, whereas compound dunes have mean grain sizes of 0·271 to 0·505 mm (medium to coarse sand), reaching a maximum size of granules. Coarser grain sizes are also related to greater water depths within the channels, particularly regarding maximum grain size.

DISCUSSION

Since bedform height controls the thickness of the resulting cross-strata sets as a partial preservation of the original foreset (Paola & Borgman, 1991; LeClair & Bridge, 2001; Leclair, 2011; Reesink *et al.*, 2015), the results presented herein imply that there may be predictable trends in the distribution of cross-strata set thickness for the deposits of large rivers in the rock record. The basic assumption of previous research that recognized large river deposits in the rock record is that the abundance of large dunes is reflected in a high proportion of large-scale cross-strata sets in the rock record (Miall, 2006; Fielding, 2007). However, a previous work by Reesink *et al.* (2014) challenged this view, showing large river deposits from the Rio Paraná dominated by small dunes and ripples. The here presented results from the world's largest fluvial channel show that, even in the thalweg of an exceedingly larger and deeper river, the dominant bedforms are smaller than what would be expected, since superimposed dunes are remarkably common on both stoss and lee sides of large compound dunes in the deep channels of the Amazon and Solimões rivers (Fig. 3). The implications of this finding are important for the interpretation of channel size based on cross-strata set thickness in the rock record, since the preserved sets would be formed by the migration of these superimposed bedforms down the lee side of host dunes, resulting in low-angle cosets instead of single large-scale cross-strata sets (Brookfield, 1977; Haszeldine, 1982; Almeida *et al.*, 2016a,b).

Recent works have shown that palaeodepth estimations from cross-strata set thickness in outcrops, based on the assumption that dune height scales with water depth, may be problematic (Best *et al.*, 2007; Leclair, 2011; Reesink *et al.*, 2014; Bradley & Venditti, 2017). The data presented herein confirm that, at any depth, there is a wide range of possible dune heights (Fig. 4A and B). The relationship of dune height and water depth in the Amazon River is particularly similar to that observed in the Jamuna River (Best *et al.*, 2007): despite a wide range of dune heights at any water depth, there is an evident scaling of the maximum dune height, which is about 20% and 30% of the water depth, in the case of the Amazon and Jamuna rivers, respectively.

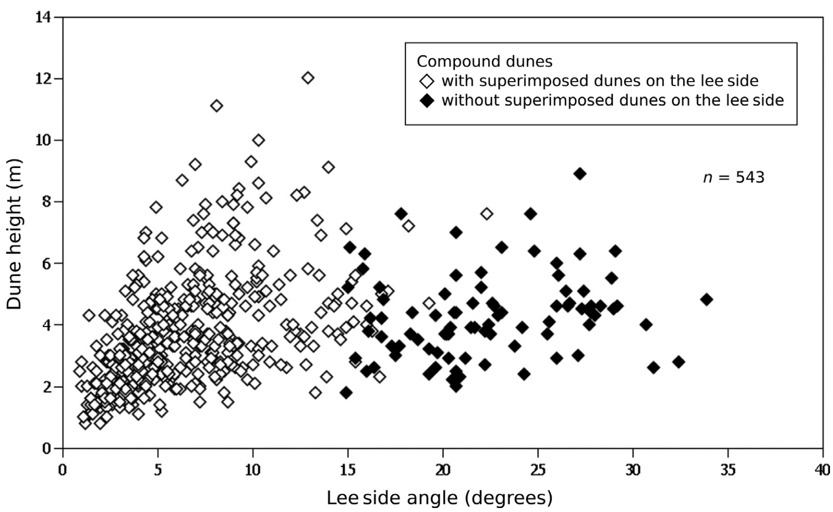

Fig. 7. Relationship between compound dune height, lee-side angle and the occurrence of superimposed dunes on the lee side.

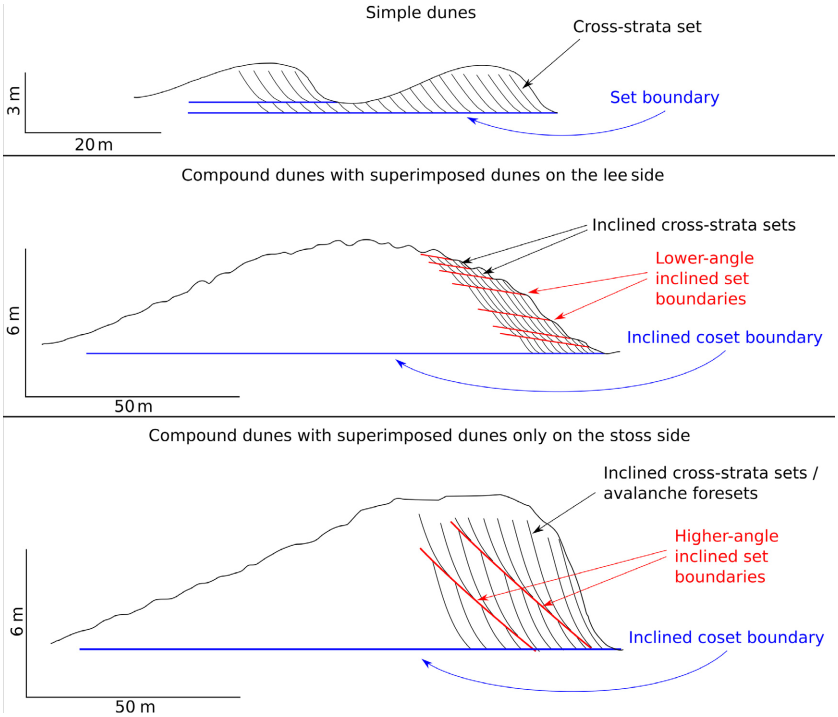

Fig. 8. Expected sedimentary structures for the simple dunes, in the shallow channel, and for the compound dunes with and without superimposed dunes on the lee side, in the deep channel.

The dominance of superimposed dunes on the lee side of the compound dunes is of great significance for the sedimentary record. Previous work on compound dunes in both aeolian and fluvial deposits has shown the effects on the sedimentary structures of superimposed dunes located on the stoss side (Reesink & Bridge, 2007, 2009, 2011) and lee side (Brookfield, 1977; Haszeldine, 1982; Almeida *et al.*, 2016a,b) of larger host dunes, resulting respectively in higher-angle and lower-angle inclined cosets. These sedimentary structures have been identified in sedimentary deposits of active rivers (Reesink & Bridge, 2011; Reesink *et al.*, 2014) and the rock record (Brookfield, 1977; Haszeldine, 1982; Almeida *et al.*, 2016a). Note that both 'higher-angle' and 'lower-angle inclined cosets' are low-angle dipping surfaces below the angle of repose of a dune (Reesink & Bridge, 2007, 2009; Almeida *et al.*, 2016a) and the terms 'higher' and 'lower' are given to distinguish them. According to these previous studies, and considering the multibeam echosounder (MBES) data presented here, the following sedimentary structures can be inferred from the studied bedforms of the Amazon River (Fig. 8): simple cross-strata sets in the shallow channel, formed by the simple dunes; and inclined cosets in the deep channel, formed by the compound dunes. Furthermore, the compound dunes would thus display two types of inclined cosets: (i) lower-angle inclined cosets, related to the occurrence of superimposed dunes on the lee side; and (ii) higher-angle inclined cosets, related to the effects of stoss side superimposed dunes on the host bedform lee side. In most of the surveyed areas of the deep channel, compound dunes present superimposed dunes on the lee side (Fig. 3), which would produce lower-angle inclined cosets, with individual cross-strata sets scaled to the height of the superimposed dunes. Only in the rare cases of compound dunes with superimposed dunes restricted to the stoss side, foresets would be produced at the scale of the large host dune, laterally transitioning to higher-angle inclined cosets.

Since the size of the bedform defines the maximum possible thickness of the preserved cross-strata sets, and the thickness of cross-stratal sets is a fraction of the formative dune height (Paola & Borgman, 1991; LeClair & Bridge, 2001; Leclair, 2011; Reesink *et al.*, 2015), sedimentary structures formed by the superimposed bedforms described herein would be relatively small, at any flow depth (Fig. 6A). Apart from rarer, larger, deep channel compound dune avalanche lee sides (6% of the total area in the reaches studied herein) that would result in metre-scale cross-strata sets and higher-angle inclined cosets, the dominant deep channel superimposed dunes and smaller shallow channel simple dunes would produce centimetre to decimetre-scale thick cross-strata sets (Fig. 8).

These latter thicknesses are usually expected in deposits of small rivers, where dunes are limited to a few metres in height (Van den Berg, 1987; Julien & Klaassen, 1995; Wilbers & Ten Brinke, 2003). Similarity of the set thicknesses occurs since published works investigated by the authors of this work from the deposits of small rivers suggest that the compound dunes with superimposed dunes on the lee side are not the dominant feature in those settings. On the contrary, their dunes are characterized by avalanche foresets (Dinehart, 1989; Carling *et al.*, 2000; Wilbers & Ten Brinke, 2003; Huizinga, 2010; Eilertsen *et al.*, 2013) and superimposed dunes occur on the stoss side of the host dunes (Carling *et al.*, 2000; Reesink & Bridge, 2011). The presence of superimposed dunes upon compound dune lee sides in the deep channel, as well as the wide scatter of dune height at any given water depth, also reveals that inferences of palaeo-water depth based on cross-strata set thickness may be misleading (Reesink *et al.*, 2015).

The lee-side angle results (Fig. 6) reveal that both shallower and deeper areas of the channel covered by mobile sediment show dunes with lee-side angles steeper than 15°, which has not been recognized to date in large rivers (Hendershot *et al.*, 2016). In shallower flows, these higher-angle dunes are primary simple dunes, whereas in deeper areas, these higher-angle dunes are superimposed on compound dunes with lee-side angles below 15°. These results also show a threshold lee-side angle at which compound dunes display superimposed dunes on their lee sides of *ca* 15 to 18°, and above which the lee-side faces may be ascribed to avalanche slopes (Fig. 7), matching the value of lee-side angles that control the onset of permanent flow separation (Kostaschuck & Villard, 1996; Best & Kostaschuck, 2002; Hendershot *et al.*, 2016). It is interesting to note that a similar relationship of higher dune form index in shallow areas, with higher lee side angles, and lower dune form index in deep areas, with lower lee-side angles (Fig. 4C), was also described in a work by Bradley & Venditti (2017), although at a very different scale. In this work, the split occurs at around 30 m of water depth, whereas Bradley & Venditti (2017) found this difference to occur at 2·5 m of water depth.

Successions dominated by centimetre to decimetre-scale cross-strata sets could be formed in channels as deep as several tens of metres, and therefore independent criteria must be used to recognize channel scale. These superimposed dunes are also migrating on much lower angle surfaces (Fig. 8), and suggest the need for careful evaluation of such low-angle surfaces in the rock record, which may be very difficult to infer with limited exposures, or impossible in core. Given the data presented herein (Fig. 6), it may be possible to recognize the deposits of deep fluvial channels based on the identification of coarse sandstones with metre-scale thick cross-stratified cosets (formed by the migration of large compound dunes) composed of centimetre to decimetre-scale thick inclined cross-strata sets (formed by the migration of the superimposed dunes) with foreset dip angles ranging from 12 to 21°. The recognition of compound dune cosets is thus key to the interpretation of river scale, since compound dunes are a main element in large river channels (Best *et al.*, 2007; Wang *et al.*, 2007), and the maximum height of these large bedforms appears better correlated with water depth (Fig. 4).

Given the lack of sequential MBES surveys at different river stages in the studied locations, the origin of conspicuous smaller bedforms both on the stoss and lee sides of larger host dunes cannot be interpreted directly from the present data. The low-angle lee-side surfaces of the large compound dunes might be attributed to changes in flow stage, with the large bedform being progressively deformed by an increase in sediment accumulation on the lee side (Kostaschuck & Villard, 1996) or by erosion of the host dune crest. It is possible that the weakening of flow separation resulting from the low-angle lee side enables the active migration of smaller bedforms also on the lee surface, giving rise to the observed morphology of compound dunes.

The rock record of large rivers

Despite the great contribution of modern day large rivers to the global sediment transport and their common occurrence in subsiding areas related to active tectonic environments, the recognition of large rivers in the rock record is relatively scarce. Examples of interpreted large river deposits are the Cretaceous McMurray Formation in western Canada (Hubbard *et al.*, 2011) the Triassic Hawkesbury Sandstone in south-eastern Australia (Miall, 2006; Fielding, 2007) and the Pleistocene deposits in central-western Amazonia (Rossetti *et al.*, 2005; Horbe *et al.*, 2013). Two main types of criteria are often used to infer river scale: (i) thickness of preserved channel-forms, channel-fill successions or bar-forms scaled to channel depth; and (ii) average or maximum thickness of preserved cross-strata sets, considered to be a function of channel depth.

The Middle McMurray Formation exhibits 30 to 40 m thick point-bar deposits, interpreted from large-scale inclined heterolithic strata (IHS) and related to kilometre-scale scroll-bars imaged in three-dimensional seismic surveys (Hubbard *et al.*, 2011; Jablonski & Dalrymple, 2016). Despite the thick channel-fill elements, ripple cross-laminated sandstones and heterolithic strata are more abundant than the 0·5 to 2·0 m thick cross-bedded sandstones, even close to the channel bases (Jablonski & Dalrymple, 2016). Previous models to explain this apparent discrepancy are grain-size controls on bedform development and tidal influence (Jablonski & Dalrymple, 2016, and references therein). The data herein suggests the possibility of the actual larger bedforms on the deeper parts of the channel being preferably preserved as cross-strata cosets resulting from smaller bedforms, ripples in the McMurray case, migrating on their lee sides. It is important to note that in the absence of well-developed large-scale IHS or available seismic images, similar successions would be unlikely to be interpreted as deep channel deposits based on the cross-strata set size distribution alone.

Another example of interpreted large river deposits are the Pleistocene sands exposed at up to 30 m tall river banks in central-western Amazonia. These sands are genetically related to the largest active rivers on Earth and compose large-scale fining-upward cycles dominated by tabular and trough cross-bedded medium to fine sands, with the local occurrence of coarse sand near the base of the fining-upward cycles and frequent intercalated silts and muds near their tops (Rossetti *et al.*, 2005; Horbe *et al.*, 2013). Again, the preserved 0·1 to 0·3 m thick cross-strata sets do not differ significantly from what is found in much smaller river deposits, and the low-angle cross-strata set bounding surfaces hamper the recognition of the 0·6 to 1·5 m thick cross-strata cosets, which are locally concave upward and downstream (Almeida *et al.*, 2016a). In fact, the preserved cross-strata set thicknesses are compatible with the partial preservation of bedforms with a size comparable to those found as superimposed dunes on larger bedforms in the modern Amazonas and Solimões rivers.

An example of large river deposits interpreted based on cross-strata set thickness is the Triassic Hawkesbury Formation of south-eastern Australia, where 2 to 3 m thick and up to 8 m thick, often concave upward and downstream, cross-strata sets abound (Conaghan & Jones, 1975; Rust & Jones, 1987; Miall & Jones, 2003). Closer inspection reveals cosets with internal smaller cross-strata sets within these structures, more frequent away from the axis of the concave forms. These deposits have been interpreted as large thalweg dunes (Almeida *et al.*, 2016a). Some of the large-scale cross-strata sets may be interpreted locally as bar foresets (see discussion in Almeida *et al.*, 2016a). Therefore, even in the best-known case of large-scale cross-strata in large river deposits, the sedimentary product of bedform superposition indicating the dominance of compound dunes is remarkable. In the three examples above, the reinterpretation of centimetre-scale cross-strata sets as formed by smaller bedforms migrating on the lee-surfaces of larger bedforms can be reconciled with an origin in deep channels.

CONCLUSIONS

High-resolution multibeam echo sounder bathymetric maps of two reaches of the Amazon River were surveyed during peak flood, and reveal that small dunes can be frequent in large rivers, suggesting significant implications for interpretations of the rock record. Despite being dominated by large-scale compound dunes at greater flow depths, these data show how small dunes can be widespread, both in shallower (as primary bedforms) and deeper (as secondary) flows in the world's largest river (Fig. 6A).

The presence of large sets of cross-strata has been thought to be the most common attribute needed to recognize the deposits of large rivers (Miall, 2006; Fielding, 2007). However, the very common presence of small dunes in both shallow and deep channels indicates that large river deposits may principally comprise bedform elements that are found within small rivers. Although very large compound dunes do occur in the deeper areas of the channel, their morphology, characterized by very low lee-side angles with downclimbing superimposed dunes, suggests that large metre-scale cross-strata sets might be rare or absent. Given that the bedform height is the possible maximum thickness of the resulting cross-strata set, the maximum preserved cross-strata set thickness must be significantly smaller than what is expected for dunes deprived of superimposed dunes on their lee sides.

Low lee-side angle dunes are a common feature among large rivers (Hendershot *et al.*, 2016) and are indeed present in the surveyed reaches of the present work, being represented by large compound dunes. However, the compound dunes generally display superimposed dunes on their lee side at angles lower than 15 to 18° (Fig. 7), corresponding to 94% of the area of the lee sides of compound dunes. Steeper lee-side angles with no superimposed dunes, interpreted as avalanche slopes, were thus limited in area. The superimposed dunes possess higher lee-side angles, commonly steeper than 15° (Fig. 6B), which have rarely been recognized in large rivers (Hendershot *et al.*, 2016). This relationship of large, low-angle, compound dunes and superimposed bedforms is present in other large rivers whose data resolution allows visualization, such as the Yangtze (Wang *et al.*, 2007), Paraná (Amsler & Prendes, 2000; Parsons *et al.*, 2005) and Mississippi (Abraham & Pratt, 2002).

Previous studies of the morphology of compound dunes in the Amazon River (Strasser, 2002, 2008) and other large rivers in the world, such as the Yangtze (Wang *et al.*, 2007), Jamuna (Best *et al.*, 2007), Paraná (Reesink *et al.*, 2014) or Mississippi (Harbor, 1998), suggest that decimetre-scale cross-strata sets are much more likely to be preserved and found in the rock record than larger metre-scale cross-sets. In this work, a collection of shallow and deep channel bedform examples is provided, indicating how ubiquitous small dunes are in the largest river of the world and, even there where the largest dunes are observed, they possess smaller superimposed dunes on the lee side that might be misleading when interpreting the rock record. The size of the superimposed dunes on the large compound dunes is comparable to dunes formed in small rivers, and criteria to differentiate between them should thus be considered in interpretation of ancient alluvium, such as coset recognition, lee-side angle, facies association and grain size. Therefore, successions dominated by decimetre-scale cross-strata sets superimposed on larger, low-angle surfaces, but showing rarer preservation of large-scale avalanche foresets near the base of fining-upward cycles that are tens of metres thick, may be characteristic of the deposits of large sand-bed river channels.

ACKNOWLEDGEMENTS

This research was funded by the São Paulo Research Foundation (FAPESP) through Research Grants #2014/16739-8, #2016/19736-5, #2017/06874-3, #12/50260-6 (FAPESP-NSF-NASA Biota/Dimensions of Biodiversity). We also thank CAPES (PROEX-558/2011) and PRFH-PETROBRAS for student scholarships, and CNPq for researcher scholarships (302905/2015-4, 301775/2012-5). We also are grateful for fieldwork funding provided by the Jack and Richard Threet Chair in Sedimentary Geology (JLB) and the Department of Geology (JS) at the University of Illinois. We also thank the careful reviews and insights that helped to improve the paper of Greg Sambrook Smith and Jeffrey A. Nittrouer, as well as Editor Nigel Mountney.

REFERENCES

Abraham, D. and **Pratt, T.** (2002) Quantification of bed-load transport on the upper Mississippi River using multibeam survey data and traditional methods. US Army Engineer Research and Development Center (ERDC)/Coastal and Hydraulics Laboratory (CHL), Coastal and Hydraulics Engineering Technical Note (CHETN). Available at: http://chl.wes.army.mil/library/publications/chetn.

AGÊNCIA NACIONAL DE ÁGUAS (ANA) – Brazilian Water Agency. HidroWeb: sistemas de informações hidrológicas. Available at: http://hidroweb.ana.gov.br/HidroWeb (October 2016).

Allen, J.R.L. (1984) *Sedimentary Structures: Their Character and Physical Basis*. Elsevier, Amsterdam, 663 pp.

Allen, J.R.L. and **Collinson, J.D.** (1974) The superimposition and classification of dunes formed by unidirectional aqueous flows. *Sed. Geol.*, **12**, 169–178.

Almeida, R.P., **Galeazzi, C.P.**, **Freitas, B.T.**, **Janikian, L.**, **Ianniruberto, M.** and **Marconato, A.** (2016a) Large barchanoid dunes in the Amazon River and the rock record: implications for interpreting large river systems. *Earth Planet. Sci. Lett.*, **454**, 92–102.

Almeida, R.P., **Freitas, B.T.**, **Turra, B.B.**, **Figueiredo, F.T.**, **Marconato, A.** and **Janikian, L.** (2016b) Reconstructing fluvial bar surfaces from compound cross-strata and the interpretation of bar accretion direction in large river deposits. *Sedimentology*, **63**, 609–628.

Amsler, M.L. and **Prendes, H.H.** (2000) Transporte de sedimentos y processes fluviales associados. In: *El Río Paraná em su trama médio, Contribuicíon al conocimiento y practicas ingenieriles en un gran río de llanura* (Eds C. Paoli and M. Schreider), pp. 233–305. Universidad Nacional del Litoral, Santa Fé.

Ashley, G.M. (1990) Classification of large-scale subaqueous bedforms: a new look at an old problem. *J. Sed. Petrol.*, **60**, 160–172.

Best, J.L. and **Kostaschuck, R.** (2002) An experimental study of turbulent flow over a low-angle dune. *J. Geophys. Res.*, **107**, 18-1–18-19.

Best, J.L., **Ashworth, P.J.**, **Sarker, M.H.** and **Roden, J.E.** (2007) The Brahmaputra-Jamuna River, Bangladesh. In: *Large Rivers: Geomorphology and Management* (Ed. A. Gupta), pp. 395–433. Wiley InterScience, Sussex.

Bradley, R.W. and **Venditti, J.G.** (2017) Reevaluating dune scaling relations. *Earth-Sci. Rev.*, **165**, 356–376.

Brookfield, M.E. (1977) The origin of bounding surfaces in ancient aeolian sandstones. *Sedimentology*, **24**, 303–332.

Carling, P.A., **Williams, J.J.**, **Gölz, E.** and **Kelsey, A.D.** (2000) The morphodynamics o fluvial sand dunes in the River Rhine, near Mainz, Germany. II. Hydrodynamics and sediment transport. *Sedimentology*, **47**, 253–278.

Coleman, J.M. (1969) Brahmaputra river: channel processes and sedimentation. *Sed. Geol.*, **3**, 129–239.

Conaghan, P.J. and **Jones, J.G.** (1975) The Hawkesbury Sandstone and the Brahmaputra: a depositional model for xontinental sheet sandstones. *J. Geol. Soc. Aust.*, **22**, 275–283.

De Reu, J., **Bourgeois, J.**, **Bats, M.**, **Zwertvaegher, A.**, **Gelorini, V.**, **De Smedt, P.**, **Chu, W.**, **Antrop, M.**, **De Maeyer, P.**, **Finke, P.**, **Van Meirvenne, M.**, **Verniers, J.** and **Crombé, P.** (2013) Application of the topographic position index to heterogeneous landscapes. *Geomorphology*, **186**, 39–49.

Dinehart, R.L. (1989) Dune migration in a steep, coarse-bedded stream. *Water Resour. Res.*, **25**, 911–923.

Eilertsen, R.S., **Olsen, N.R.B.**, **Rüther, N.** and **Zinke, P.** (2013) Channel-bed changes in distributaries of the lake Øyeren delta, southern Norway, revealed by interferometric sidescan sonar. *Norw. J. Geol.*, **93**, 25–35.

Ernstsen, V.B., **Noormets, R.**, **Winter, C.**, **Hebbeln, D.**, **Bartholomä, A.**, **Flemming, B.W.** and **Bartholdy, J.** (2006) Quantification of dune dynamics during a tidal cycle in an inlet channel of the Danish Wadden Sea. *Geo Mar. Lett.*, **26**, 151–163.

Fielding, C.R. (2007) Sedimentology and stratigraphy of Large River Deposits: recognition in the ancient record, and distinction from 'Incised Valley Fills'. In: *Large Rivers: Geomorphology and Management* (Ed. A. Gupta), pp. 97–113. Wiley InterScience, Sussex.

Gallant, J.C. and **Wilson, J.P.** (2000) Primary topographic attributes. In: *Terrain Analysis: Principles and Applications* (Eds J.P. Wilson and J.C. Gallant), pp. 51–86. John Wiley and Sons, New York, NY.

Gupta, A. (2007) Introduction. In: *Large Rivers: Geomorphology and Management* (Ed. A. Gupta), pp. 1–5. Wiley InterScience, Sussex.

Harbor, D.J. (1998) Dynamics of bedforms in the Lower Mississippi River. *J. Sed. Res.*, **68**, 750–762.

Haszeldine, R.S. (1982) Descending tabular cross-bed sets and bounding surfaces from a fluvial channel in the Upper Carboniferous of North-East England. *J. Sed. Petrol.*, **53**, 1233–1247.

Hendershot, M.L., **Venditti, J.G.**, **Bradley, R.W.**, **Kostaschuck, R.A.**, **Church, M.** and **Allison, M.A.** (2016) Response of low-angle dunes to variable flow. *Sedimentology*, **63**, 743–780.

Horbe, A.M.C., **Motta, M.B.**, **Almeida, C.M.**, **Dantas, E.L.** and **Vieira, L.C.** (2013) Provenance of Pliocene and recent sedimentary deposits in western Amazonia, Brazil: consequences for the paleodrainage of the Solimões-Amazonas River. *Sed. Geol.*, **296**, 9–20.

Hovius, N. (1998) Controls of sediments supply by large rivers. In: *Relative Role of Eustasy Climate and Tectonism in Continental Rocks* (Eds K. Shanley and P. McCabe). SEPM Spec. Publ., **59**, 3–16.

Hubbard, S.M., **Smith, D.G.**, **Nielsen, H.**, **Leckie, D.A.**, **Fustic, M.**, **Spencer, R.J.** and **Bloom, L.** (2011) Seismic geomorphology and sedimentology of a tidally influenced river deposit, Lower Cretaceous Athabasca oil sands, Alberta, Canada. *AAPG Bull.*, **95**, 1123–1145.

Huizinga, R.J. (2010) Bathymetric surveys at highway bridges crossing the Missouri River in Kansas City, Missouri, using a multibeam echo sounder, 2010. U.S. Geol. Surv. Scientific Investigations Report, 2010–5207, 61 pp.

Jablonski, B.V.J. and **Dalrymple, R.W.** (2016) Recognition of strong seasonality and climatic cyclicity in an ancient, fluvially dominated, tidally influenced point bar: Middle McMurray Formation, Lower Steepbank River, north-eastern Alberta, Canada. *Sedimentology*, **63**, 552–585.

Jackson II, R.G., (1976) Largescale ripples of the lower Wabash River. *Sedimentology*, **23**, 593–623.

Julien, P.Y. and **Klaassen, G.J.** (1995) Sand-dune geometry of large rivers during floods. *J. Hydraul. Eng.*, **121**, 657–663.

Kostaschuck, R.A. and **Villard, P.V.** (1996) Flow and sediment transport over large subaqueous dunes: Fraser River, Canada. *Sedimentology*, **30**, 727–742.

Latrubesse, E.M., **Stevaux, J.C.** and **Sinha, R.** (2005) Tropical rivers. *Geomorphology*, **70**, 187–206.

Leclair, S.F. (2011) Interpreting fluvial hydromorphology from the rock record: large-river peak flows leave no clear signature. In: *From River to Rock Record: the Preservation of Fluvial Sediments and Their Subsequent Interpretation* (Eds S.K. Davidson, S. Leleu and C.P. North), SEPM Spec. Publ., **97**, 113–123.

Leclair, S.F. and **Bridge, J.S.** (1997) Preservation of cross-strata due to migration of subaqueous dunes over aggrading and non-aggrading beds: comparison of experimental data and theory. *Geosci. Can.*, **24**, 55–66.

LeClair, S.F. and **Bridge, J.S.** (2001) Quantitative interpretation of sedimentary structures formed by river dunes. *J. Sed. Res.*, **71**, 713–716.

Lunt, I.A. and **Bridge, J.S.** (2007) Formation and preservation of open-framework gravel strata in unidirectional flows. *Sedimentology*, **54**, 71–87.

Miall, A.D. (2006) How do we identify big rivers? And how big is big? *Sed. Geol.*, **186**, 39–50.

Miall, A.D. and **Jones, B.G.** (2003) Fluvial architecture of the Hawkesbury Sandstone (Triassic), near Sydney, Australia. *J. Sed. Res.*, **73**, 531–545.

Nittrouer, J.A., **Mohrig, D.** and **Allison, M.A.** (2011) The lowermost Mississippi River: a mixed bedrock-alluvial channel. *Sedimentology*, **58**, 1914–1934.

Paola, C. and **Borgman, L.** (1991) Reconstructing topography from preserved stratification. *Sedimentology*, **33**, 553–565.

Parsons, D.R., **Best, J.L.**, **Orfeo, O.**, **Hardy, R.J.**, **Kostaschuk, R.** and **Lane, S.N.** (2005) Morphology and flow fields of three-dimensional dunes, Rio Paraná, Argentina: results from simultaneous multibeam echo sounding and acoustic Doppler current profiling. *J. Geophys. Res.*, **110**, F04S03 1–F04S03 9.

Potter, P.E. and **Hamblin, W.K.** (2006) Big rivers worldwide: Part 1 origins: Provo, Utah, Brigham Young University. *Geol. Stud.*, **48**, 78.

Reesink, A.J.H. and **Bridge, J.S.** (2007) Influence of superimposed bedforms and flow unsteadiness on formation of cross strata in dunes and unit bars. *Sed. Geol.*, **202**, 281–296.

Reesink, A.J.H. and **Bridge, J.S.** (2009) Influence of bedform superimposition and flow unsteadiness on the formation of cross strata in dunes and unit bars—Part 2, further experiments. *Sed. Geol.*, **222**, 274–300.

Reesink, A.J.H. and **Bridge, J.S.** (2011) Evidence of bedform superimposition and flow unsteadiness in unit-bar deposits, South Saskatchewan River, Canada. *J. Sed. Res.*, **81**, 814–840.

Reesink, A.J.H., **Ashworth, P.H.**, **Sambrook Smith, G.H.**, **Best, J.L.**, **Parsons, D.R.**, **Amsler, M.L.**, **Hardy, R.J.**, **Lane, S.N.**, **Nicholas, A.P.**, **Orfeo, O.**, **Sandbach, S.D.**, **Simpson, C.J.** and **Szupiany, R.N.** (2014) Scales and causes of

heterogeneity in bars in a large multi-channel river: Río Paraná, Argentina. *Sedimentology*, **61**, 1055–1085.
Reesink, A.J.H., **Van den Berg, J.H.**, **Parsons, D.R.**, **Amsler, M.L.**, **Best, J.L.**, **Hardy, R.J.**, **Orfeo, O.** and **Szupiany, R.N.** (2015) Extremes in dune preservation: controls on the completeness of fluvial deposits. *Earth-Sci. Rev.*, **150**, 652–665.
Rossetti, D.F., **Toledo, P.M.** and **Góes, A.M.** (2005) New geological framework for Western Amazonia (Brazil) and implications for biogeography and evolution. *Quatern. Res.*, **63**, 78–89.
Rubin, D.M. and **Hunter, R.E.** (1982) Bedform climbing in theory and nature. *Sedimentology*, **29**, 121–138.
Rust, B.R. and **Jones, B.G.** (1987) The Hawkesbury Sandstone south of Sydney, Australia: Triassic analogue for the deposit of a large, braided river. *J. Sed. Petrol.*, **57**, 222–233.
Sambrook Smith, G.H., **Ashworth, P.J.**, **Best, J.L.**, **Lunt, I.A.**, **Orfeo, O.** and **Parsons, D.R.** (2009) The sedimentology and alluvial architecture of a large braid bar, Río Paraná, Argentina. *J. Sed. Res.*, **79**, 629–642.
Sambrook Smith, G.H., **Best, J.L.**, **Orfeo, O.**, **Vardy, M.E.** and **Zinger, J.A.** (2013) Decimeter-scale *in situ* mapping of modern cross-bedded dune deposits using parametric echo sounding: A new method for linking river processes and their deposits. *Geophys. Res. Lett.*, **40**, 3883–3887.
Strasser, M.A. (2002) Estudo da geometria das formas de fundo no curso médio do Rio Amazonas. MSc. Dissertation, Universidade Federal do Rio de Janeiro, Rio de Janeiro, 100 pp.
Strasser, M.A. (2008) Dunas fluviais no rio Solimões–Amazonas – dinâmica e transporte de sedimentos. Ph.D. Thesis, Universidade Federal do Rio de Janeiro, Rio de Janeiro, 148 pp.
Van den Berg, J.H. (1987) Bedform migration and bedload transport in some rivers and tidal environments. *Sedimentology*, **34**, 681–698.
Wang, Z., **Chen, Z.**, **Shi, Y.**, **Li, M.**, **Zhang, Q.** and **Wei, T.** (2007) Fluvial bedforms and hydrodynamic controls along the Mid-Lower Yangtze channel. *Sci. China (Ser. D)*, **37**, 1223–1234. (in Chinese).
Wignall, P.B. and **Best, J.L.** (2000) The Western Irish Namurian Basin reassessed. *Basin Res.*, **12**, 59–78.
Wilbers, A.W.E. and **Ten Brinke, W.B.M.** (2003) The response of subaqueous dunes to floods in sand and gravel bed reaches of the Dutch Rhine. *Sedimentology*, **50**, 1013–1034.
Yalin, M.S. (1964) Geometrical properties of sand waves. *J. Hydraul. Div.*, **90**, 105–119.

Manuscript received 27 July 2017; revision accepted 27 February 2018